NASA TECHNICAL NOTE

NASA TN D-2225

A PARAMETRIC STUDY OF MASS-RATIO AND TRAJECTORY FACTORS IN FAST MANNED MARS MISSIONS

by Duane W. Dugan

Ames Research Center

Moffett Field, Calif.

NATIONAL AERONAUTICS AND SPACE ADMINISTRATION • WASHINGTON, D. C. • FEBRUARY 1965

A PARAMETRIC STUDY OF MASS-RATIO AND TRAJECTORY FACTORS IN FAST MANNED MARS MISSIONS

By Duane W. Dugan

Ames Research Center
Moffett Field, Calif.

NATIONAL AERONAUTICS AND SPACE ADMINISTRATION

For sale by the Office of Technical Services, Department of Commerce,
Washington, D.C. 20230 -- Price $3.00

A PARAMETRIC STUDY OF MASS-RATIO AND TRAJECTORY FACTORS IN FAST MANNED MARS MISSIONS

By Duane W. Dugan

Ames Research Center
Moffett Field, Calif.

SUMMARY

A parametric study is made of several factors which affect the magnitude of the gross-payload fractions for manned Mars missions of total duration less than one synodic period of Mars. Velocity requirements are found and used to determine the best possible ratios of gross payload to initial mass in a near-Earth orbit. Several mission parameters are varied to assess their effects upon the gross-payload ratios. Included among the parameters studied are: date of opposition of Mars included within the mission period; type of mission mode; propulsion characteristics; date of arrival at Mars; length of stay time at Mars; delayed and premature departures from Mars and from correctly oriented orbits about Earth; total transit time; and the fraction of gross payload unloaded at various phases of the mission. Associated trajectories are examined for velocities of entry into the martian and terrestrial atmospheres, the perihelion distances of return trajectories, and the communication distances between Earth and the mission spacecraft.

INTRODUCTION

After the lunar mission, a manned expedition to the planet Mars appears to be a reasonable step, from the scientific and technical standpoints, in the manned exploration of the solar system. Particular scientific motivation is furnished by the possibility that some form of extraterrestrial life may be found and studied. In addition, the environmental conditions, such as temperature and atmospheric pressure, are believed to be less hostile to man on Mars than on Venus and Mercury.

Although a manned mission to Mars may not be undertaken for some time, preliminary investigations of the many factors involved in such missions are desirable now to assist in defining at an early date the major research problems whose solutions are essential to the success of the mission.

A number of preliminary studies relating to round-trip missions to Mars have been reported. Some are concerned chiefly with fly-by missions and with Mars orbiting missions without landing (e.g., refs. 1 and 2); others, such as reference 3, treat the manned landing-and-return mission, but the scope is restricted to specific payloads and to relatively few mission modes. It

appears that a parametric but simplified study of a wide range of mission modes and opportunities would be useful. Such a study is the subject of this paper.

The first part of the study is concerned with obtaining velocity requirements for ballistic flights as a function of transit times from Earth to Mars and from Mars to Earth for an appropriate range of launch dates over a complete cycle of oppositions of Mars in the period from 1971 to 1988. In the second part, these velocity requirements are used for obtaining maximum ratios of gross payload to initial mass in Earth orbit as functions of total transit time, stay time at Mars, unloaded fractions of gross payload, and of the year of opposition. The corresponding velocities of entry into the martian and terrestrial atmospheres and trajectory characteristics of outbound and return legs as well as the effects of early and late departures from both Earth and Mars are investigated. The study includes a comparison of maximum gross-payload fractions and of other mission characteristics which result from employing several different mission modes of the direct and of the Mars-orbit rendezvous types. Two types of propulsion systems are considered, one chemical with a specific impulse, I_{sp}, of 445 seconds, the other nuclear with an I_{sp} of 820 seconds.

In general, only those missions lasting less than the synodic period of Mars (780 days) are considered here. In some instances characteristics are calculated for missions based on Hohmann-type trajectories lasting from 900 to 1000 days for comparison with those of these "fast" missions.

ANALYSIS

Some general aspects of manned landing and return missions to Mars may be inferred from a study of figure 1. In this figure the orbits of Earth and Mars are projected onto the plane of the ecliptic, together with dates and relative positions of these two planets for oppositions of Mars between the years 1971 and 2000. Also shown are the locations of the ascending and descending nodes of Mars' orbit, which is inclined 1.85° to the ecliptic plane. Although the synodic period of Mars is nearly 780 days or 26 months, the actual interval between successive oppositions included in figure 1 may be as much as four weeks longer or a little over two weeks shorter than 26 months. This irregularity is due, for the most part, to the eccentricities of the orbits of Earth (0.016726) and especially of Mars (0.093367). Also because of these orbital eccentricities, the distances of nearest approach of the planets vary from 35×10^6 to nearly 63×10^6 miles.

Figure 1 suggests trends in the relative energy requirements for round-trip missions to Mars which have a total duration, including stay time at Mars, of less than the synodic period of Mars. On the basis of the noted variable distance between the two planetary orbits, such requirements should be lower for oppositions which occur when Mars is in the neighborhood of its perihelion than for oppositions which coincide more nearly with Mars' aphelion passage. Likewise, it can be anticipated that reentry velocities into the

Earth's atmosphere will tend to be lower if the mission departs Mars when Mars is in the neighborhood of its perihelion rather than close to aphelion. The oppositions in figure 1 which appear to present the most favorable opportunities for round-trip missions are those of 1971, 1986, and 1988.

From such considerations it appears advisable to examine the effect of planetary configurations upon mission characteristics. Accordingly, the present study includes a number of mission dates in the cycle of oppositions encompassing the years 1971 through 1988.

To evaluate the variations of velocity requirements with outbound and inbound trip times and with launch dates over a complete cycle of oppositions, several simplifications and approximations are incorporated into the calculations. Appendix A outlines the procedures used. Velocity increments are computed by a variant of the familiar "patched-conic" procedure. To aid in interpreting the results presented in the next section, the simplifications and assumptions used in this part of the analysis are summarized here as follows:

(1) Positions of Earth and Mars are calculated from equations based on the assumption that the orbits are unperturbed ellipses about the Sun.

(2) The orbit of Mars is assumed to lie in the ecliptic plane. This assumption is made in order to avoid the highly inclined single-impulse heliocentric transfer trajectories required when the departure and target planets do not lie in the same plane at the time of arrival. Unless they are in the same plane, the inclination of the heliocentric transfer trajectory with respect to the ecliptic approaches 90° as the difference in the celestial longitudes of the departure and target planets approaches 180°. In such cases, the required launch velocities and rates of closure at arrival become unreasonably large. Undesirably large inclinations can be avoided with relatively small increases in mission velocity requirements beyond those calculated for coplanar planetary orbits. A simple approach to this is discussed in appendix A and results of calculations made according to this method are shown in figure 2 for a typical example of an Earth-to-Mars trip. According to the figure, a second impulse during midcourse is advantageous only for angular distances typically between 170° and 190°. Likewise, the typical example indicates that differences between velocity requirements for single-impulse type trajectories calculated from two- and three-dimensional equations are insignificant except when angular distances β are greater or less than 180° by about 20°. Hohmann-type trajectories involve 180° of angular travel, but for "fast" round-trip missions the angular distances involved are likely, in general, to be somewhat different from 180°. Hence, for the most part, the assumption that the orbit of Mars is coplanar with that of Earth should give results adequate for the present exploratory purposes. The out-of-plane requirements are checked in this study to evaluate the validity of this assumption.

(3) Equations of Newtonian celestial mechanics for the restricted two-body problem are used to calculate velocities and other pertinent data in planetocentric and heliocentric conic orbits of the mission spacecraft.

These orbits are patched to give an approximation to the actual trajectory which would be followed by the spacecraft under the stipulated conditions. In reference 4 it is stated that velocity increments obtained in a three-dimensional sphere-of-influence patched-conic procedure agreed within 3 percent with those obtained with "exact" n-body calculations.

(4) Heliocentric velocities at points of transition from hyperbolic planetocentric orbits to the heliocentric transfer orbit or vice versa are calculated as though they were orbital velocities at the appropriate positions of the departure and target planets.

(5) Relative velocities between mission spacecraft and departure or target planets at pertinent points of transition from planetocentric hyperbolic orbits to heliocentric transfer orbits or vice versa are assumed equal to the appropriate hyperbolic excess velocities.

(6) Gravity losses involved in departing from or arriving at planetocentric parking orbits are neglected, and the altitudes of these orbits are assumed to be zero. The relatively small errors introduced by each of these simplifications tend to compensate one another in the present study except for relatively high-energy trips from Mars to Earth.

(7) Velocities of entry into planetary atmospheres are calculated at the surface of the planet rather than at an appropriate altitude above the surface.

Calculations by means of a more detailed procedure (e.g., using sphere of influence to compute velocities in heliocentric transfer orbits and in planetocentric hyperbolic orbits) indicate that errors introduced by assumptions and simplifications (3) to (7) do not exceed more than a few percent.

Following the description in appendix A of the procedures for generating incremental velocity requirements is a second section describing how these velocity increments used in conjunction with other mission parameters give ratios of the gross payload to the initial mass in Earth orbit. The equation developed there for the ratio of gross payload to initial mass in Earth orbit, $\overline{M}_L$, is

$$\overline{M}_L = \frac{R_1R_2R_3R_4}{1 - k_1(1 - R_2R_3R_4) - k_2(1 - R_3R_4) - k_3(1 - R_4)}$$

where

R_i $\quad (1 + \sigma_i)e^{-\frac{\Delta V_i}{c_i}} - \sigma_i \; ; \quad i = 1, 2, 3, 4$

σ_i ratio of mass of inerts to mass of propellants in ith stage

k_j fraction of gross payload unloaded at various points in the mission; $j = 1, 2, 3$

A high-speed digital computer was used to perform the many calculations involved in each of the foregoing procedures.

RESULTS AND DISCUSSION

Some of the results obtained from the programs previously described are presented and discussed in the following sections.

Velocity Requirements

Although the velocities associated with trips to Mars and back are regarded here chiefly as inputs to a program for calculating mass ratios, they can provide a basis for understanding and anticipating the effects on mass ratios of the year of opposition, date of arrival at Mars, total transit times, stay times at Mars, mission modes, and other parameters. In general, the conditions for which the sums of the major velocity requirements are least will serve as guides in finding those conditions for which the gross-payload fractions are largest. Accordingly, a brief survey of factors affecting major velocity requirements is made here.

Examples of the effects of transit time and arrival date upon major velocity requirements and atmosphere-entry velocities are presented in figure 3. The various velocities required for several transit times are plotted against the date of arrival at Mars. The date of departure from Mars is the arrival date plus the stay time T_S. (In fig. 3, $\Delta\tilde{V}_3$ and $\Delta\tilde{V}_E$ are shown for a 7-day stay at Mars.) Velocities of entry into the martian atmosphere may be obtained from the values of $\Delta\tilde{V}_2$ from which they differ by an additive constant, namely, the circular velocity of a Mars-centered orbit (0.3183 in terms of Earth escape speed, or 11,670 fps).

A characteristic trend is noted in figure 3, namely, that velocity increments associated with the Earth-to-Mars trip, $\Delta\tilde{V}_1$ and $\Delta\tilde{V}_2$, reach their minimums for arrival dates after opposition, whereas return velocities $\Delta\tilde{V}_3$ and $\tilde{V}_{E_\oplus}$ are lowest if departure from Mars occurs before opposition. It can also be seen that increasing the time on either leg beyond about 250 days will cause little reduction of minimum major velocity requirements.

If the total transit time T and the stay time T_S are specified, the total velocity increments required in a given mission mode will have a single minimum for any given arrival date. This minimum value is generally insensitive within ± 4 or 5 days to the transit time out T_1 (or to trip time on return leg, T_2). Because of the opposite trends of outbound and inbound velocity requirements noted in figure 3, however, a plot of the foregoing minimum values as a function of arrival date exhibits a number of stationary values. Figure 4(a) illustrates the phenomena for the rendezvous mode which utilizes propulsion braking to acquire an orbit about Mars and atmospheric braking at Earth. In the example, the smallest minimum occurs for arrivals before opposition in the case of total transit times of 300 and 340 days, but after opposition for longer total trip times. At some value of T, the two minimums, one before, the other after opposition, should be equal. In cases for which total velocity requirements are nearly equally low for arrivals

either before or after opposition, other considerations may affect the selection of the arrival date. Figure 4(b) shows another effect of arrival date, namely that outbound trip times are relatively longer for early arrivals than for those after opposition. The longer outbound trips could be advantageous if waste products are to be jettisoned along the way. Figure 3(d) shows that velocities of entry into the terrestrial atmosphere in the neighborhood of opposition arrival dates are markedly lower for early than for late arrivals at Mars. Unfortunately, as in the example shown in figure 4(a), the choice of an early arrival is generally advantageous only for missions of relatively high energy; for example, the penalty for selecting the best early arrival date rather than the best late arrival date for the 460-day mission shown in the figure is an increase in total velocity requirements of nearly 13,000 fps. If propulsion braking is specified to limit atmosphere-entry velocities at Earth, it is possible that the earlier arrivals will be advantageous also for the lower energy missions.

The effect of total transit time upon minimum total-velocity requirements is shown in figure 5 for one type of rendezvous mode (propulsion braking at Mars) and for the direct mode in figure 5. The stay time at Mars is 7 days in the examples. For comparison, the total major velocity requirements for missions employing Hohmann-type trajectories in both legs in the direct mode are listed for two periods. The use of these Hohmann-type trajectories requires very long stay times, and the advantages in reduced velocity requirements are not necessarily large. For example, in 1971 the sum of the major velocity increments in the direct mode for a transit time of 410 days and a stay time of 7 days is only about 15 percent greater than that required in the Hohmann-type mission which requires 502 days of travel time and a stay period of 451 days. If out-of-the-plane velocity requirements are included, the 15-percent advantage cited for the Hohmann-type mission reduces to a little over 4 percent. (In the example "fast" mission, total plane-change velocities amount to less than 200 fps, whereas they are nearly 3900 fps in the two Hohmann-type trajectories.) A more distinct advantage of the Hohmann-type trajectories is that atmosphere-entry velocities at Earth are typically about 37,000 to 38,000 fps whereas they are considerably greater, about 63,000 fps, in the short mission used for comparison.

The effect of the date of arrival at Mars on the minimum total velocity requirements for several total transit times and over a complete cycle of oppositions between the years 1971 and 1988 is shown in figure 6. The variation over the cycle is quite pronounced for relatively short trips in which energy requirements are high, but diminishes for longer trips of lower energy. For the two mission modes shown, velocity requirements are generally largest during the opposition of 1978, although, in most cases, only slightly greater than those for the immediately preceding and following oppositions of 1975 and 1980.

Gross-Payload Fractions

Among the considerable number of factors which affect the magnitude of the gross-payload fractions associated with "fast" manned landing-and-return missions to Mars, the following are considered here: (a) choice of mission mode; (b) total transit time; (c) characteristics of propulsion used; (d) date of opposition of Mars; (e) unloading of portions of gross payload during mission; and (f) length of stay time at Mars.

Unless specifically noted otherwise, atmospheric braking is assumed to be used for direct descent to the surface of Earth upon return.

It should also be noted that all results presented here are based upon the assumption that the orbit of Mars lies in the plane of the ecliptic. As discussed in an earlier section, velocity increments required to change the inclination of the heliocentric transfer orbit either at launch or during midcourse in order to take into account the actual inclination of Mars' orbit need not be large. These velocity increments are calculated here in the manner previously described. Some of the largest of these increments encountered in the present study are shown in figure 7 as a function of total transit time. Also shown is the variation of gross-payload fraction with total transit time. Figure 7 indicates that total out-of-plane velocity changes need not exceed a few hundred feet per second. The figure also shows that typically for "fast" missions, plane-change velocities in the return trip are relatively insignificant. Since the total of the major velocity increments in the example mission amounts to more than 42,000 fps, these additional velocity requirements should not materially affect conclusions based upon their neglect.

Effect of mission mode.- In figure 8 is shown a comparison of gross-payload fractions possible in two types of rendezvous modes and in the direct mode for missions arriving at Mars in 1971. Chemical propulsion with a specific impulse of 445 seconds and a constant inert fraction σ (based upon propellant mass) of 0.10 is assumed for all stages.[1] A fraction k_2 of the gross payload is considered to be unloaded either in a parking orbit about Mars (excursion vehicle, etc.) or at the surface (heat-shield structure, landing gear, etc.). A stay time of 7 days is assumed for the comparison. For comparatively short travel times, gross-payload fractions are seen to be larger for the direct than for the propulsive-type rendezvous mode. If travel time is greater, however, larger fractions can be achieved in this type of rendezvous method than in the direct method for similar unloaded fractions k_2. The value of k_2 will vary somewhat with the mission mode; in the rendezvous mode, the excursion vehicle probably represents a slightly larger fraction of the gross payload than do the heat shield, landing gear, deceleration devices, etc., required for the direct descent of the entire spacecraft to the surface. Figure 8 shows that if atmosphere braking is used to acquire the parking orbit about Mars in a rendezvous-type mission, considerably larger gross-payload fractions can be obtained. It can also be seen that the best

[1] If σ is considered to be a function of velocity increment, calculations show that it may be about 0.12 to 0.13 at the lowest major increments encountered. The effect on maximum $\bar{M}_L$ is negligible.

travel time is about two months shorter in this mode than in the other type of rendezvous mode. The advantages shown for atmospheric braking at Mars relative to propulsive braking will be partly offset by requirements of greater mass of heat shield for the entire vehicle, of greater structural strength for the parent spacecraft, and of additional propulsion for correcting the initial orbit.

Propulsion characteristics.- A comparison between gross-payload fractions possible with chemical propulsion, specific impulse of 445 secs, and with nuclear propulsion, specific impulse of 820 secs, is given in figure 9. As discussed in appendix A, the inert fraction, σ, for nuclear propulsion is considered to be a function of the velocity increment.[2] The period chosen for comparison includes the opposition of 1975. Results for the rendezvous mode with propulsion braking at Mars are presented in figure 9(a). Also shown for nuclear propulsion is the rendezvous mode which employs atmospheric braking to attain an orbit about Mars. In figure 9(b), the comparison is made for the direct mission mode. Because the velocity requirements at departure from Mars are considerably greater in the direct than in the rendezvous mode, two stages of propulsion are used for the return trip in the case of chemical propulsion in order to avoid negative values of payloads in many instances. In general, figure 9 indicates that in 1975 maximum gross-payload fractions with nuclear propulsion are about three times larger than those with chemical propulsion. It might be noted that the relative efficiencies of mission modes shown for nuclear propulsion in 1975 are similar to those previously noted for chemical propulsion in 1971.

Date of opposition.- Figure 10 presents the variations of gross-payload ratios with total transit time for the three types of mission modes discussed previously, but for the period including the opposition of 1980. The effect of the date of opposition upon the maximum payload ratios possible under similar conditions of propulsion and unloading fraction can be seen from comparing the results shown in figures 8, 9, and 10. The relative magnitudes are generally in accord with the variation of minimum total velocity requirements over a cycle of oppositions presented in figure 6. The payload fractions for missions in 1980 are essentially the same or only slightly larger than those in 1975, depending upon the mission mode.

Unloading.- The dependence of the gross-payload fraction upon the magnitude of the unloaded fraction of the gross payload is clearly indicated in figure 8. The figure also shows that the total transit time required to maximize the gross-payload fraction is essentially independent of the unloaded fraction. The effects of unloaded fractions on other characteristics of optimum mission trajectories, namely, date of arrival and individual trip times, amount to only a few days for the ranges of the unloaded fractions considered to be of practical significance. As a result, the various velocity increments and entry velocities are also essentially independent of the k_i.

---

[2]Values of σ for nuclear propulsion assumed here range from about 0.17 for a ΔV of 33,000 fps to 0.25 for a ΔV of 8,000 fps.

In the missions considered so far, the unloading was assumed to take place after the vehicle had attained a parking orbit about Mars or descended directly to the surface. In the rendezvous mode employing propulsion to achieve capture about Mars, it is pertinent to examine the effects of separating the excursion vehicle from the parent craft prior to the application of thrust. The smaller vehicle would then descend directly to the surface of Mars, using atmospheric braking for the most part. A comparison between the gross-payload fractions obtained by unloading the excursion vehicle before or after a parking orbit is attained by the parent spacecraft is given in figure 11. The advantages of the early over the later separation of the excursion vehicle are small or modest, depending upon the value of k_1 (or k_2) involved. On the other hand, some increase in the mass of the excursion vehicle (chiefly of the heat shield and of guidance facilities) would be required in the case of early separation. Figure 12 indicates that in the neighborhood of transit times for which payload fractions are greatest, the atmosphere-entry velocities may be 8000 to 9000 fps higher in direct descent than in a descent from orbit. The net advantage of early unloading over the unloading in orbit in the mission mode considered is not likely to be large, percentagewise.

Length of stay time.- All data used for comparisons in the foregoing have been based upon a nominal stay time at Mars of 7 days. The effect of the length of stay time upon the gross-payload ratios is shown in figure 13. It may be noted that for the range of stay times shown, those longer than 7 days increase the gross-payload fractions for short total transit times but decrease them for longer. Another noticeable effect is that the total required travel times associated with maximum payload ratios decrease with increasing length of stay. Hence, the total mission time increases more slowly than stay time. In the examples given, each additional 40 days of stay time increases the total mission time by about 20 days. Actually, since the curves of payload ratios are generally quite flat in the region of their maximums, the travel times can be reduced somewhat from those associated with the maximums without seriously reducing the payload fraction. In any case, the combination of greater propellant requirements and increased life support for planned stay times of increasing duration will be reflected in greater initial mass requirements or reduced gross payloads, or both.

The ultimate in stay times might be considered to be that involved in the use of Hohmann-type trajectories to Mars and return, in which case the waiting period at Mars is comparable with the travel time. The total transit time, stay time, date of arrival at Mars, and possible gross-payload ratios for various values of k_2 for each type of mission mode using Hohmann-type trajectories are listed in figure 13 for comparison. As noted earlier, velocity increments required for plane changes in Hohmann trajectories are generally considerably larger than those in fast missions. If these plane changes are taken into account, assuming that they are made by chemical propulsion with a specific impulse of 445 secs and with inert fractions appropriate to the magnitude of the velocity increments, the gross-payload ratios in the Hohmann-type missions are reduced to about 78 percent of the values listed in figure 13, whereas those in the fast missions are not appreciably affected (see fig. 7). Even so, the advantage in terms of gross-payload fraction lies

with the Hohmann-type trajectories if comparison is restricted to the same mission mode in each case. However, the use of these trajectories in a rendezvous mode appears questionable because of the long time which would be spent by part of the crew in a parking orbit about Mars (438 days in the example). If atmospheric braking can be used to effect capture into an orbit about Mars, a fast mission including a stay time of one to several months in the rendezvous mode (fig. 13(c)) would be more efficient, in terms of propellant-mass ratios, than the Hohmann-type mission using the direct mode.

Other Mission Characteristics

Although the gross-payload fraction is an important factor in the assessment of mission requirements, several other mission characteristics are also significant. Selected here for discussion are early and late departures from Earth; delayed and premature departures from Mars; atmosphere-entry velocities; outbound and inbound transit times; dates of arrival at Mars; the distance of nearest approach to the Sun; and communication distances between Earth and the mission spacecraft.

Early and late departures from Earth.- As noted earlier, the velocity requirements for the subject missions are calculated on the assumption that departure is initiated from a near-Earth orbit. This orbit is assumed to have the proper orientation for launching the mission craft at the required time into the appropriate heliocentric trajectory. No assessment is made of the weight penalties involved in adjusting the initial orbit to take into account the effects of delayed departures. Attention is restricted here to other weight penalties incurred by departing earlier or later than some nominal scheduled time.

Figure 14 shows the date of departure from Earth orbit associated with the gross-payload fraction $\bar{M}_L$ for scheduled departures. The examples include two types of rendezvous modes and the direct mode for periods including the opposition of 1980. The largest value of $\bar{M}_L$ in all the examples occurs within a relatively narrow range of departure dates between approximately 90 and 110 days before the date of opposition. As noted subsequently, dates of arrival at Mars may differ by as much as two months, depending upon the mission mode. The figure also shows that the decrease in gross-payload fraction in each case is more rapid for departures made after the most opportune date than for those made earlier. Likewise, the relative decrements in $\bar{M}_L$ with late departure dates are greater in the direct and rendezvous modes with atmospheric braking at Mars than in the rendezvous mode with propulsion braking at Mars. Another effect of departing on dates other than the scheduled one is that the total transit time is reduced for late, and increased for early departures.

The rather large losses in payload fraction indicated in figure 14 for nonoptimum departure dates can be minimized in some instances by adjusting certain mission parameters such as the date of arrival at Mars and the ratio of the outbound and inbound trip times. Figure 15 illustrates the improvement

which results from this reoptimization procedure. At each point on the curves of $\bar{M}_L$ shown in figure 14, another curve can be drawn with total transit time held constant but with date of arrival at Mars and individual trip times varied. Several such curves are shown in figure 15. As illustrated in the figure, an outer envelope curve can be drawn to include the largest possible values of the gross-payload fraction at any given departure date. For departures earlier or later by more than about 10 to 20 days than the date at which $\bar{M}_L$ is largest, the outer envelope rather than the inner curve assesses more accurately the penalties for off-schedule departures.

If the gross payload is assumed essentially constant at the value based on the departure date associated with the greatest value of the gross-payload fraction, the increase in initial mass required for departing the (adjusted) Earth orbit earlier or later than the nominal time can be estimated. The additional mass, of course, will be propellants and inerts.

Figure 16 shows the percent increase of initial mass as a function of early and late departures for various mission periods, mission modes, and stay times. In general, penalties for departing earlier or later than 20 to 30 days become significantly large. In figure 16(a), the effect of the particular opposition period of the mission is shown to be relatively small for late departures, but appreciably large for premature launch dates. Part (b) of the figure indicates that the choice of mission mode is highly significant with respect to required increases in initial mass in the case of late departures. In both the rendezvous mode that depends upon atmospheric braking at Mars and in the direct mode, the penalties for departures later than about 20 days are significantly large; in the rendezvous mode employing propulsion braking at Mars, they are about one-fourth to one-third as large as in the other two modes shown. The effect on mass increase of increasing the planned stay time at Mars is shown in figure 16(c) to be essentially insignificant for the range of stay times given.

Delayed departure from Mars.- Another consideration in the subject mission is the possibility that departure from Mars may be delayed for some reason. An example of the effects of delays on the over-all mass ratio is given in figure 17. In calculating the gross-payload fractions required in case of delayed departures, the return transit time was adjusted to make the launch velocity increment ΔV_3 a minimum in each case. As shown in figure 17, this procedure resulted in improving the original payload fractions in the case of the higher energy missions but created a serious deficit in the fractions for missions utilizing near-maximum payload ratios. To allow for unavoidable delays in departure in the more efficient missions, additional propellants would need to be carried for the resulting higher energy return trips to Earth. As shown in the lower part of figure 17, the return trips for delayed departures require more time than for scheduled departures in the case of the higher energy missions, but less time if near-maximum payload fractions are utilized. Total mission time, however, increases with increasing delays in all cases shown in the figure.

Premature departures from Mars.- Next consider the effect of an earlier than planned departure from Mars. Figure 18 illustrates the effect on payload fraction and on total transit times of such contingencies. For all planned total travel times shown in the figure, gross-payload fractions are more favorable when Mars is departed earlier than planned. This means, of course, that an excess of propellants could be used to shorten the return trip or perhaps to bring back more scientific samples. Likewise, although the total travel time is increased for early departures, in the region of more favorable payload fractions the actual total mission time is less than for scheduled departures.

From the foregoing discussion of delayed and premature departures from Mars for the return to Earth, it might be useful to plan for a stay period at Mars somewhat longer than actually intended in order to provide a margin of safety in the mission. Some advantage accrues from this procedure, inasmuch as a combination of outbound and return trajectories can be chosen to reduce propellant requirements of the entire mission to below those based upon optimizing the return trajectory only.

Atmosphere-entry velocities.- Velocities of entry into the atmosphere of Earth upon return are shown in figure 19. The dates given, 1971, 1975, and 1980, refer to the opposition of Mars included in the mission period. Two types of rendezvous modes and the direct mode are included in the figure. One significant characteristic of the entry velocities in all cases shown is that they increase with increasing total transit time in the regions where more favorable gross-payload fractions are found. In the neighborhood of the maximum values of the gross-payload ratios (the approximate total travel times associated with the maximums are indicated by arrows), entry velocities vary from about 48,000 fps (rendezvous mode with atmospheric braking at Mars, 1971) to nearly 74,000 fps (rendezvous mode with propulsion braking at Mars, 1975). In the direct mission mode, entry into the Earth's atmosphere is made at about 64,000 fps in both 1975 and 1980. The influence of the heliocentric distance of Mars at the time of departure from the planet can be seen in the disparity between entry velocities for 1971 (Mars near perihelion) and for 1975 and 1980 (Mars in neighborhood of aphelion). The effect of the unloaded fraction k_2 is not significantly large. Discontinuities observed for entry velocities of 1975 missions are associated with the occurrence of maximum values of gross-payload fractions for arrival at Mars both before and after the date of opposition, as discussed previously.

Figure 20 shows that entry velocities increase not only with increasing transit time but also with increasing stay time for the range of stay times shown. The velocities shown are those associated with maximum gross-payload fractions in each case. The effect of increasing stay time is considerably greater in 1975 than in 1980 missions. In 1980, for example, each additional 10 days of stay time means an increase of about 400 to 600 fps in entry velocity, depending upon the mission mode; in 1975, the corresponding increase in entry velocity is from approximately 900 to 1200 fps. In both periods, the increase is least for the rendezvous mode with propulsion braking at Mars, and nearly the same for the other two modes considered here. At some much

longer stay time, the entry velocities can be expected to decrease and reach the values typical of Hohmann-type missions (37,500 fps in 1971, and 38,230 fps in 1978).

In view of the very large atmosphere-entry velocities at Earth associated with the rendezvous mode employing propulsion braking at Mars, the effects of using propulsion thrust to reduce them are examined here. An example of using chemical propulsion (σ_i proportional to ΔV_i) to reduce entry velocities at Earth to parabolic speed is given in figure 21, and the variations of gross-payload fractions with total transit time are compared with all-atmospheric braking at Earth. In the former instance, k_3 represents the ratio of the mass of the mission module to the gross payload; in both cases, k_2 is the fraction of the gross payload represented by the martian excursion vehicle left in orbit about Mars at departure. Nuclear propulsion is assumed for all stages other than that used for reducing entry velocities. The example indicates that propulsion braking to reduce entry velocities at Earth requires significantly more propellant than atmospheric braking and about two months of additional travel time. For the stay time used in the example (47 days), the unretarded entry velocity is about 77,000 fps. If atmospheric braking at Mars is assumed, the corresponding entry velocity at Earth is somewhat less, 70,000, and the gross-payload fraction for $k_2 = 0.6$ is about 34 percent for a total transit time of 400 days (cf. figs. 13(c) and 20(b)). The use of atmospheric braking at either Mars or Earth or at both thus increases the efficiency and decreases the required travel time of the mission in comparison with the use of corresponding propulsion braking. However, it should be pointed out that the feasibility of safe entry into the atmosphere of the Earth at the high velocities cited remains to be demonstrated.

Velocities of entry into the martian atmosphere in the cases of the direct mode and of the rendezvous mode with atmospheric braking are illustrated in figure 22. In the direct mode, the figure indicates that the entry velocities associated with maximum gross-payload fractions are approximately 32,000 fps in 1980, 27,000 fps in 1975, and 26,000 fps in 1971. Corresponding velocities in the rendezvous mode are somewhat less than in the direct mode in 1980 (29,000 fps), but are essentially the same in 1975 and 1971.

The effect of stay time at Mars on entry velocities into the martian atmosphere is shown in figure 23. In general, for stay times up to about 60 days, each additional 10 days of stay time involves an increase of 400 to 600 fps in entry velocity, depending upon the mission mode and the date of opposition included in the mission.

Transit times, outbound and return.- Another mission characteristic of interest is the division of time between the outbound and return legs of the mission. Such information is summarized in figure 24 for three types of mission modes and for three mission periods. The total trip times shown are those for which the payload fraction is largest in each case. In general, if there are three velocity stages, as in the rendezvous mode with propulsion braking at Mars, the total transit time is divided nearly equally between the outbound and return trips; if only two major velocity increments are required, as in the direct mode and the other rendezvous mode, more time is required for

the return leg than for the Earth-to-Mars trip. Although increasing the stay time has the effect already noted of reducing the total trip time for which the payload fraction is maximum, it does not materially change the ratio shown for the trip times out and back.

Dates of arrival at Mars.- The date of arrival at Mars is significant for its relationship with the martian season. In figure 1, the beginning of each season in the northern hemisphere of Mars is given. The celestial longitudes of Mars at the beginning of northern spring, summer, autumn, and winter are 84°, 174°, 264°, and 354°, respectively. The longitude of perihelion of the martian orbit is nearly 335°; hence, as for the Earth, northern winter occurs when the planet is relatively close to the Sun. Because of the orbital eccentricity, the seasons vary in length. In terms of Earth days, the lengths of the northern seasons are, respectively, 199, 184, 146, and 158 days for spring, summer, autumn, and winter.

Figure 25 shows the dates of arrival at Mars as a function of total transit times for three types of mission modes and for periods including the oppositions of 1971, 1975, and 1980. Arrivals at Mars take place at dates later relative to opposition the farther the planet is from the Sun during opposition. The effect of the magnitude of the unloaded fraction k_2 is to cause the arrival date to increase by generally a few days with increasing k_2.

Figure 26 presents the date of arrival associated with maximum gross-payload fractions as a function of planned stay time at Mars. For the range of stay times shown, increasing the stay period requires somewhat earlier arrivals. For stay times longer than those included in the figure, the trend should be reversed, since for the long waiting periods characteristic of Hohmann-type missions, arrivals occur considerably later after opposition than any of those shown (e.g., 186 days in 1975, 171 days in 1978). The figure also shows that the date of arrival can vary as much as two months with mission mode, other things being the same. From figures 25 and 26, and from data given in figure 1, the seasons during which the stay time on Mars would occur are obtained for the years 1971, 1975-76, and 1980. They are listed below according to the mission mode which might used.

Mission mode	Year	Northern season
Rendezvous mode with propulsion braking at Mars	1971	Midwinter
	1975	Midspring
	1980	Midsummer
Rendezvous mode with atmospheric braking at Mars, and direct mode	1971	Late fall
	1975	Early spring
	1980	Early summer

The arrival date thus has a bearing on investigations of the martian seasonal phenomenon commonly termed "the wave of darkening."

Nearest approach to the Sun.- A study of the characteristics of the trajectories employed to go from Earth to Mars and subsequently from Mars back to Earth reveals one particular feature of concern in mission planning. As shown in figure 27, the vehicle on the return leg approaches the Sun as closely as 0.4 to 0.6 a.u. when gross-payload fractions near the maximum values are considered. Figure 27(a) shows the effect of the opposition period on the perihelion distance; figure 27(b) indicates the effect of mission mode; and the influence of the planned stay time is shown in figure 27(c). From part (a) of the figure, it appears that the heliocentric distance of Mars at the time of departure from that planet is associated with the perihelion distance of the return leg. The closest approach to the Sun seems to occur when the heliocentric distance at departure is greatest (1975 and 1980). With regard to mission mode, figure 27(b) shows that the nearest approach to the Sun occurs with the rendezvous mode which uses propulsion braking at Mars. It is clear from figure 27(c) that when the stay time is increased, the return trip tends to approach closer to the Sun. However, if stay times are prolonged enough, the perihelion distance will increase until the distance of the orbit of the Earth is attained, as in the Hohmann-type missions.

Communication distance.- Figure 28 presents the distance between the Earth and Mars as a function of time measured from the date of opposition for the years 1971, 1975, and 1980. The dates of departure from Mars associated with maximum gross-payload ratios for various mission modes are indicated in the figure for a 7-day stay at Mars. For longer stay times, the distances would increase somewhat, since the combination of longer stay times and earlier arrivals causes a net increase in the date of departure. The distances in each case represent approximately the maximum communication distances involved in the mission. Actually, the distance between the returning vehicle and Earth increases somewhat following departure from Mars. The variation of communication distance between the vehicle and Earth with time since departure from Mars is illustrated in figure 29. The maximum distance is only about 10 percent greater than the distance at departure; however, figure 29 shows that a considerable time (about 100 days) may elapse before the communication distance becomes less than that at departure from Mars.

Another important aspect of the communications problem in the mission is illustrated in figure 30. Here the outbound and inbound trajectories of the mission used for an example in the previous figure are shown. Typically, an opposition of the vehicle and Earth occurs on the outbound leg, and an inferior conjunction takes place near the end of the return trip, as shown. During such periods, when the Sun is in or close to the line of sight between the vehicle and Earth, solar noise will present difficulties in communications.

CONCLUDING REMARKS

The foregoing presentation has indicated the influence of a number of parameters on the attainment of maximum gross-payload fractions in fast manned Mars missions. Certain broad conclusions may be drawn from the many comparisons made, but such matters as selection of a mission mode or the width and shape of a launch window will depend upon many other considerations besides

the information presented here. Crew size, type of ecological system used (open, closed), weights of vehicle components and of equipment, propulsion-system characteristics, booster capabilities, Earth launch sites, safety and reliability, will all play an important part in formulating the method of accomplishing the mission. Several trends indicated by the present study are summarized here. Unless noted otherwise, direct descent by atmospheric braking is assumed at Earth return.

Simplified calculations of total velocity requirements for fast manned-landing missions to Mars over a full cycle of oppositions (1971 to 1988) indicate that minimum requirements do not vary by more than about 10 to 15 percent (4,000 to 5,000 fps), depending upon the mission mode assumed.

The use of nuclear propulsion with a specific impulse of 820 secs permits gross-payload fractions about 2.5 to 3 times larger than those possible with chemical propulsion with a specific impulse of 445 secs for the opposition of 1975.

The substitution of atmospheric for propulsion braking in achieving capture into a low circular orbit about Mars at arrival not only increases gross-payload fractions by about 1-1/2 times, but also reduces total travel times by nearly 2 months. In the direct mission mode, gross-payload fractions are about 10 percent smaller than those in the rendezvous mode with propulsion braking at Mars, and the total travel time is 50 to 70 days shorter, other things being equal.

With any mode, maximum gross-payload fractions decrease with increasing stay time up to at least three months in fast missions. For stay times of several hundred days, Hohmann-type missions permit gross-payload ratios larger than do fast missions for the same mission mode. Energy requirements are higher for delayed departures from Mars, and lower for premature departures. Planning for longer than intended stay times at Mars rather than for possible delays in departure can more economically provide a margin of safety in the mission.

For a stay time of 7 days at Mars, entry velocities into the martian atmosphere range from about 26,000 fps (1971) to 32,000 fps (1980), depending upon the mission mode considered. Likewise, entry velocities into the terrestrial atmosphere upon return vary from about 48,000 fps (rendezvous mode with atmospheric braking at Mars, 1971) to nearly 74,000 fps (rendezvous mode with propulsion braking at Mars, 1975). In the direct mode, both in 1975 and 1980, Earth entry velocities are approximately 64,000 fps. Up to about 3 months, each additional 10 days of stay time at Mars increases the atmosphere-entry velocities at Earth by roughly 1000 fps in 1975 and 500 fps in 1980. Using propulsion braking to reduce to parabolic speed the atmosphere-entry velocities in the 1975 mission (rendezvous mode with propulsion braking at Mars) reduced maximum gross-payload fractions to about 1/3 to 1/2 of those attained with no propulsion braking at Earth and required about 2 months of additional travel time.

Departures from Earth orbit earlier or later than the nominal date associated with maximum gross-payload fractions require significant increases in the initial mass only when they are more than 10 days from the nominal date.

In the fast missions considered, return trajectories associated with maximum gross-payload ratios have perihelion distances as small as about 0.4 to 0.6 a.u., depending upon the opposition period of the mission, the mission mode, and the length of the stay time at Mars. Communication distance between the mission vehicle and Earth can be about 2 a.u. in missions conducted during the oppositions of 1975 and 1980 with the rendezvous mode using propulsion braking at Mars.

Ames Research Center
National Aeronautics and Space Administration
Moffett Field, Calif., July 24, 1964

APPENDIX A

CALCULATIONS OF VELOCITIES AND MASS RATIOS

This section describes the procedures followed in calculating the data required in the present study. The notation is summarized in appendix B.

MISSION VELOCITIES

For this study a large number of calculations were required to explore velocity requirements over wide ranges of transit times and launch dates and over a complete cycle of oppositions. Therefore, several simplifications are made in the analysis to obtain the data required in each phase of a mission without unduly long and complicated calculations.

One simplification made at the outset is to assume that the elliptic orbits of Mars and Earth lie in the same plane, namely that of the ecliptic. This is done in order to avoid highly inclined heliocentric transfer orbits between Mars and Earth. The inclination of these transfer orbits with respect to the plane of the ecliptic approaches 90° as the angular distance travelled by the mission vehicle approaches 180°. For such highly inclined orbits, the launch velocities from Earth or Mars and the rates of closure of the vehicles with the planets become inordinately large. In practice, these highly inclined orbits can be avoided with relatively small additional velocity increments beyond those required in the case of coplanar planetary orbits.

In one simple approach, the vehicle can be assumed to follow the trajectory in the orbital plane of the departure planet, as in the two-dimensional case, until it reaches a point at which the difference in celestial longitudes of the vehicle and of the target planet at the known time of arrival is 90°; at this point the angle of inclination required for the transfer trajectory to intersect the actual arrival position of the target planet is a minimum (equal to the celestial latitude of the target planet at arrival relative to the orbit of the departure planet). The magnitude of the velocity increment required to effect the plane change thus depends on the velocity in the transfer orbit at the point described and on the appropriate relative celestial latitude. For an Earth-to-Mars trajectory, for example, the velocity increment ΔV_{p_1} required for a plane change can be estimated from the equation

$$\Delta V_{p_1} = 2V_T \left| \sin \frac{1}{2} \iota \sigma_A' \right|$$

where V_T is the heliocentric transfer-orbital velocity at the point in question. (The notation used in this paper is summarized in appendix B). Since the celestial latitude of Mars does not exceed 1.85° (0.0324 radian), the increment can be closely approximated from

$$\Delta V_{p_1} = V_T \left| {}^{l}\vec{\sigma}_A \right|$$

The heliocentric velocity of the vehicle as it approaches to within 90° of the arrival point will be comparable in magnitude with the orbital speed of the Earth, or about 10^5 fps. Hence, the plane-change velocity increment can be expected to vary from zero to not much more than roughly 3000 fps, depending chiefly upon the celestial latitude of Mars at arrival. The foregoing applies also to return trips, Mars to Earth.

It should be noted that the simple procedure described here for alleviating the excessively large velocities encountered in single-impulse type trajectories by employing a second impulse is likely to give conservative (somewhat large) values for the plane-change velocity increments. Somewhat smaller values could be obtained if the variation of velocity along the transfer trajectory were to be included in an optimization procedure. For example, in reference 4, Fimple uses a suitable combination of plane changes made both during the launch maneuver and during midcourse to minimize plane-change velocity requirements.

Earth Departure

The velocity increment calculated is that required to inject a vehicle from an orbit about the Earth into a heliocentric conic orbit connecting the centers of Earth and Mars. A vehicle following the trajectory from a massless Earth to a massless Mars arrives on a preselected date after a trip lasting T_1 days. As noted, the orbits of both Mars and Earth are regarded as unperturbed Keplerian ellipses lying in the plane of the ecliptic, so that the positions of both planets at appropriate times can readily be computed. If the angle β is the difference between the celestial longitudes of Mars at arrival and of Earth at departure, and $r\vec{\sigma}_A$ and $r_{\oplus D}$ are the corresponding heliocentric distances of the planets (see sketch (a)), the following equations can be used to find the eccentricity e_1 and the semimajor axis a_1 of a heliocentric conic trajectory which passes through the positions of the two planets at the stated times.

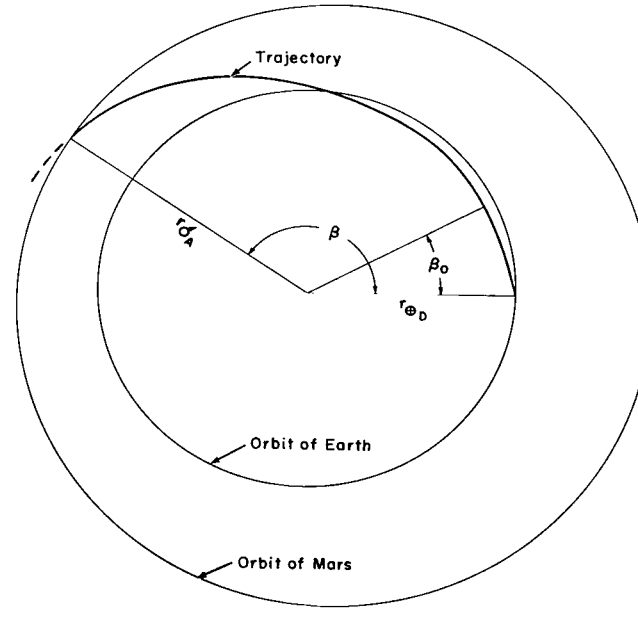

Sketch (a)

$$e_1 = \frac{r_{\sigma_A} - r_{\oplus_D}}{r_{\oplus_D} \cos \beta_o - r_{\sigma_A} \cos(\beta - \beta_o)} \tag{A1}$$

$$a_1 = \frac{r_{\oplus_D}(1 + e_1 \cos \beta_o)}{\left|1 - e_1^2\right|} \tag{A2}$$

The only unknown quantity in these equations is the perihelion constant β_o. This parameter is varied in an iterative scheme to make the computed time T_{1_c} from Earth to Mars agree with the stipulated time T_1 within a specified limit. For values of β_o which give eccentricities less than unity, the equation used for computing T_{1_c} in days is

$$T_{1_c} = \frac{365.25}{2\pi} a_1^{3/2} \left[2 \tan^{-1} \frac{(1 - e_1^2)^{1/2} \tan(1/2)(\beta - \beta_o)}{1 + e_1} \right.$$

$$- \frac{e_1(1 - e_1^2)^{1/2} \sin(\beta - \beta_o)}{1 + e_1 \cos(\beta - \beta_o)} + 2 \tan^{-1} \frac{(1 - e_1^2)^{1/2} \tan(1/2)\beta_o}{1 + e_1}$$

$$\left. - \frac{e_1(1 - e_1^2)^{1/2} \sin \beta_o}{1 + e_1 \cos \beta_o} \right], \qquad e_1 < 1 \tag{A3a}$$

and for eccentricities greater than unity,

$$T_{1_c} = \frac{365.25}{2\pi} a_1^{3/2} \left[\frac{e_1(e_1^2 - 1)^{1/2} \sin(\beta - \beta_o)}{1 + e_1 \cos(\beta - \beta_o)} \right.$$

$$- 2 \tanh^{-1} \frac{(e_1^2 - 1)^{1/2} \tan(1/2)(\beta - \beta_o)}{1 + e_1} + \frac{e_1(e_1^2 - 1)^{1/2} \sin \beta_o}{1 + e_1 \cos \beta_o}$$

$$\left. - 2 \tanh^{-1} \frac{(e_1^2 - 1)^{1/2} \tan(1/2)\beta_o}{1 + e_1} \right], \qquad e_1 > 1 \tag{A3b}$$

When a value of β_o is found such that the stipulated trip time is matched satisfactorily, the eccentricity and semimajor axis corresponding to this value can be used to obtain the heliocentric velocity at any point in the trajectory. Consistent with the approximate nature of the present analysis, the residual velocity V_{R_1} which the vehicle should have relative to the Earth at the point of transition from the geocentric hyperbolic orbit to the interplanetary heliocentric trajectory is calculated as the vector difference between the velocity in the latter at a point corresponding to the position of Earth at departure and the orbital velocity of Earth at that point. It is further assumed here that this residual velocity at the point of transition is equal to the geocentric hyperbolic excess velocity. The impulsive velocity

increment ΔV_1 required at launch from an orbit h_1 miles above the surface of Earth is then given by

$$\Delta V_1 = \left(\frac{2\mu_\oplus}{R_\oplus + h_1} + V_{R_1}^2\right)^{1/2} - \left(\frac{\mu_\oplus}{R_\oplus + h_1}\right)^{1/2} \tag{A4}$$

where $\mu_\oplus$ is the gravitational parameter $(GM_\oplus)$ and $R_\oplus$ is the equatorial radius of Earth. For thrust-to-weight ratios of interest here, the effects of gravity losses amount to a few percent of ΔV_1. On the other hand, if the orbital altitude h_1 from which the mission commences is considered to be 200 to 300 miles, and if calculations are made with $h_1 = 0$, the calculated values of ΔV_1 are a few percent too high. In the procedure adopted here, gravity losses are ignored and the orbital altitude is taken as zero. In this way, calculations are considerably simplified without introducing large errors in the mass ratios determined from ΔV_1. Accordingly, equation (A4) is normalized in terms of the velocity of escape from Earth $(2\mu_\oplus/R_\oplus)^{1/2}$, and rewritten as

$$\Delta \tilde{V}_1 = \left(1 + \tilde{V}_{R_1}^2\right)^{1/2} - \left(\frac{1}{2}\right)^{1/2} \tag{A5}$$

Mars Arrival

The second velocity increment calculated is that necessary to transfer the vehicle from the heliocentric trajectory (discussed in the preceding section) into an orbit about the planet. The rate of closure between the vehicle and Mars is calculated in a manner analogous to that used to find the velocity V_{R_1} in the case of Earth departure; that is, from the vector difference between the heliocentric velocity at a point corresponding to the position of Mars at arrival and the orbital velocity of Mars at that point. Likewise, the rate of closure is taken to be the velocity of approach V_{R_2} at infinity. This velocity is then increased by gravitational acceleration to a final velocity V_f of the vehicle at its nearest approach to Mars. The final velocity is given by

$$V_f = \left(\frac{2\mu_{\sigma}}{R_{\sigma} + h_2} + V_{R_2}^2\right)^{1/2}$$

where h_2 is the altitude above the surface of Mars at nearest approach. The velocity increment ΔV_2 required to obtain an orbit about Mars depends not only upon the velocity of approach V_{R_2} and the altitude h_2, but also upon the eccentricity e_f of the orbit established. From the equation for ΔV_2,

$$\Delta V_2 = V_f - \left[\frac{\mu_{\sigma}(1 + e_f)}{R_{\sigma} + h_2}\right]^{1/2}$$

it is apparent that a highly eccentric orbit would be advantageous in minimizing ΔV_2 requirements. In terms of the total mission, however, the advantages noted for elliptical orbits over a circular orbit would be offset to

some degree by the increase in the mass of propellants required for an excursion vehicle to achieve rendezvous with a parent craft in the higher energy orbits. In the present preliminary study, attention is restricted to circular parking orbits upon arrival at Mars in the rendezvous mode with propulsion braking. Likewise, calculations for both V_f and ΔV_2 are made with h_2 taken as zero. The equation used for $\Delta\tilde{V}_2$ is thus

$$\Delta\tilde{V}_2 = (p^2 + \tilde{V}_{R_2}^2)^{1/2} - \left(\frac{p^2}{2}\right)^{1/2} \tag{A6}$$

where p is the ratio of the velocity of escape for Mars to that for the Earth.

In the rendezvous mode with atmospheric braking at Mars, and in the direct mode, the velocity of entry into the martian atmosphere can be obtained from the simplified expression for $\tilde{V}_f$, or,

$$\tilde{V}_{E_{\sigma'}} = (p^2 + \tilde{V}_{R_2}^2)^{1/2} \tag{A7}$$

Mars Departure

The third velocity increment calculated is that used at departure from Mars. The procedure for finding the orbital elements of the return heliocentric trajectory is essentially the same as that described earlier for the Earth to Mars trip. If the rendezvous mode is assumed (launch from martian orbit), gravity losses are disregarded and the orbital altitude is considered to be zero, as before. For the direct mode, however, both gravity and drag losses should be considered. In this mode it is assumed that the entire vehicle (less any mass unloaded at the surface of Mars) would first be launched into a parking or coasting orbit. For establishing a circular parking orbit at an altitude of about 300 miles, drag and gravity losses equivalent to about 2500 fps appear to be appropriate and this value is arbitrarily assigned here to represent these losses. The velocity increment ΔV_3 required to depart the orbit for the return trip is calculated from

$$\Delta V_3 = \left(\frac{2\mu_{\sigma'}}{R_{\sigma'}} + V_{R_3}^2\right)^{1/2} - \left(\frac{\mu_{\sigma'}}{R_{\sigma'}}\right)^{1/2}$$

Here V_{R_3} is analogous to V_{R_1} used to calculate the velocity increment for injection into the Earth to Mars heliocentric trajectory. The third major velocity increment is then either

$$\Delta\tilde{V}_3 = (p^2 + \tilde{V}_{R_3}^2)^{1/2} - \left(\frac{p^2}{2}\right)^{1/2} \tag{A8a}$$

for the rendezvous mode, or

$$\Delta\tilde{V}_3' = (p^2 + \tilde{V}_{R_3}^2)^{1/2} + \Delta\tilde{V}_{losses} \tag{A8b}$$

for the direct mission mode.

Earth Return

The last phase of the mission is considered here to be a capsule making a direct entry into the Earth's atmosphere and descending to Earth chiefly by atmospheric braking. Calculations for the velocity of entry into the terrestrial atmosphere $V_{E_\oplus}$ are simplified in the same manner as that used to find V_{E_σ} in a previous section. The equation used is

$$\tilde{V}_{E_\oplus} = (1 + \tilde{V}_{R_4}^2)^{1/2} \tag{A9}$$

where V_{R_4} is the rate of closure between the returning vehicle and Earth. If propulsion braking is contemplated for reducing entry velocities, the velocity increment is found by taking the difference between the velocity given by equation (A9) and the stipulated entry velocity.

The procedures outlined in the foregoing have been programmed for a high-speed digital computer. Data were obtained for individual transit times T_1 and T_2 from 60 to 360 days for a range of dates of arrival at Mars for each opposition between the years 1971 and 1988.

A second program was also constructed to investigate the conditions required to minimize the sum of the various major velocity requirements in any given mission. This program finds the least value of the sum for a given total transit time, stay time, and date of arrival at Mars. These values are then plotted as a function of the date of arrival at Mars to find the minimum of the least total velocity increments for the given total transit time and stay time.

Mass Ratios

In the following paragraphs, a description is given of the procedure used to evaluate parametrically the ratio of the mass of the gross payload to the initial mass in orbit about Earth.

In this preliminary study, only four main stages of major velocity increments are considered. The basic equation from which the analysis begins is simply

$$M_1 = M_L + \sum M_{p_i}(1 + \sigma_i) \tag{A10}$$

where M_1 is the initial mass in orbit, M_L is the mass of the gross payload, M_{p_i} is the mass of propellants used in the ith stage, and σ_i is the ratio of the mass of inerts to the mass of propellants for that stage. As indicated by equation (A10), the gross payload is defined here as the initial mass M_1 exclusive of the masses associated with providing the major propulsive requirements of the mission.

To develop an expression for the ratio of M_L to M_1 in terms of velocity requirements and of other parameters, the following relationships and definitions are helpful. First, the well-known rocket formula

$$\frac{M_{p_i}}{M_i} = 1 - e^{-\Delta V_i/c_i}$$

is used to relate propellant-mass requirements to velocity increments ΔV_i at any major stage. For convenience, two ratios are defined, in general, as

$$R_i = (1 + \sigma_i)e^{-\Delta V_i/c_i} - \sigma_i$$

and

$$\bar{M}_i = \frac{M_i}{M_1}$$

If a series of terms k_j ($\Sigma k_j < 1$) is used to represent the fractions of the payload mass M_L unloaded during the mission, the masses of the spacecraft at various points in the mission can be given as follows.

(a) After launch from Earth orbit and about to enter orbit about Mars or to descend directly to the martian surface:

$$M_2 = M_1 - M_{p_1}(1 + \sigma_1) - k_1 M_L$$

$$\bar{M}_2 = R_1 - k_1 \bar{M}_L \qquad \text{(A11a)}$$

where k_1 is the fraction of M_L separated prior to injection from the heliocentric transfer trajectory into an orbit about Mars or before entry into the martian atmosphere. In one type of rendezvous mode, $k_1 M_L$ might be the Mars excursion vehicle which would proceed to a direct descent to the surface by means of atmospheric braking. Accumulated waste products might also be included here.

(b) When the vehicle is ready to depart for Earth:

$$\frac{M_3}{M_2} = R_2 - k_2 \frac{M_1}{M_2} \bar{M}_L \qquad \text{(A11b)}$$

$$\bar{M}_3 = R_1R_2 - (k_1R_2 + k_2)\bar{M}_L \tag{A11c}$$

where k_2 is the fraction of M_L unloaded at Mars, either in a parking orbit or on the surface. In the rendezvous mode, k_2M_L might include the excursion vehicle and wastes accumulated during the martian stay, less the mass of any scientific samples removed from the planet to be transported to Earth. In the direct mode, k_2M_L would include such items as the mass of the heat shield, parachutes, retropropulsion, landing gear, launching gear, and wastes, less mass of samples.

(c) After launch from the martian orbit or surface and after the mission module is discarded preparatory to direct descent to surface of Earth:

$$\frac{M_4}{M_3} = R_3 - k_3\frac{\bar{M}_L}{\bar{M}_3} \tag{A11d}$$

$$\bar{M}_4 = R_1R_2R_3 - [R_3(k_1R_2 + k_2) + k_3]\bar{M}_L \tag{A11e}$$

where k_3 is the fraction of the gross payload unloaded during the return trip prior to entry into the terrestrial atmosphere. Here k_3M_L would be the mission module containing the life-support equipment, excess food, water, and oxygen; some auxiliary power units; and other items not required in the direct descent to the surface of Earth by an atmosphere-entry capsule.

(d) Entry into terrestrial atmosphere following propulsion deceleration and separation of retrorocket:

$$\frac{M_5}{M_4} = R_4 \tag{A11f}$$

$$\bar{M}_5 = R_1R_2R_3R_4 - R_4[R_3(k_1R_2 + k_2) + k_3]\bar{M}_L \tag{A11g}$$

With the use of the relationships of equations (A11) in equation (A10), the expression for the ratio of the mass of the gross payload to the initial mass in orbit about the Earth $\bar{M}_L$ is obtained as

$$\bar{M}_L = \frac{R_1R_2R_3R_4}{1 - k_1(1 - R_2R_3R_4) - k_2(1 - R_3R_4) - k_3(1 - R_4)} \tag{A12}$$

The general equation for computing $\bar{M}_L$ for any number of velocity stages with unloading of mass between velocity increments has the form

$$\bar{M}_L = \frac{\prod_1^n (R_i)}{1 - \sum_{j=1}^{n-1} k_j\left[1 - \prod_{j+1}^{n} (R_i)\right]} \tag{A13}$$

where n is the number of velocity stages and j is an integer between 1 and $(n - 1)$. Any of the k_j can be set to zero. Likewise, setting any velocity increment equal to zero reduces the corresponding factor R to unity.

A computer program was devised to solve equation (A12) to find maximum values of $\bar{M}_L$ for a prescribed set of propulsion parameters, and for given values of total transit time T, stay time T_S, unloaded fraction k_j, and date of arrival at Mars. These maximum values are then plotted as a function of the date of arrival to determine the greatest value of the individual maximums. The value of the inert fraction σ of any stage is generally considered to be a constant when propulsion by chemical rocket engines is assumed. In the case of nuclear propulsion, the σ's are calculated as functions of the velocity increments. Reference 5 includes an equation for the structural factor γ for rocket engines in terms of the stage weight. The equation is of the form

$$\gamma = \frac{1 + a(1 - e^{-\Delta V/c})}{1 + b(1 - e^{-\Delta V/c})}$$

where a and b are ratios of various sums of weight ratios of component parts of the rocket system. In terms of the parameter σ based on the weight of propellants as used here, the equation becomes

$$\sigma_i = \frac{1 + a(1 - e^{-\Delta V_i/c_i})}{(b - a)(1 - e^{-\Delta V_i/c_i})} \tag{A14}$$

The program provides for substaging any or all of the main velocity stages. Optimum staging techniques are assumed so that the propulsive factor R_{i_n} for n stages is calculated from

$$R_{i_n} = \left[(1 + \sigma_i)e^{-\Delta V_i/nc_i} - \sigma_i\right]^n \tag{A15}$$

In general, substaging is used in the present study only when major velocity increments are so large that negative R-values can be anticipated.

APPENDIX B

NOTATION

a	semimajor axis of conic orbits, a.u.
c_i	effective velocity of efflux from rocket engines of ith velocity stage, fps
e	eccentricity of conic orbit
G	universal gravitational constant
h_1, h_2	altitude of circular orbit above surface of Earth and Mars, respectively
k_j	fraction of gross payload unloaded after ith velocity increment
l	celestial latitude
M	mass
M_i	mass at ith velocity stage of mission
M_L	mass of gross payload, or initial mass less mass required for propulsion
M_1	initial mass in Earth orbit just prior to departure for Mars
p	ratio of surface escape velocity of Mars to that of Earth
r	heliocentric distance
r_p	perihelion distance
R	equatorial radius of planet
R_i	ith propulsive factor, $(1 + \sigma_i)e^{-\Delta V_i/c_i} - \sigma_i$
T	total transit time of mission
T_1	trip time, Earth to Mars
T_2	trip time, Mars to Earth
T_S	stay time at Mars
V_E	atmosphere-entry velocity

V_R	velocity of mission vehicle relative to planet at point of transition from planetocentric hyperbolic orbit to heliocentric transfer trajectory or vice versa
β	difference between celestial longitude of Mars at arrival and that of Earth at departure
β_o	perihelion constant of heliocentric trajectory from Earth to Mars
ΔV_i	required velocity increment at ith velocity stage of mission
ΔV_p	velocity increment required for plane change
μ	gravitational parameter, GM
σ_i	inert fraction, or ratio of mass of inerts to mass of propellants for the ith velocity stage

Subscripts

A	arrival
D	departure
f	final conditions at Mars
1	conditions or requirements at start of mission
2	conditions or requirements at arrival at Mars
3	conditions or requirements at departure from Mars
4	conditions or requirements at return to Earth before entry
5	conditons following entry into terrestrial atmosphere
$\oplus$, $\sigma^{\prime}$	Earth and Mars, respectively

Supercripts

—	normalized to initial mass in Earth orbit
~	normalized to surface escape velocity of Earth

REFERENCES

1. General Dynamics/Astronautics: A Study of Early Manned Interplanetary Missions - Final Summary Report AOK 63-0001, Jan. 31, 1963.

2. Lockheed Missiles and Space Company: Manned Interplanetary Mission Study. Summary Report 8-32-63-1, vol. 1, March 1963.

3. Space Technology Laboratories, Inc.: Manned Mars Landing and Return Mission Study. Final Report, vol. II, 28, March 1964.

4. Knip, Gerald, Jr., and Zola, Charles L.: Three-Dimensional Trajectory Analysis for Round-Trip Missions to Mars. NASA TN D-1316, 1962.

5. Fimple, W. R.: Optimum Midcourse Plane Changes for Ballistic Interplanetary Trajectories. AIAA Jour., vol. 1, no. 2, Feb. 1963, pp. 430-4.

6. Wang, C. J.: Nuclear Propulsion for Orbit-Based Spacecraft. Transactions of the Seventh Symposium on Ballistic Missile and Space Technology held at the USAF Academy, Colorado, Aug. 13-16, 1962, vol. 1, pp. 365-85.

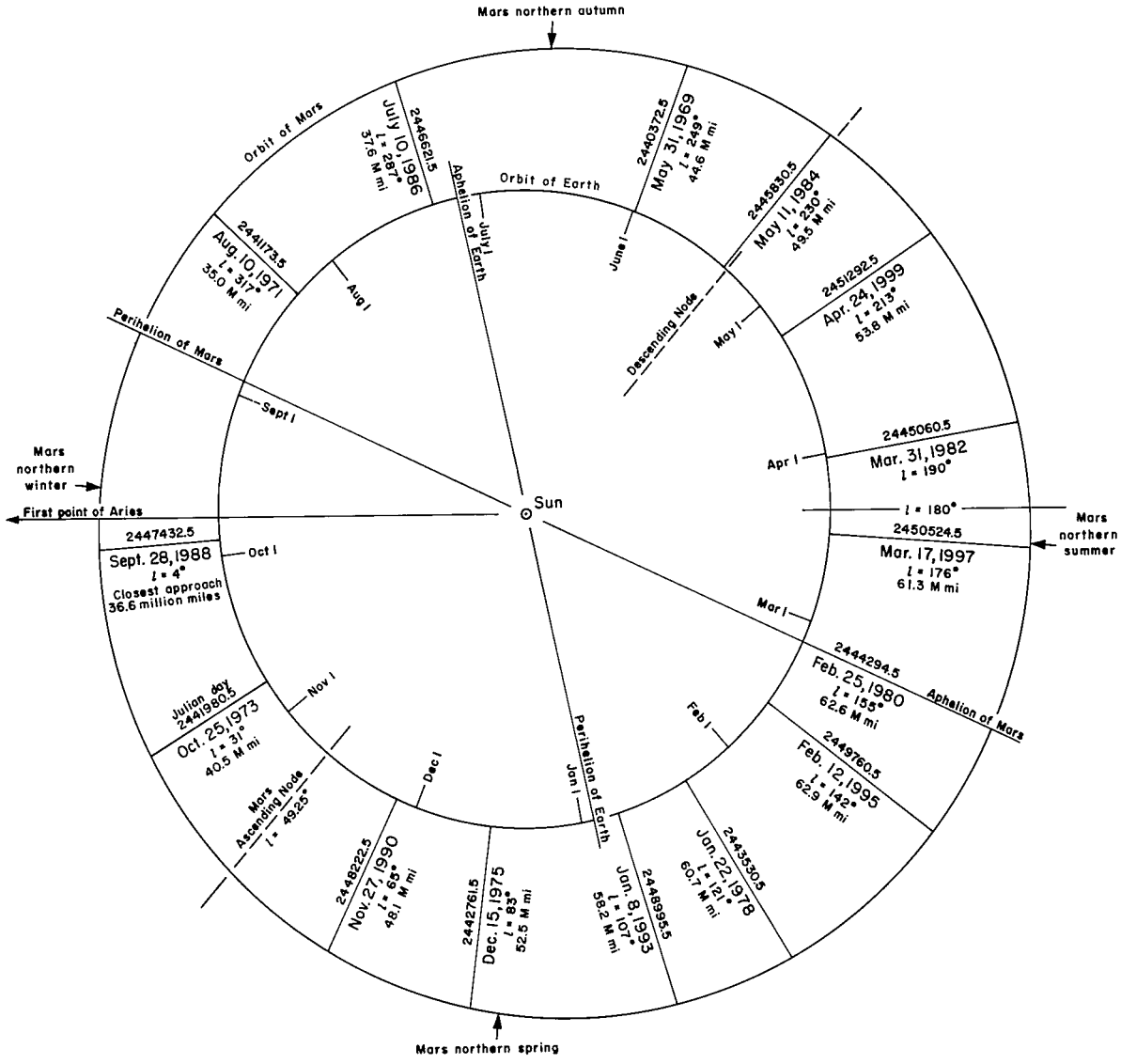

OPPOSITIONS OF MARS 1970 to 2000

Figure 1.- Orbital data for Mars and Earth, including oppositions of Mars from 1970 to 2000 AD.

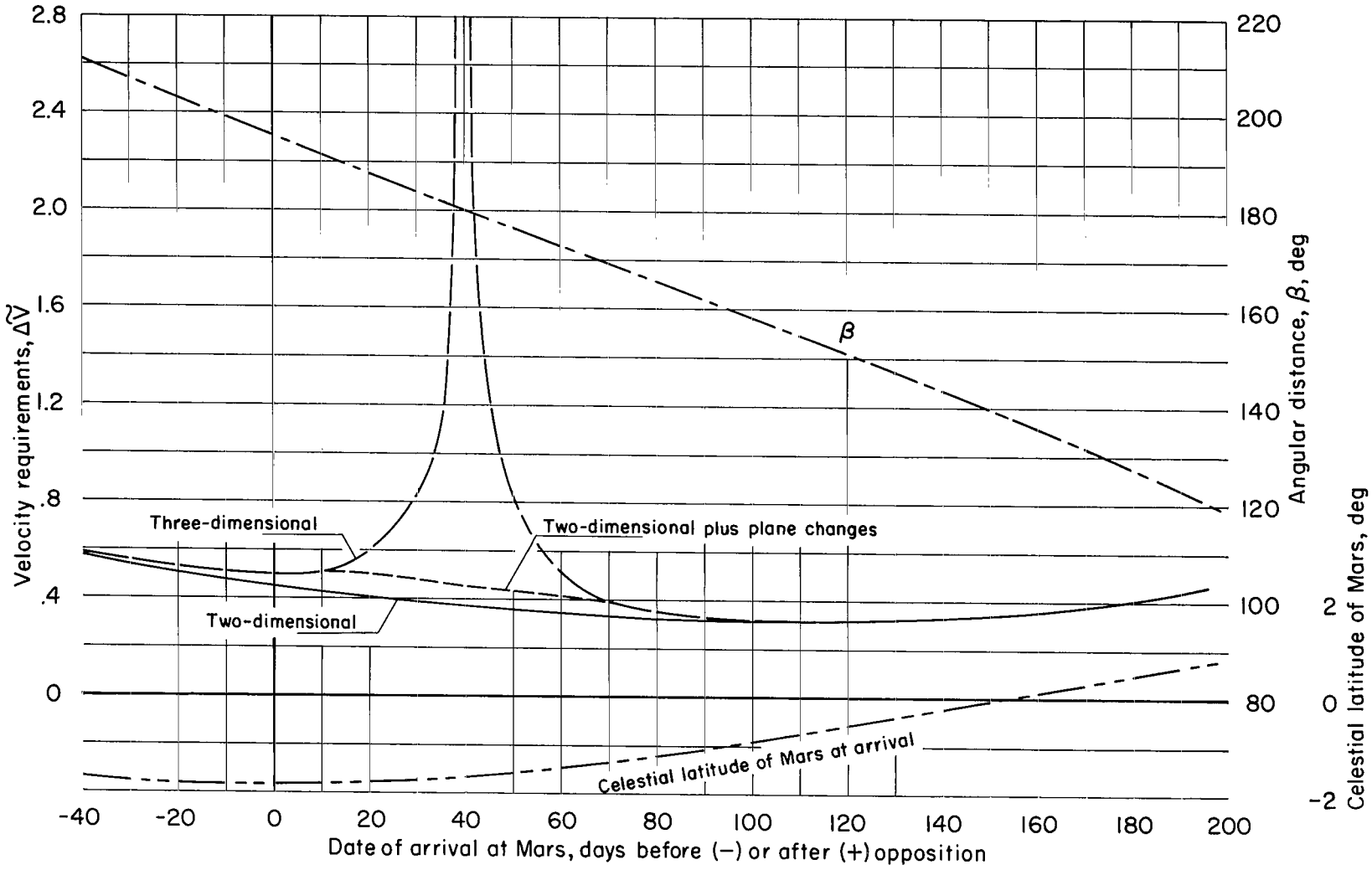

Figure 2.- Comparison of results of various methods of calculating velocity requirements for a 200-day trip from Earth to Mars; 1971.

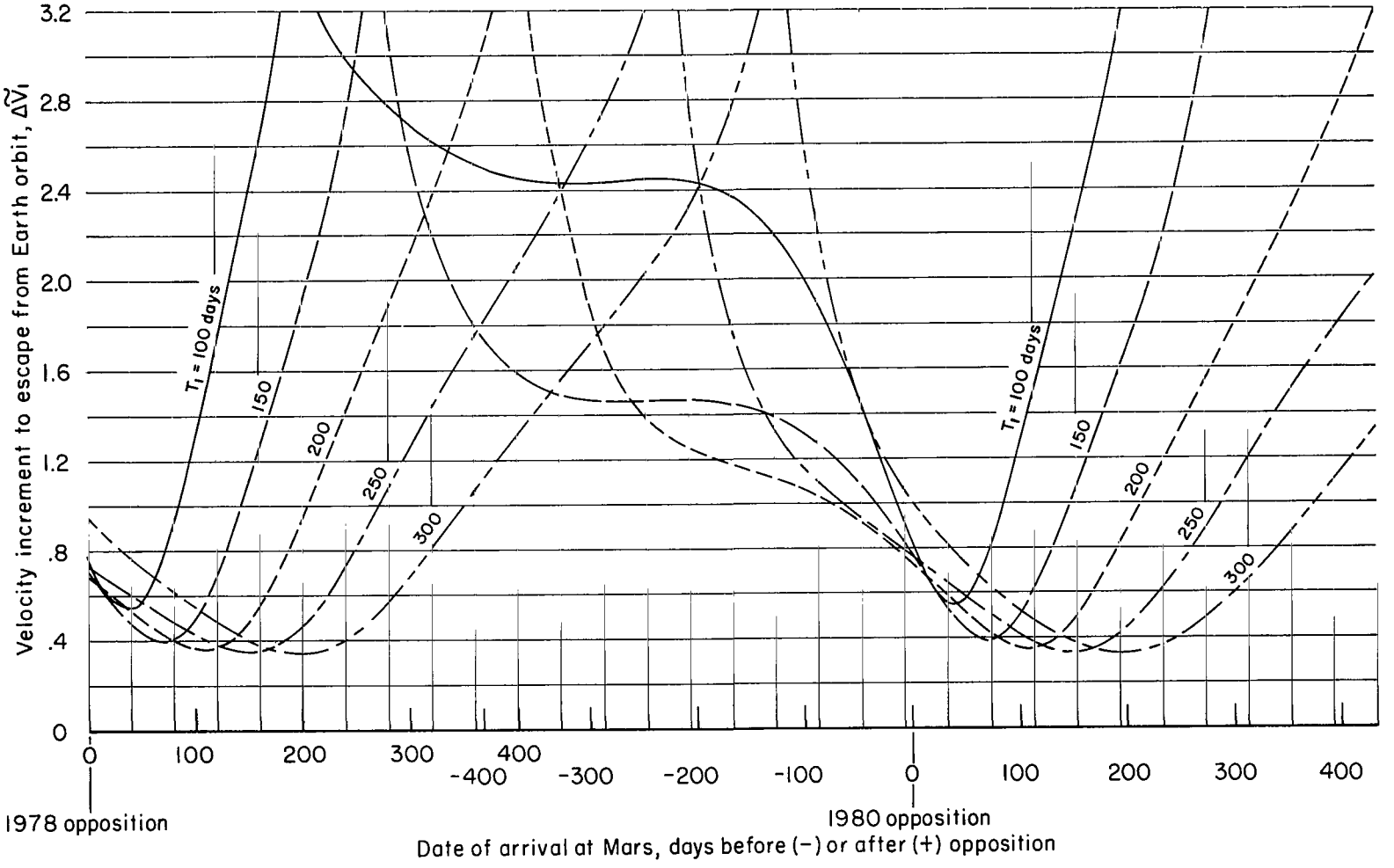

(a) Velocity increments required to depart orbit about Earth.

Figure 3.- Variation of velocities in Mars manned landing and return missions with date of arrival at Mars; 1978 to 1981.

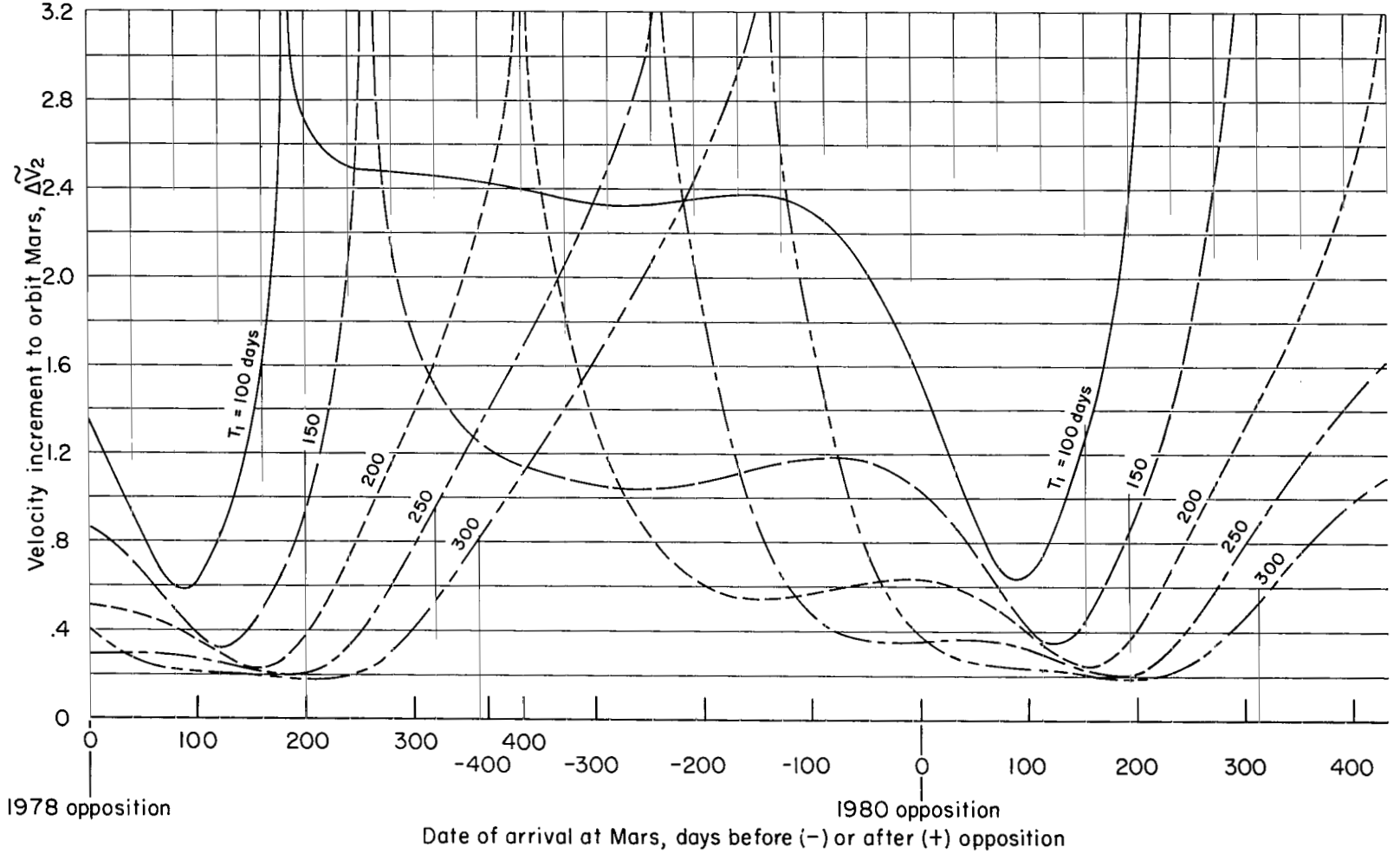

(b) Velocity increments required to acquire orbit about Mars.

Figure 3.- Continued.

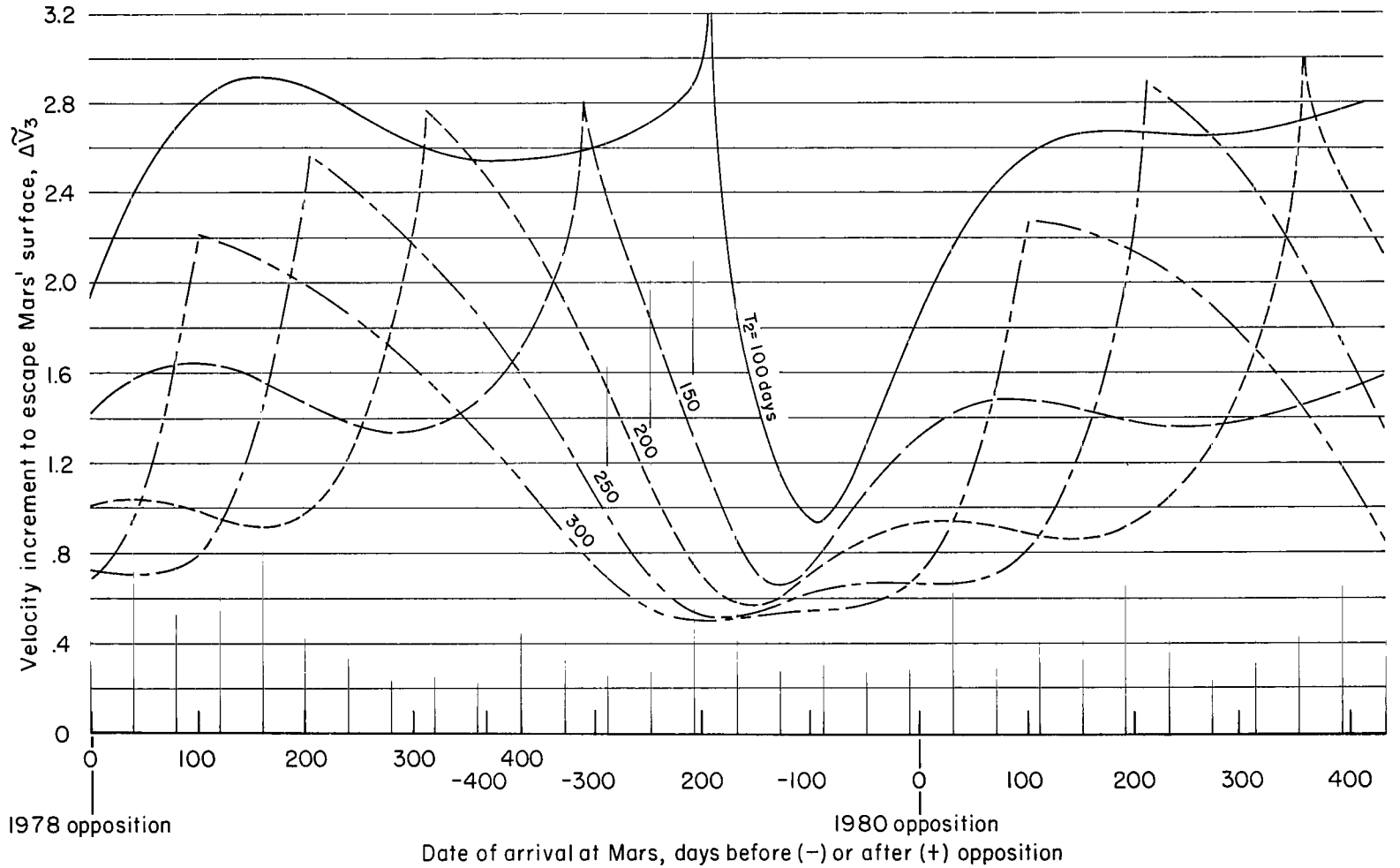

(c) Velocity increments required to launch from surface of Mars after 7-day stay. (No gravity or drag losses included.)

Figure 3.- Continued.

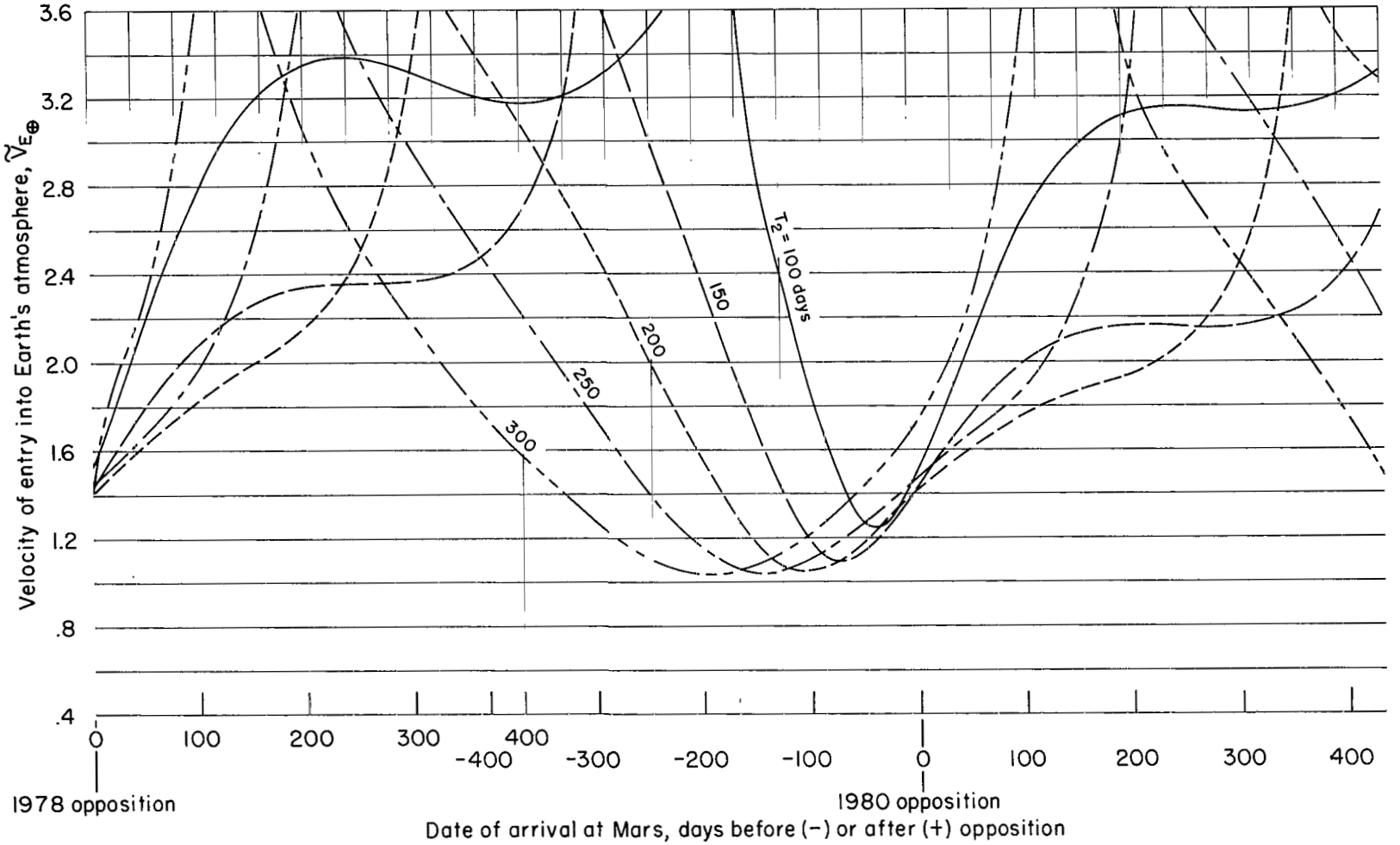

(d) Velocity of entry into atmosphere of Earth; 7-day stay at Mars.

Figure 3.- Concluded.

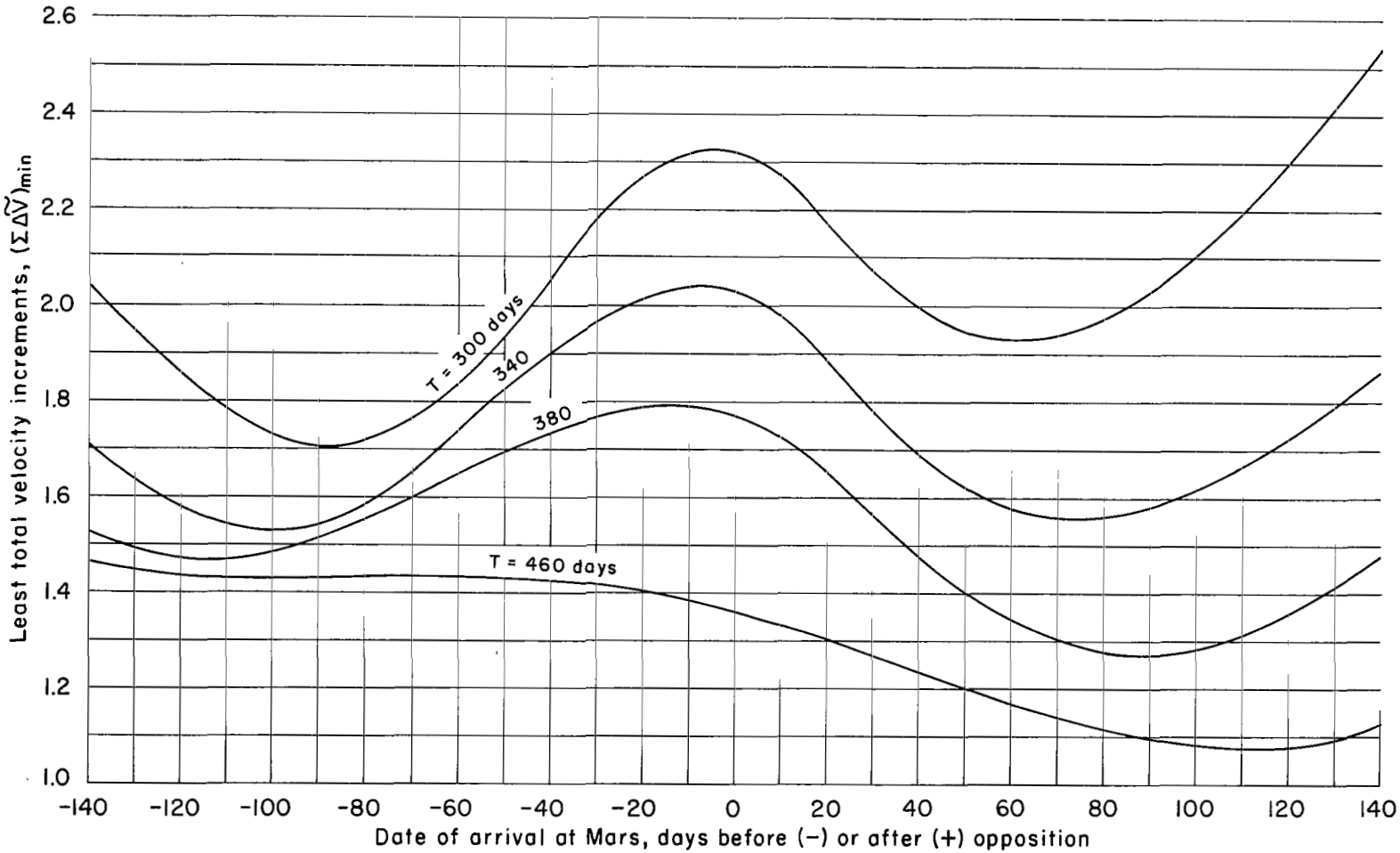

(a) Total velocity requirements.

Figure 4.- Effects of date of arrival at Mars on mission characteristics (rendezvous mode with propulsion braking at Mars; 1975; 7-day stay).

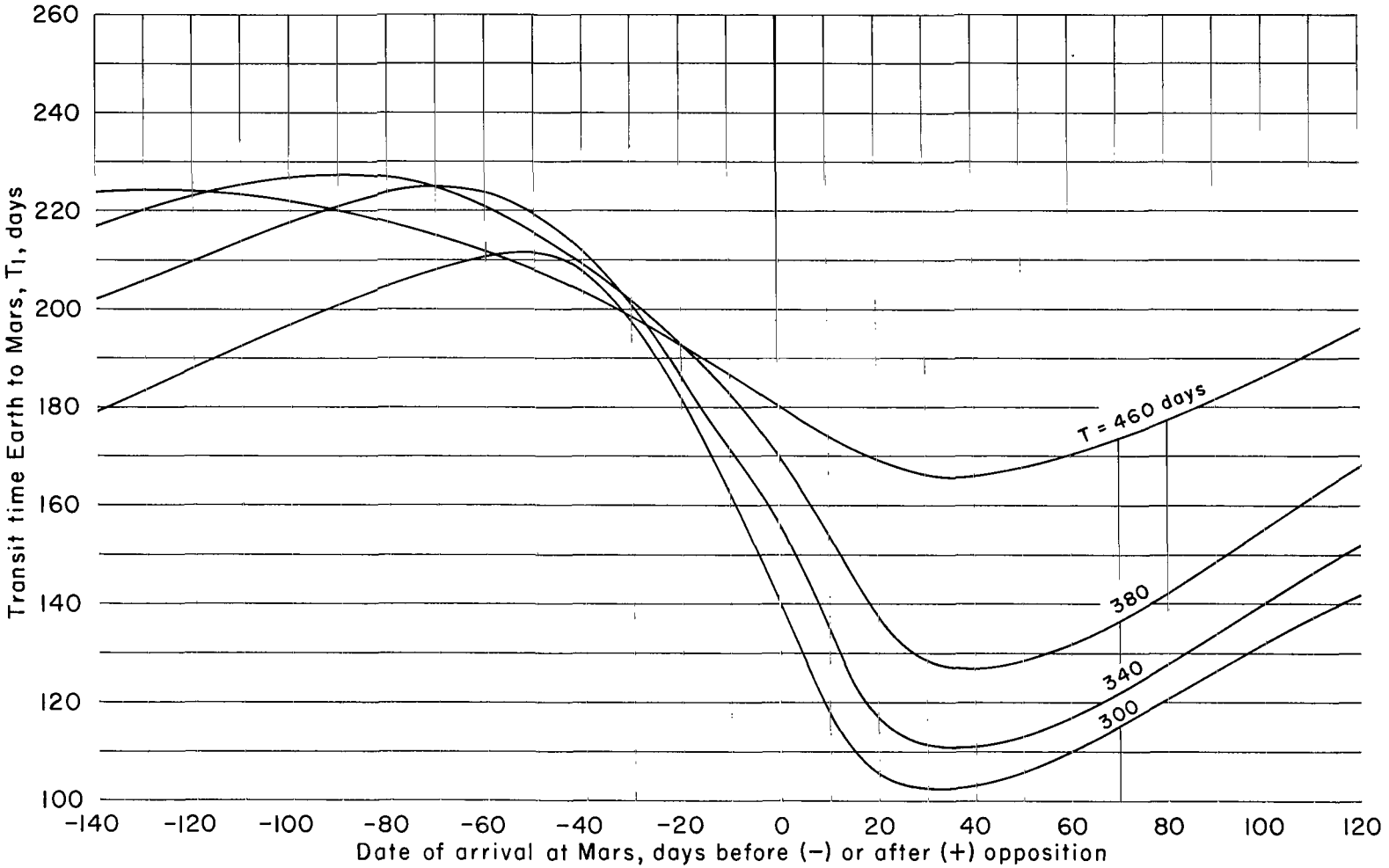

(b) Transit time from Earth to Mars.

Figure 4.- Concluded.

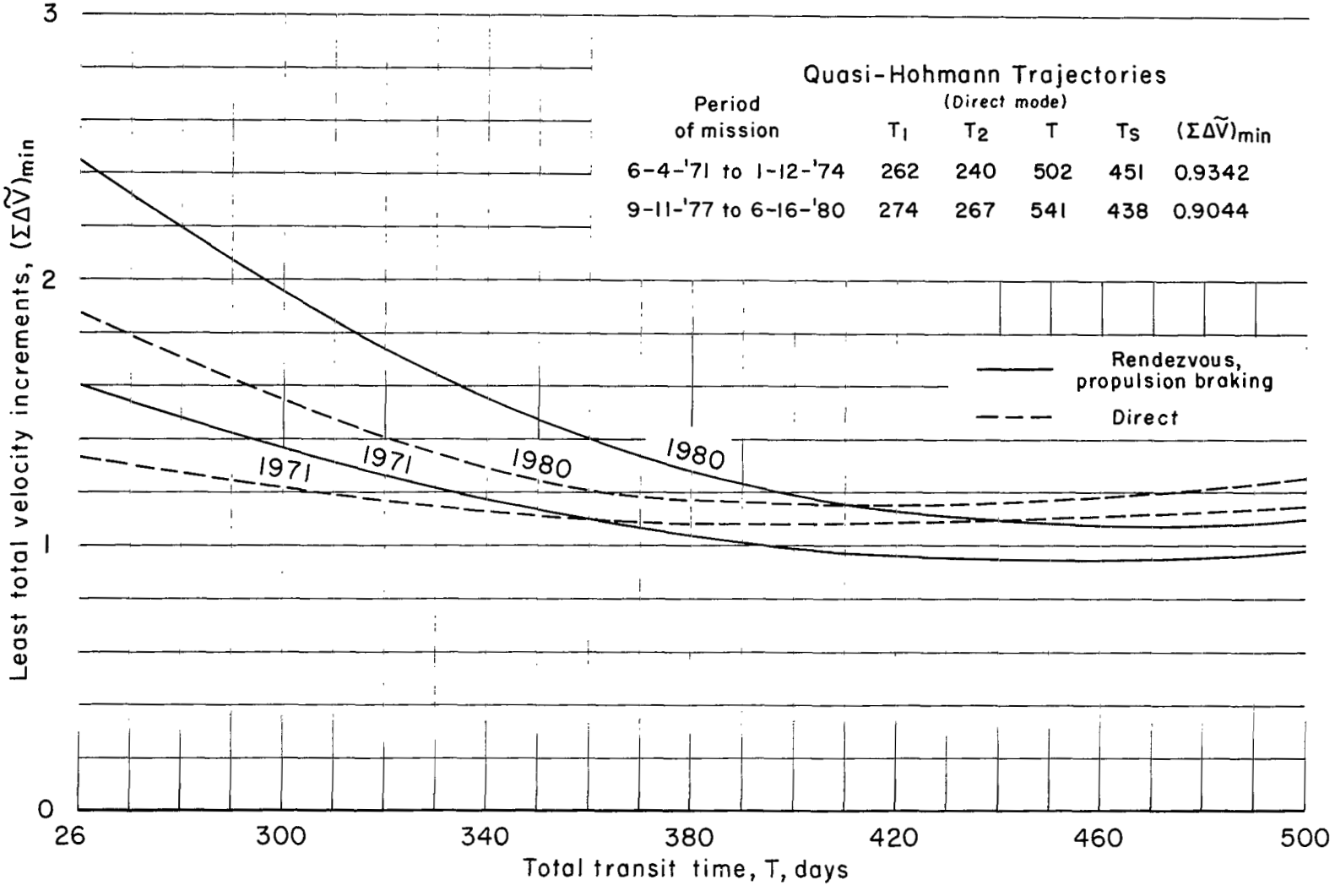

Figure 5.- Variation of least total velocity requirements with total transit time; 7-day stay.

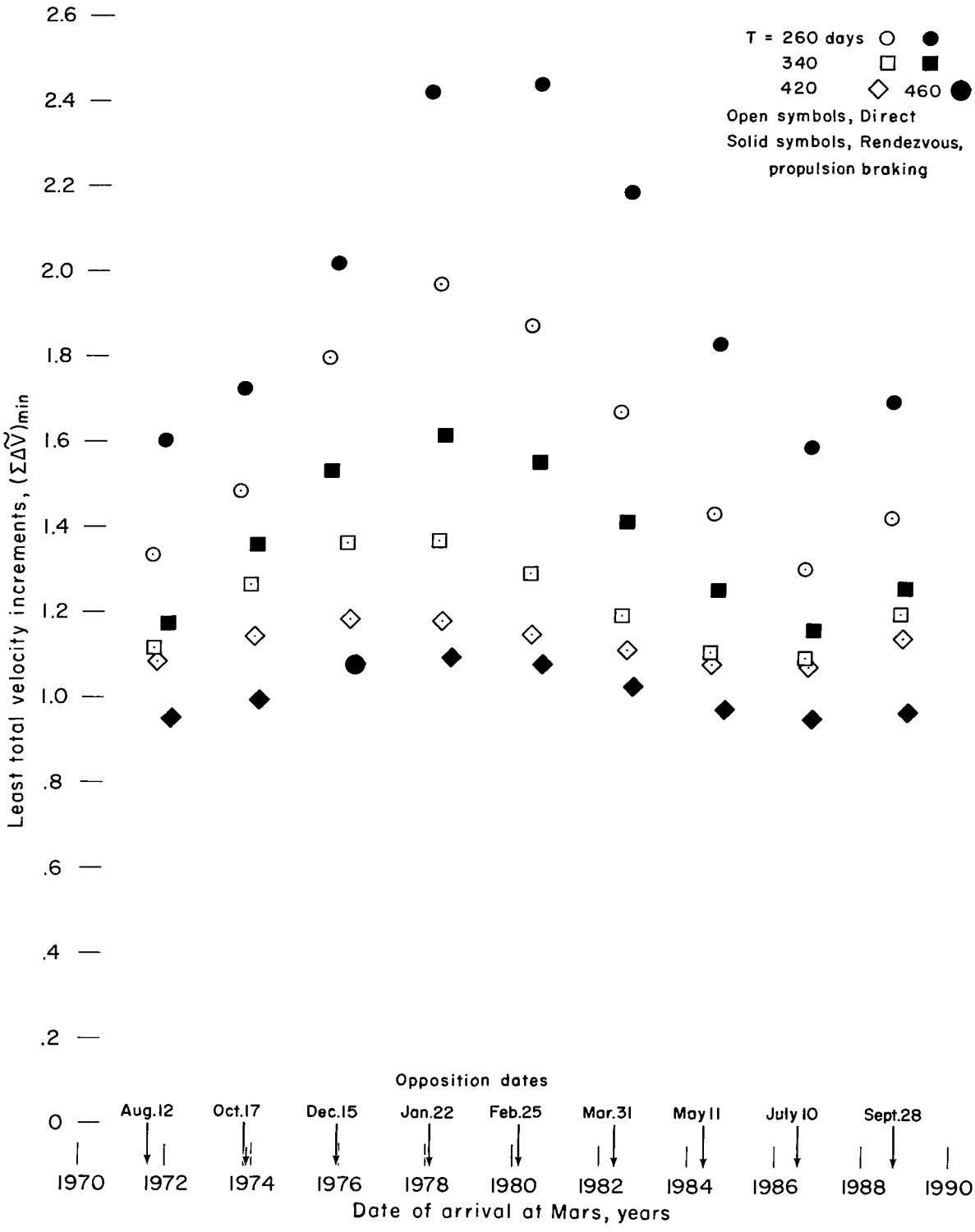

Figure 6.- Variation of minimum total velocity requirements with total transit time and with date of arrival at Mars from 1970 to 1990. No propulsion braking at Earth.

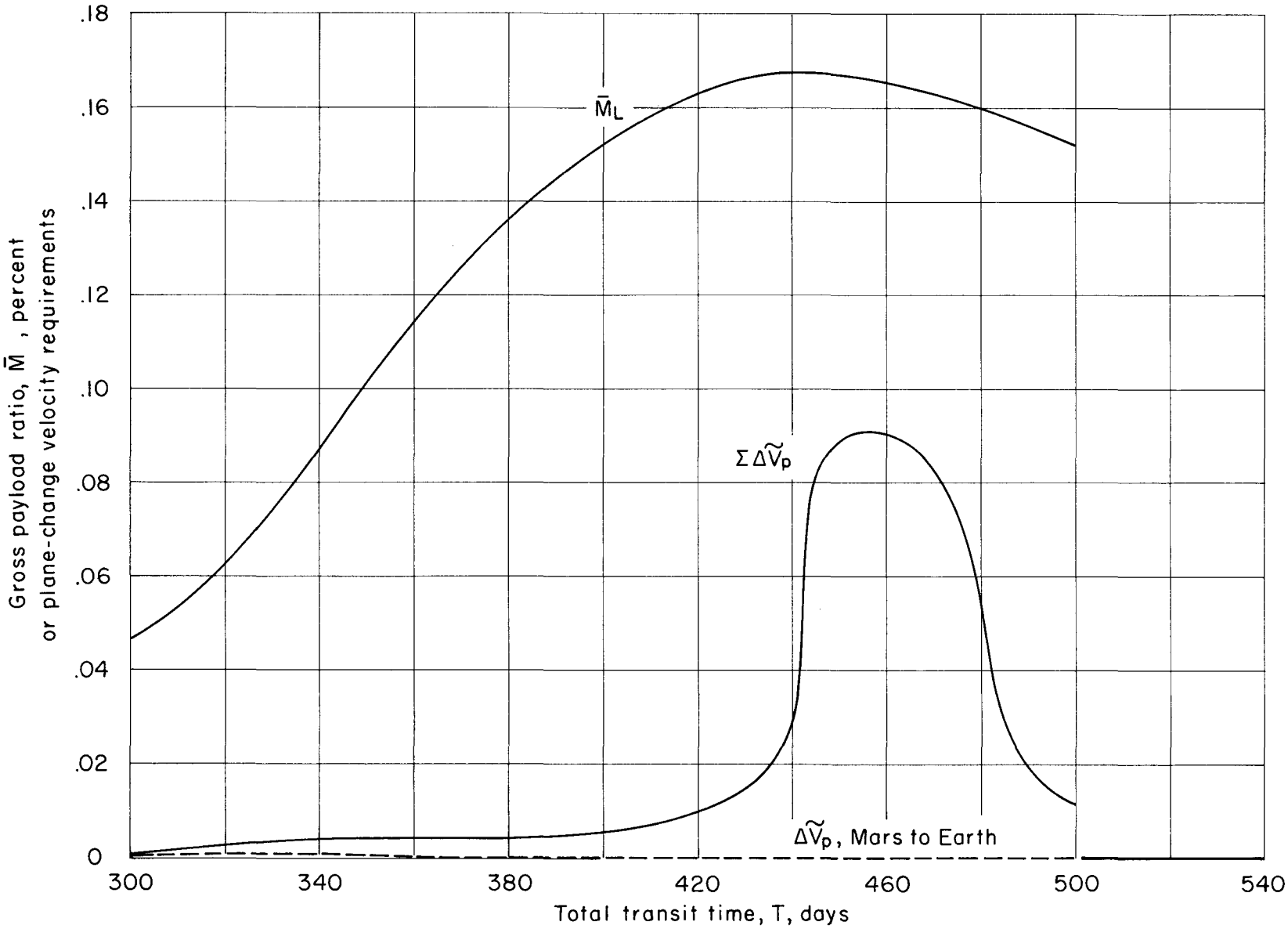

Figure 7.- Example of plane-change velocity requirements; rendezvous mode with propulsion braking at Mars; 1975-1976; $k_2 = 0.4$; 47-day stay.

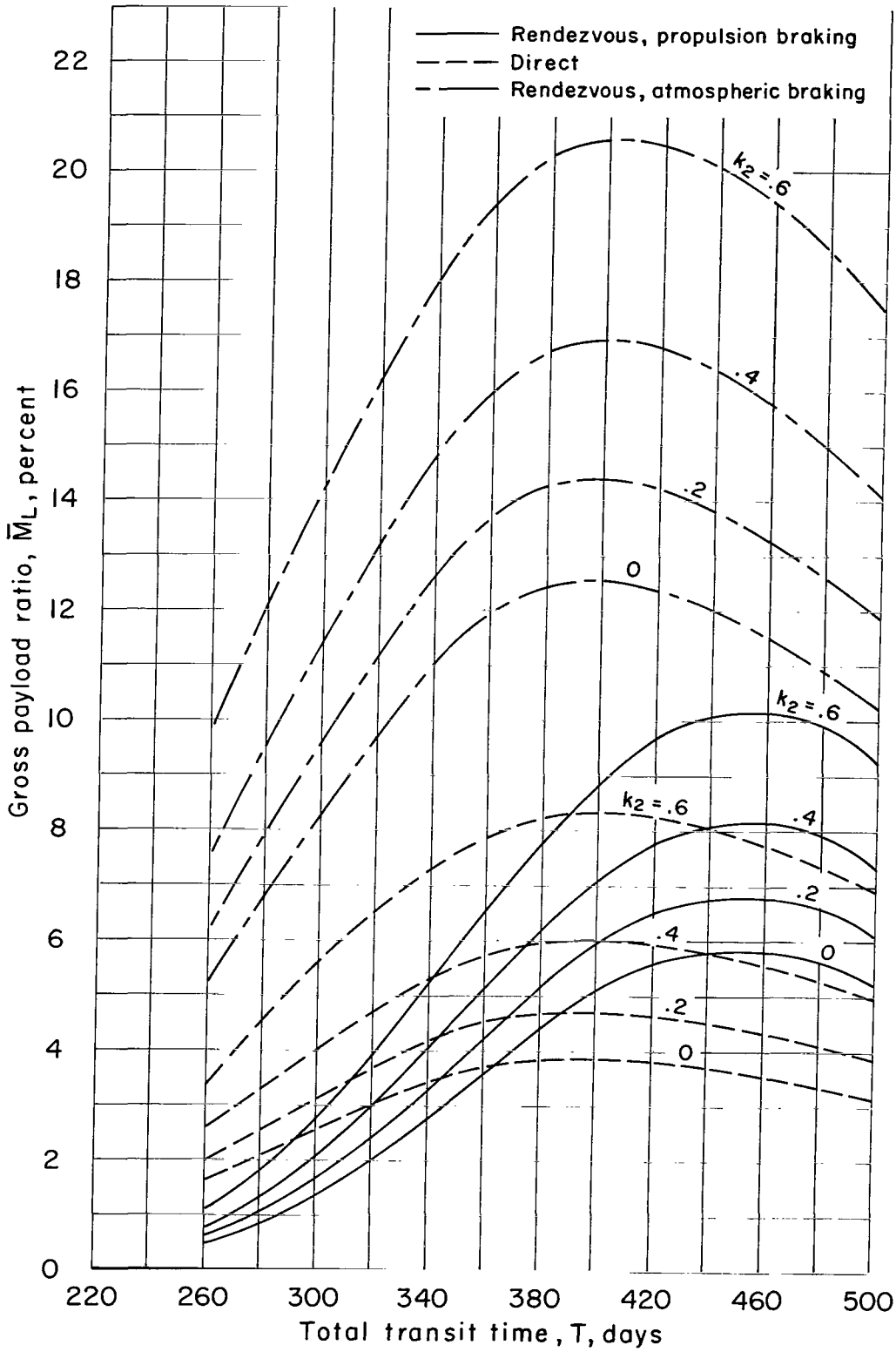

Figure 8.- Effect of mission mode on gross-payload fraction; 1971; 7-day stay.

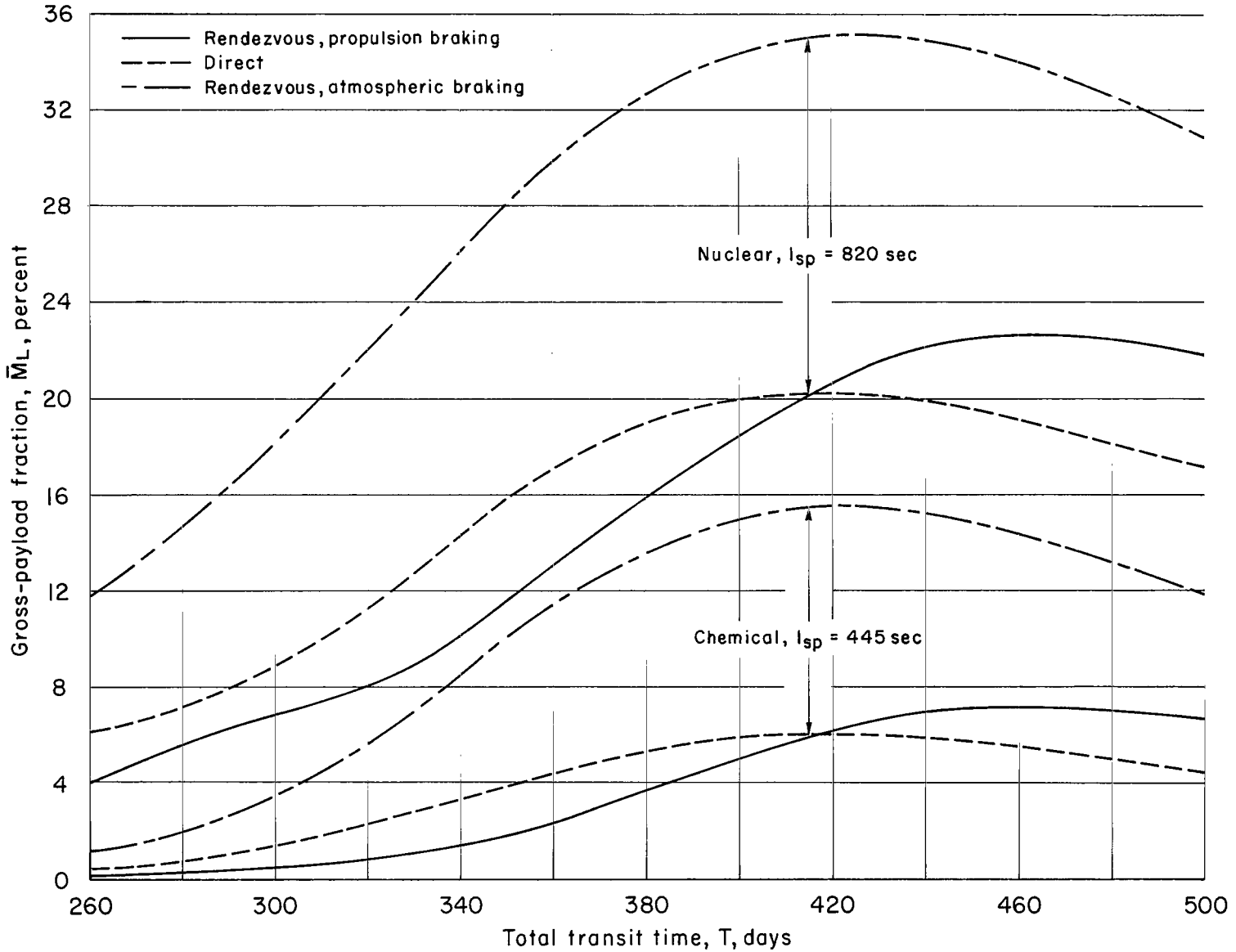

Figure 9.- Effect of propulsion system specific impulse on gross-payload fraction; 1975; 7-day stay; $k_2 = 0.6$.

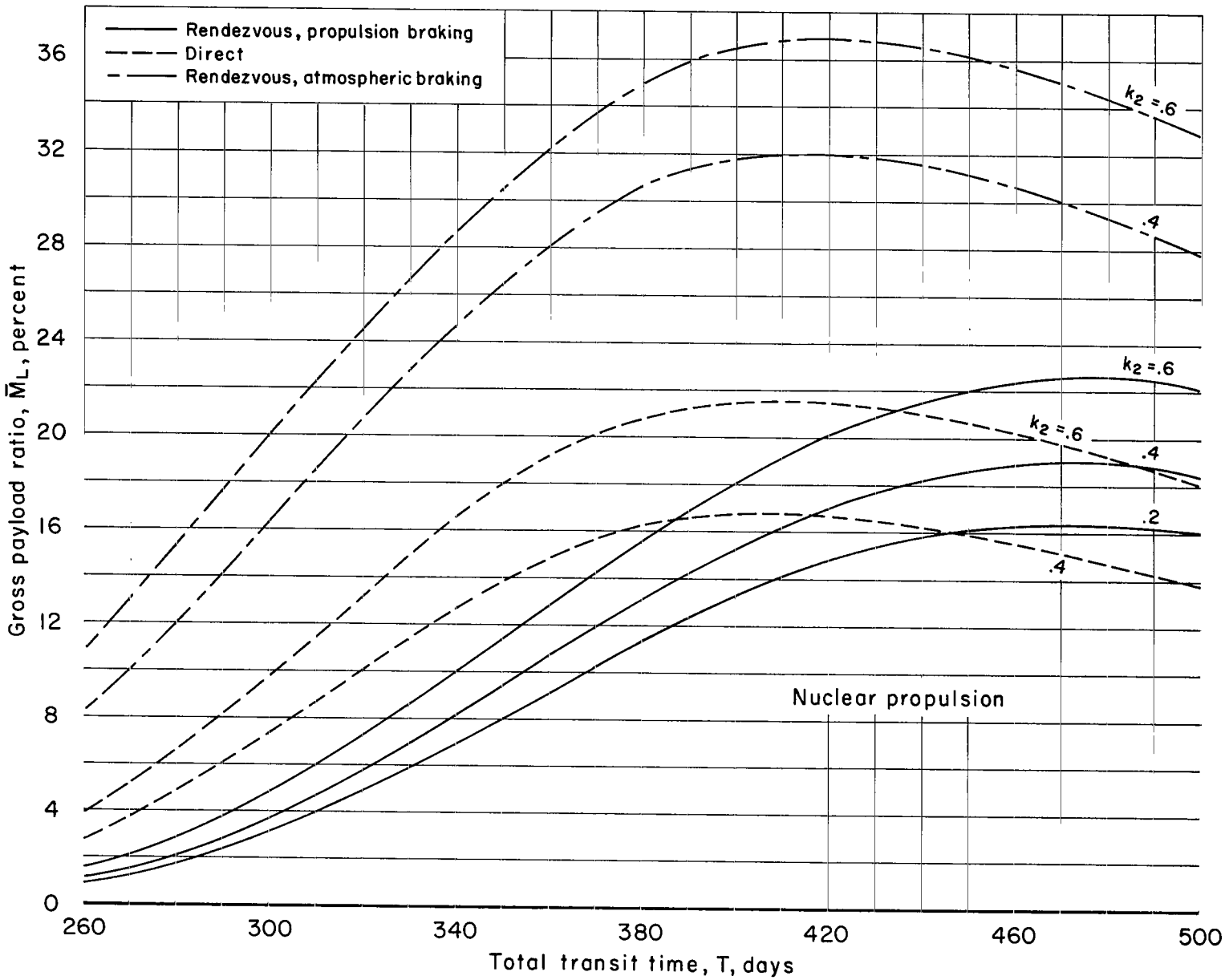

Figure 10.- Comparison of gross-payload fractions obtained by three methods; 1980; 7-day stay.

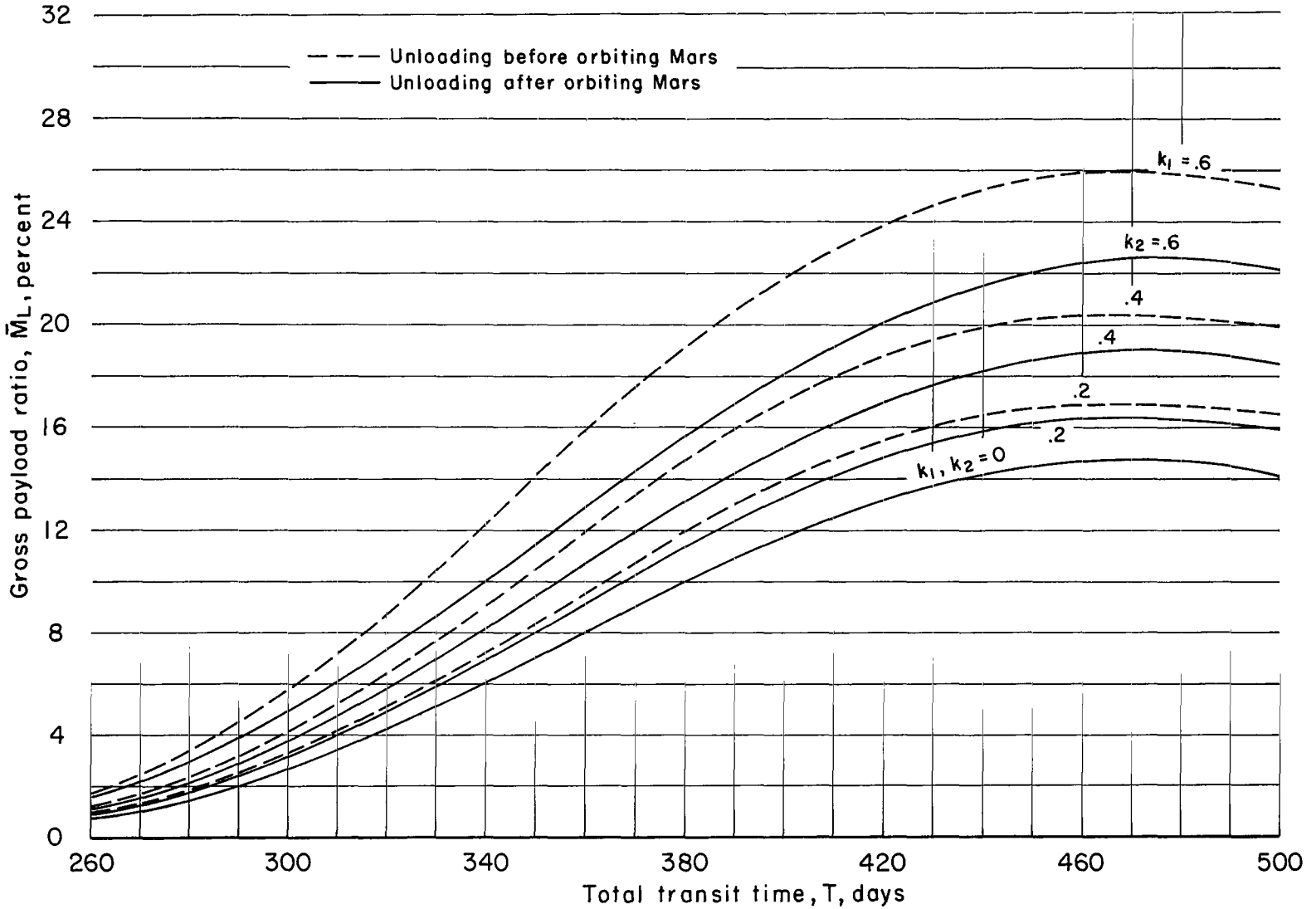

Figure 11.- Effect of unloading before orbiting Mars in rendezvous mode with propulsion braking at Mars; nuclear propulsion; 1980; 7-day stay.

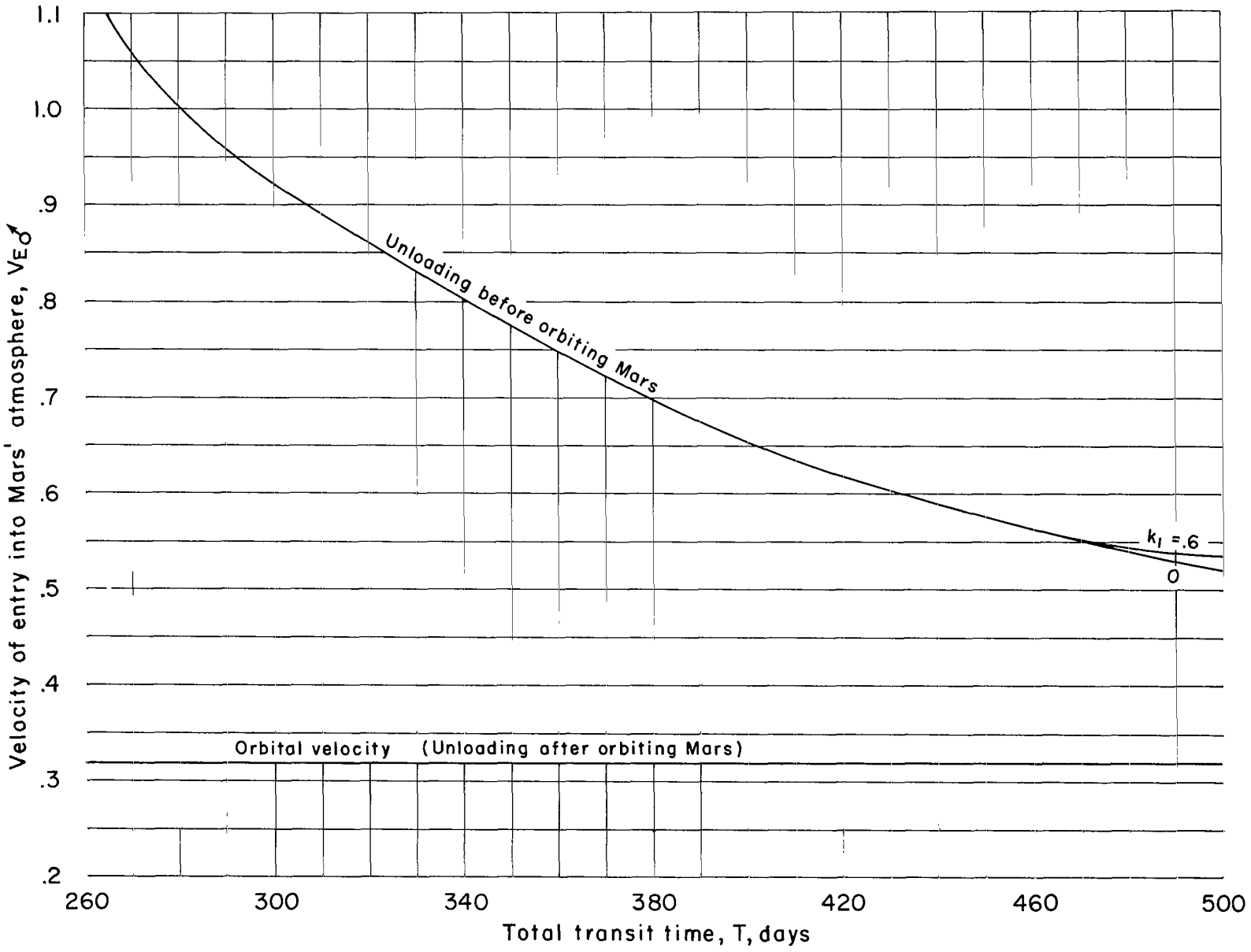

Figure 12.- Effect of unloading before orbiting Mars on velocity of entry of excursion vehicle into martian atmosphere; 1980; 7-day stay.

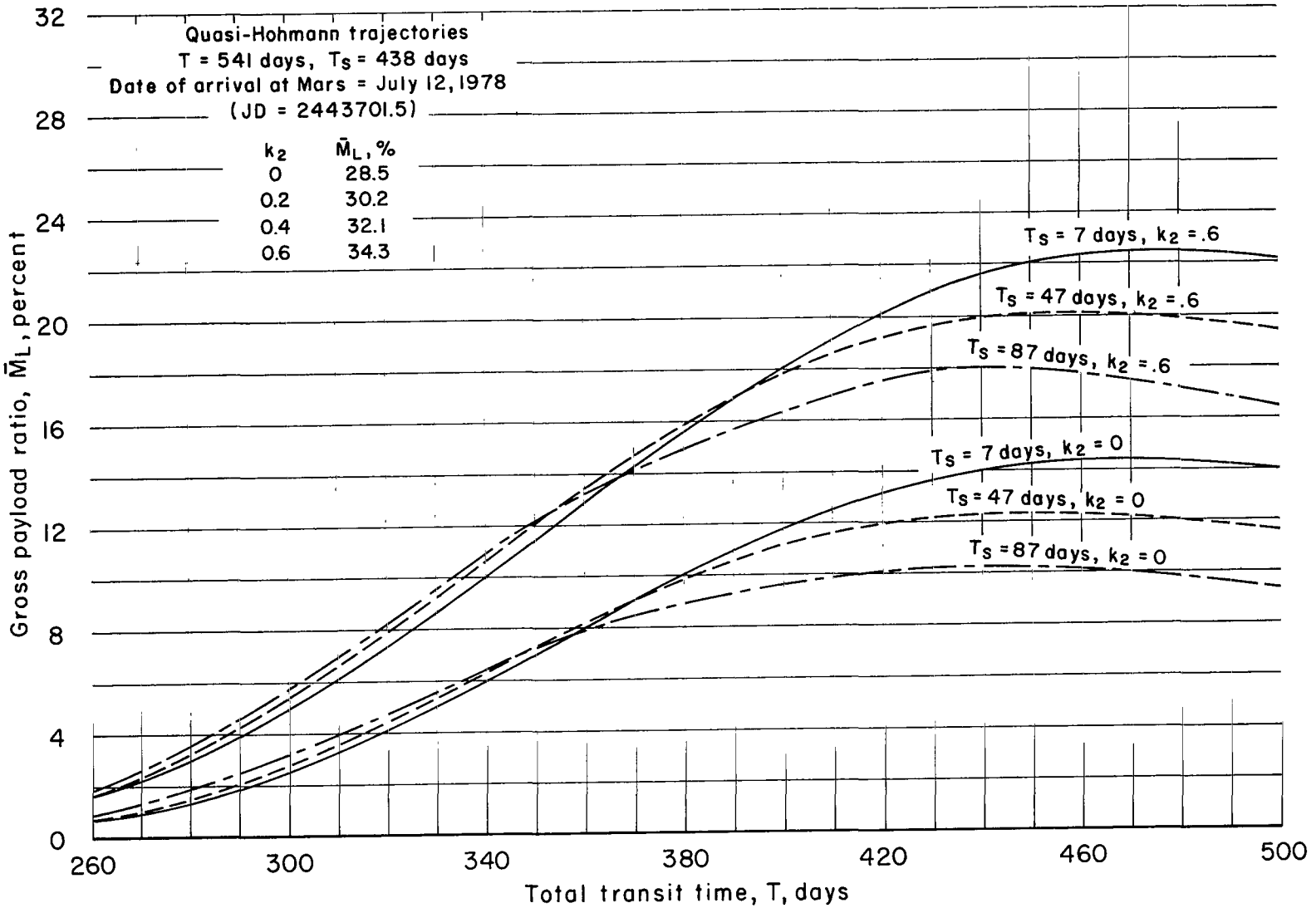

(a) Rendezvous mode with propulsion braking at Mars.

Figure 13.- Effect of stay time on gross-payload ratios; nuclear propulsion; 1980.

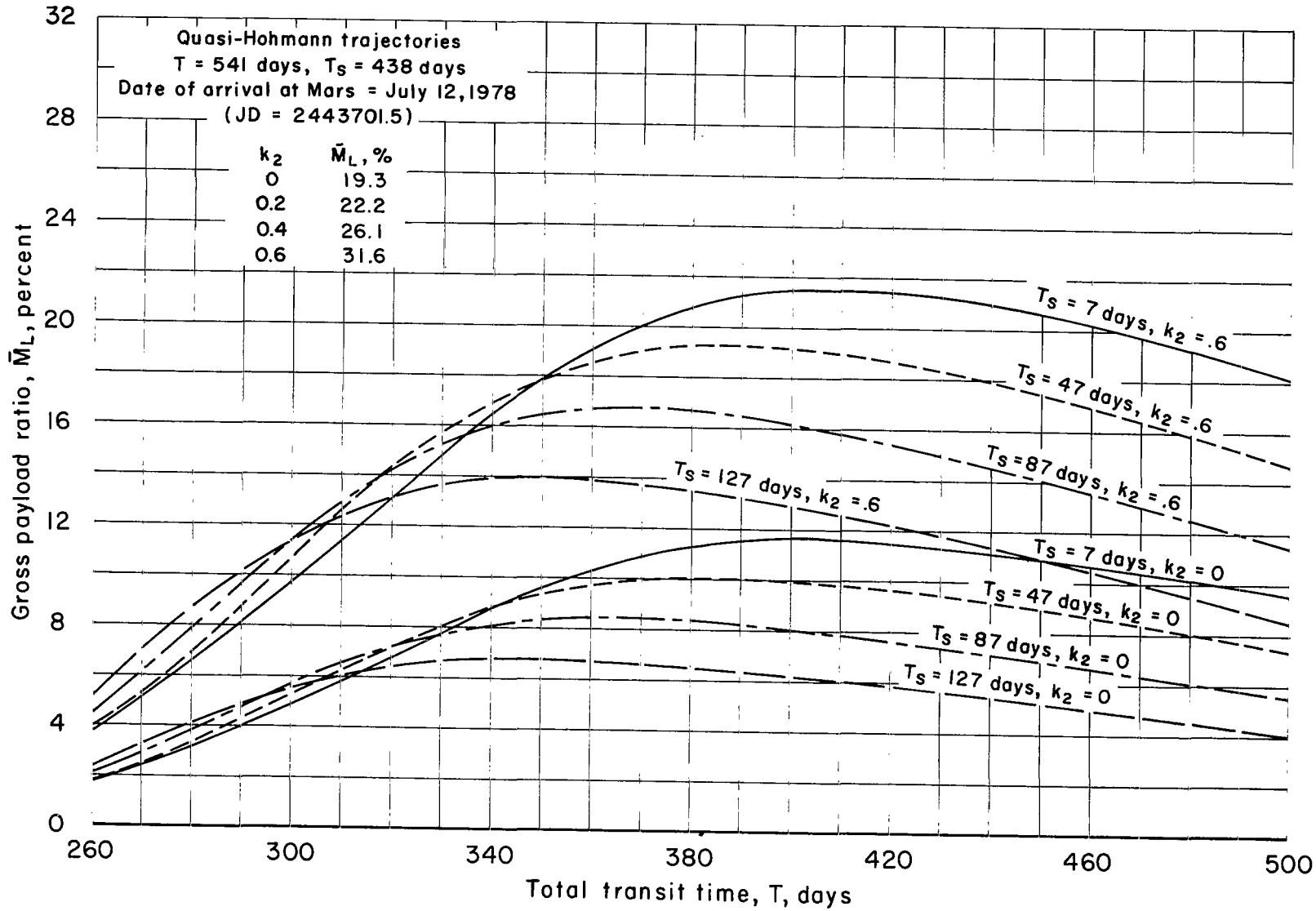

(b) Direct mode.

Figure 13.- Continued.

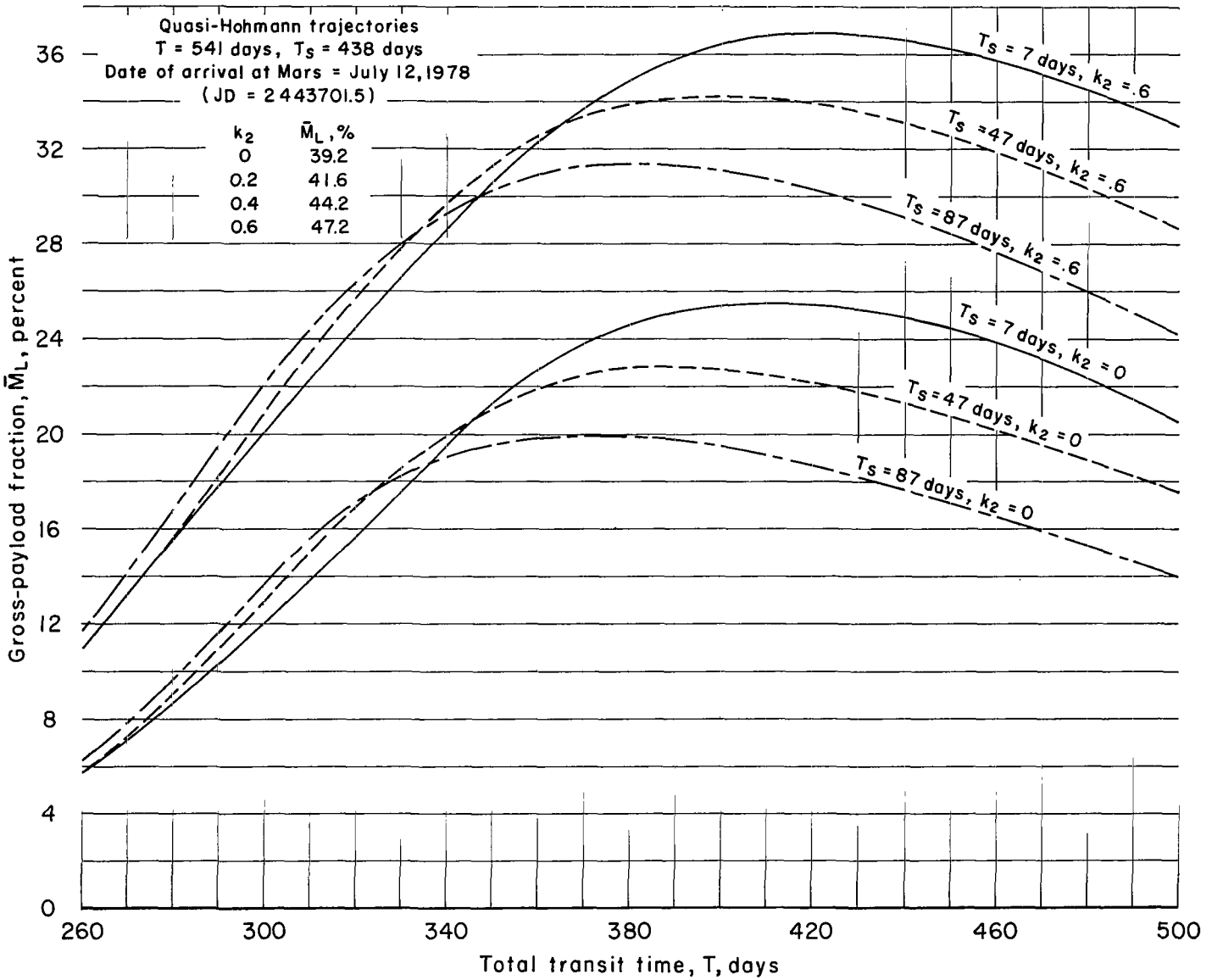

(c) Rendezvous mode with atmospheric braking at Mars.

Figure 13.- Concluded.

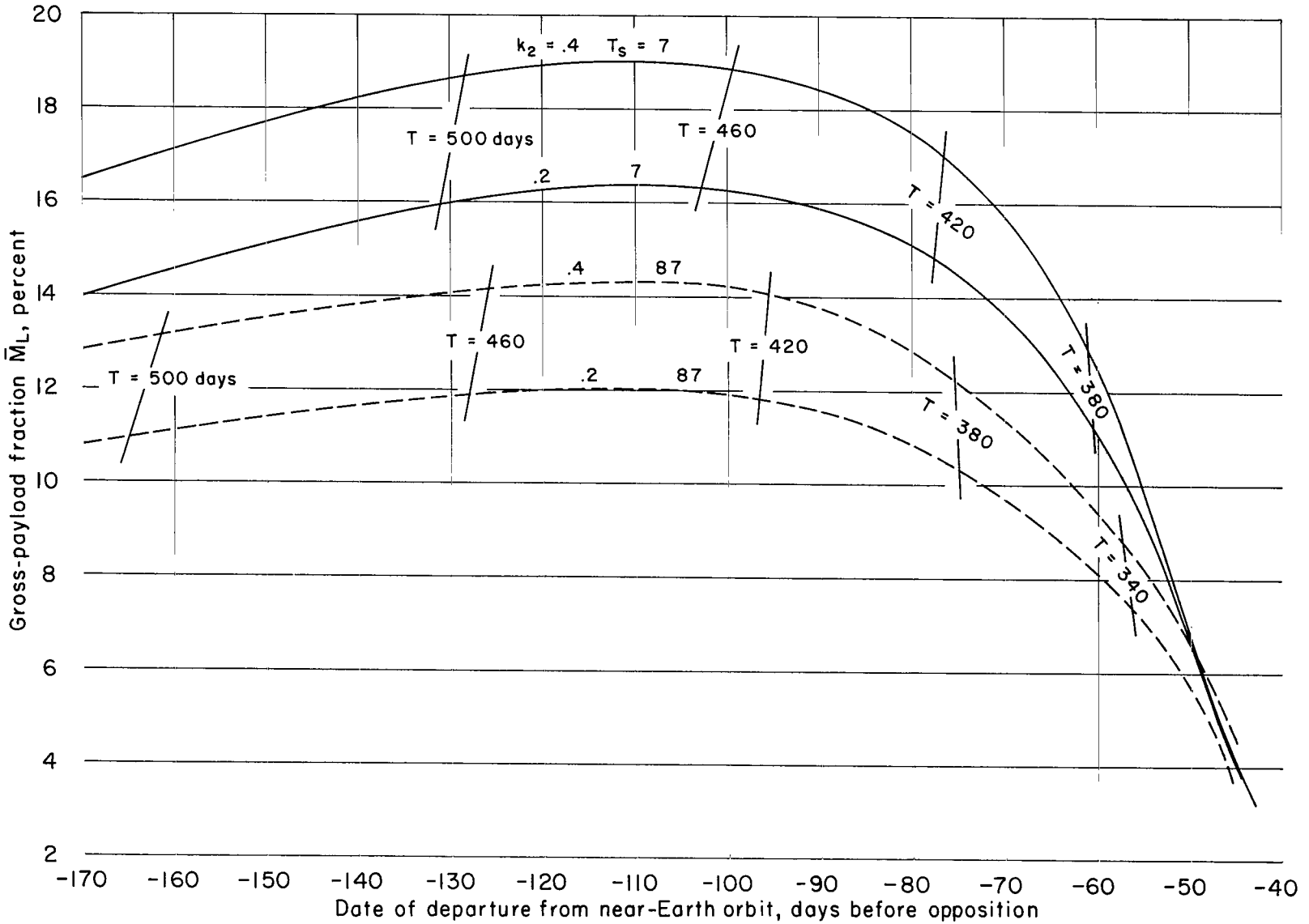

(a) Rendezvous mode with propulsion braking at Mars.

Figure 14.- Variation of gross-payload fraction with date of departure from Earth; 1980.

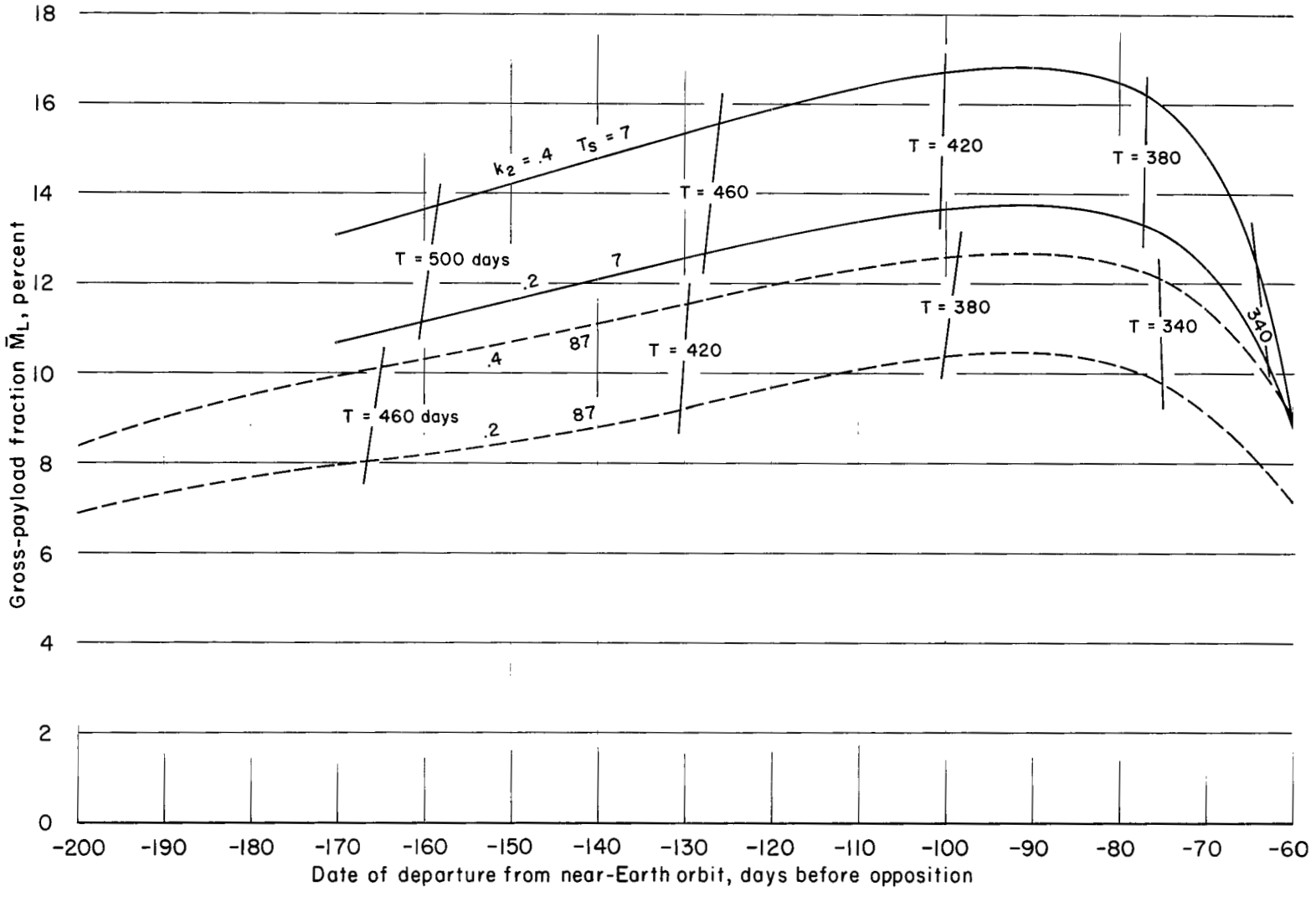

(b) Direct mode.

Figure 14.- Continued.

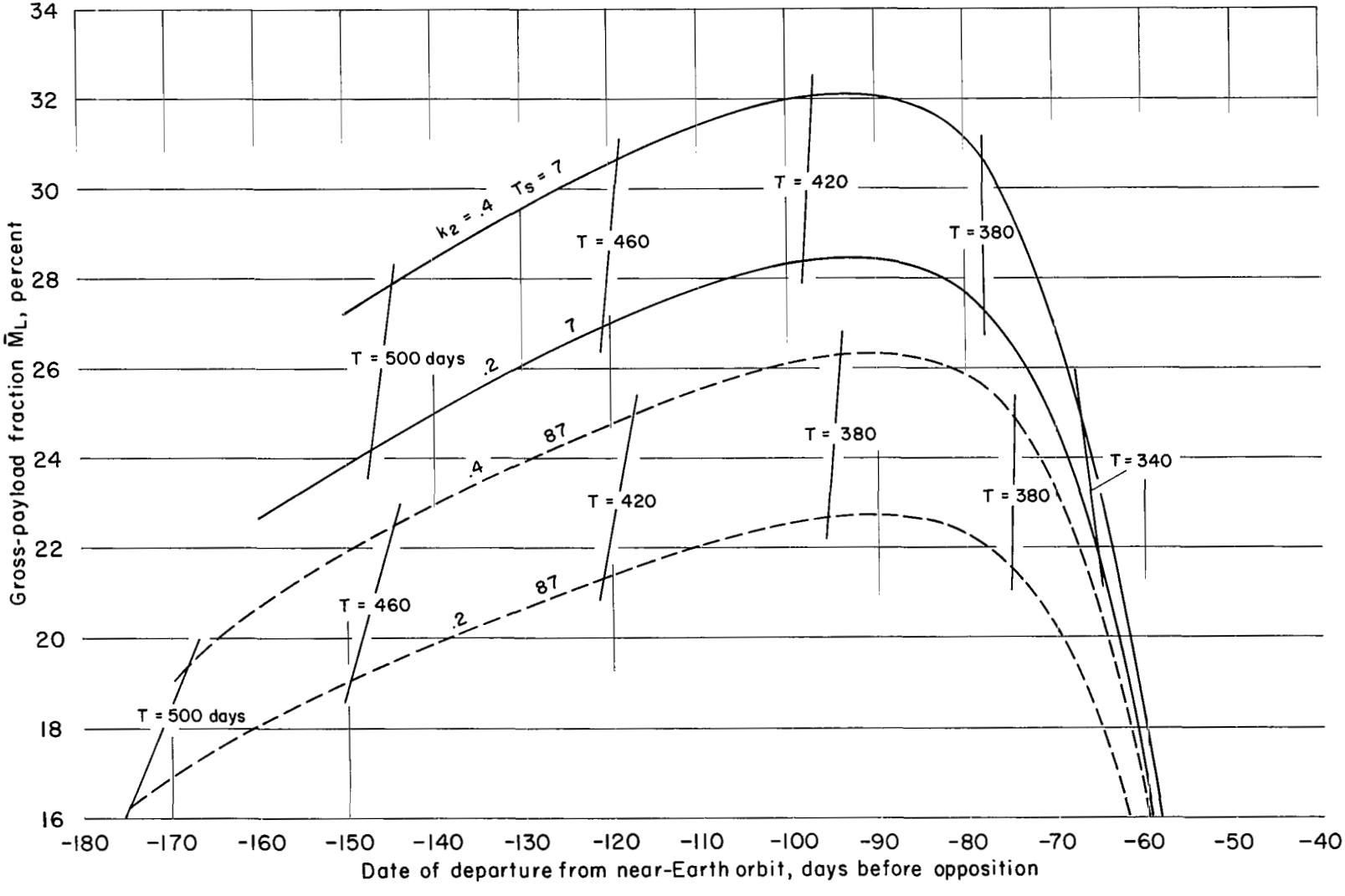

(c) Rendezvous mode with atmospheric braking at Mars.

Figure 14.- Concluded.

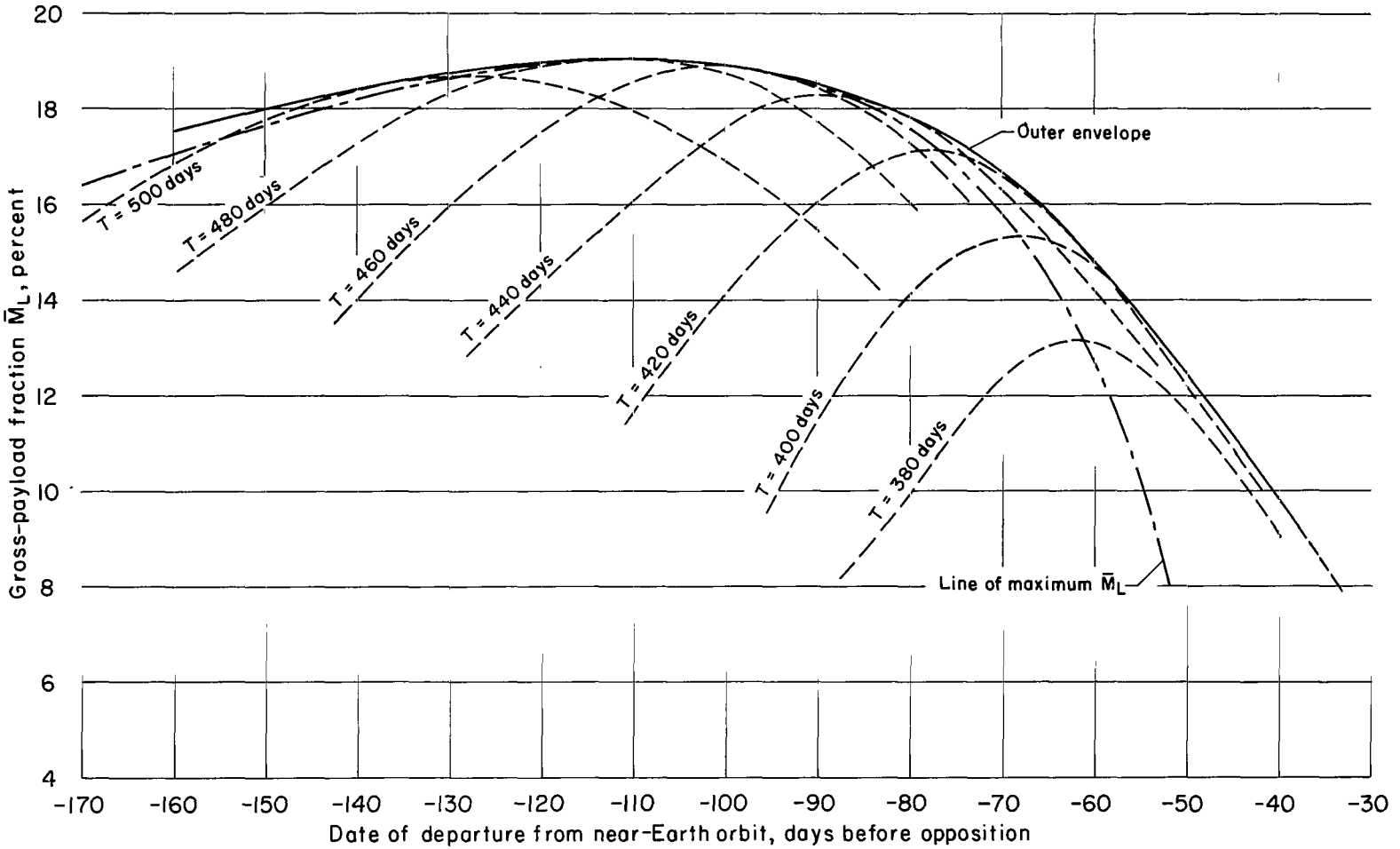

Figure 15.- Effect of reoptimization on penalties incurred by early or late departures from Earth; rendezvous mode with propulsion braking at Mars; k_2 = 0.4; 7-day stay; 1980 opposition.

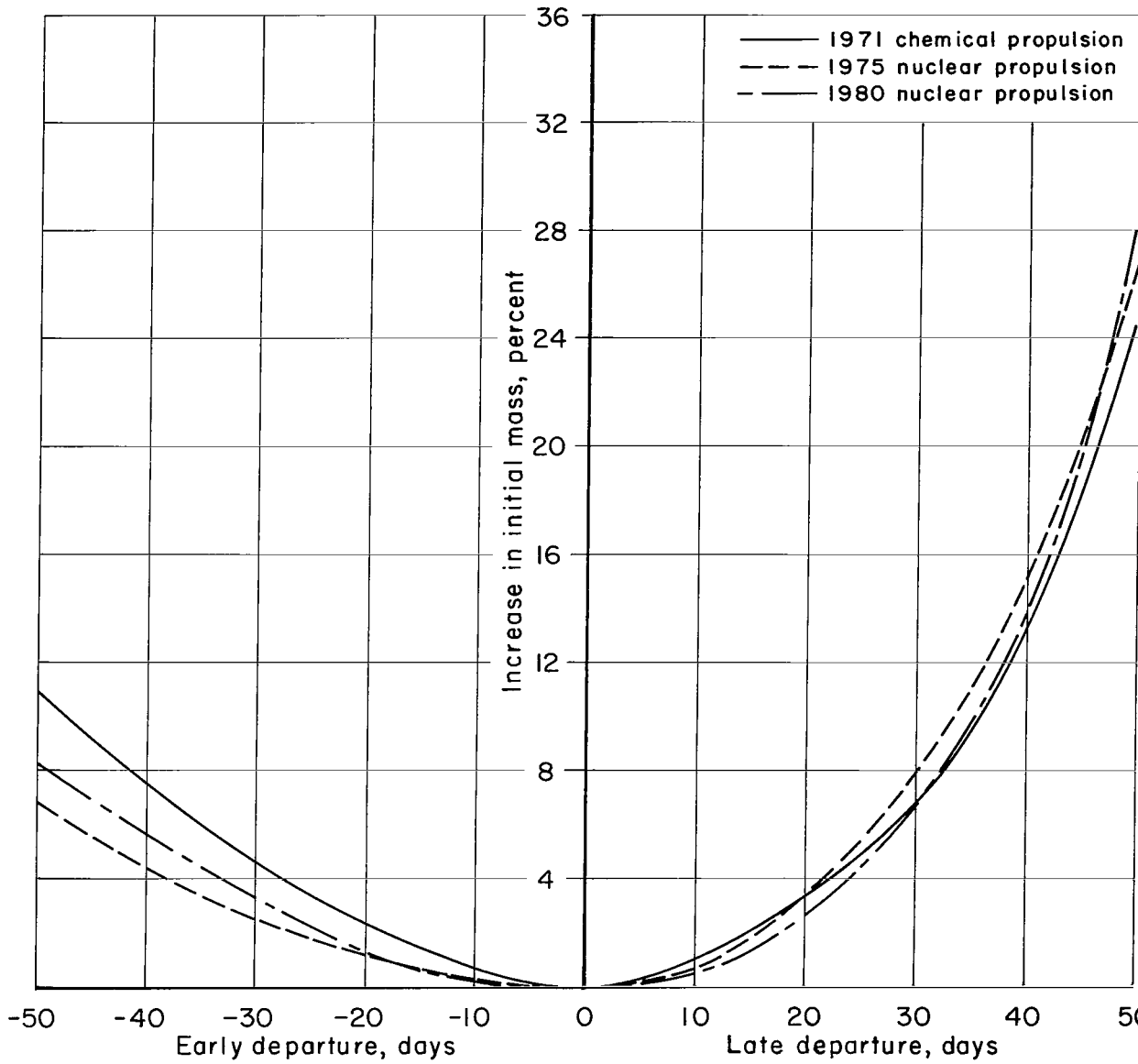

(a) Rendezvous mode with propulsion braking at Mars; $k_2 = 0.4$; 7 day stay; 1971, 1975, 1980.

Figure 16.- Effects of early and late departures from adjusted Earth orbits in terms of required increases in initial mass.

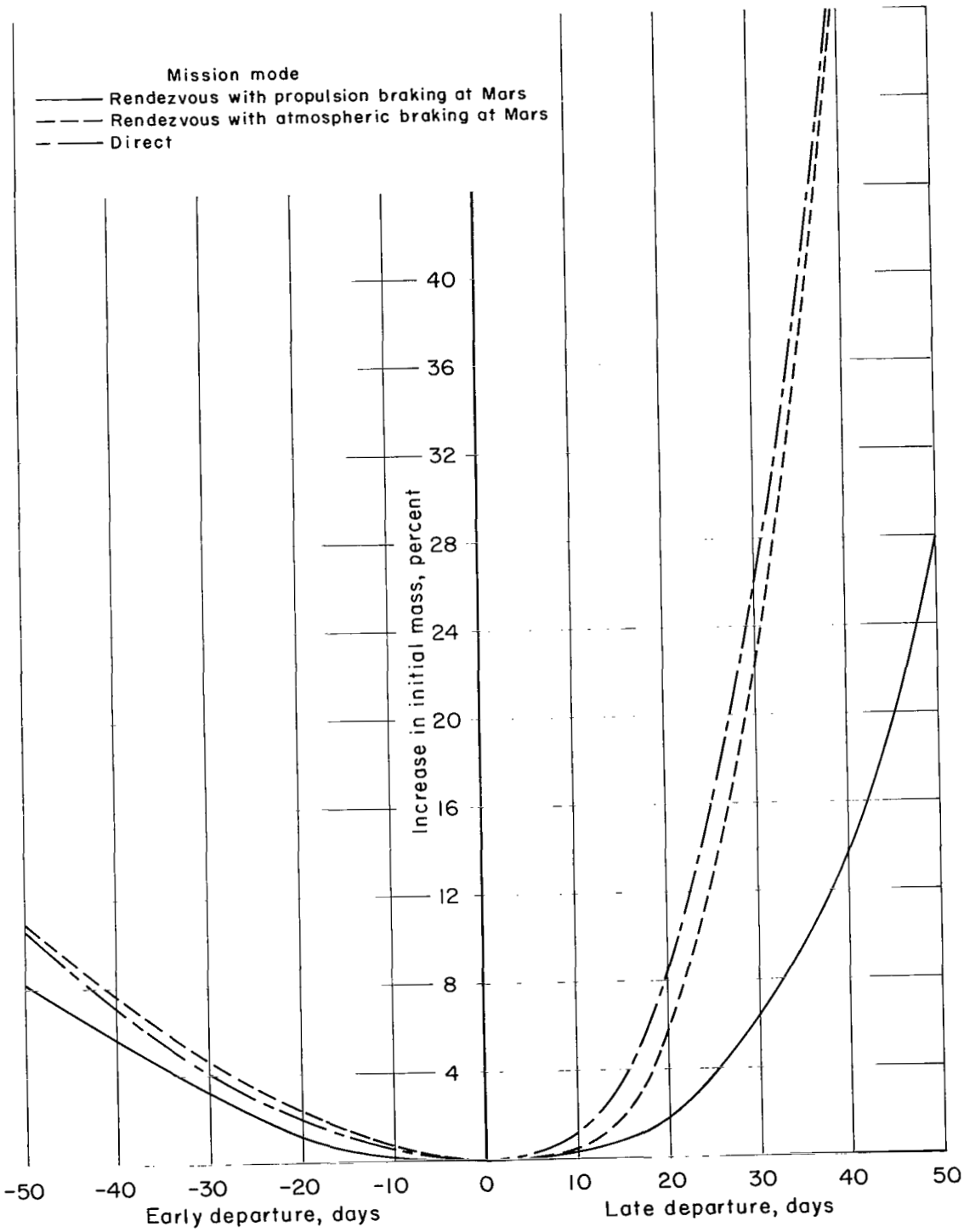

(b) Effect of mission mode; k_2 = 0.4; 7-day stay; 1980.

Figure 16.- Continued.

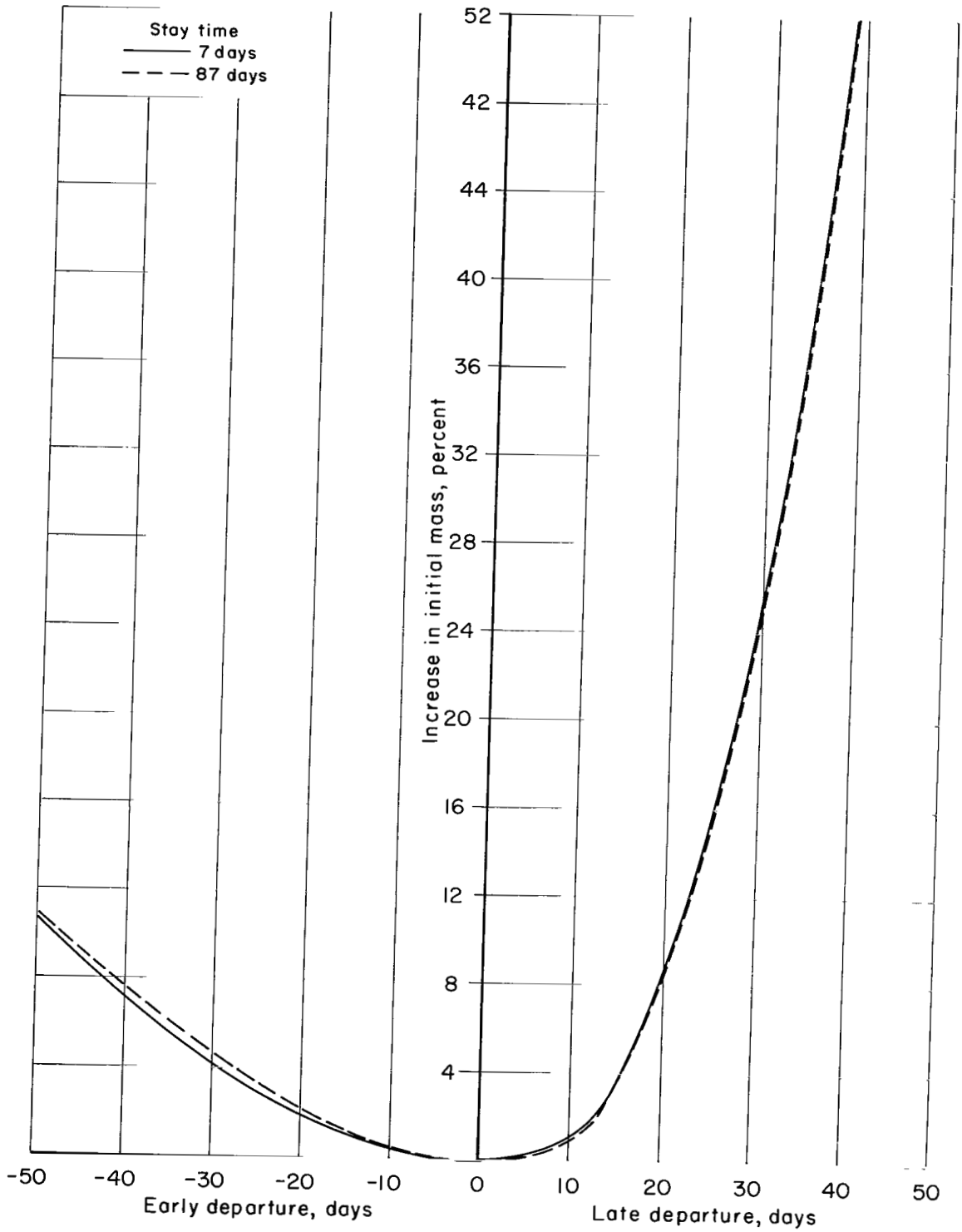

(c) Effect of stay time at Mars; rendezvous mode with atmospheric braking at Mars; $k_2 = 0.4$; 1980.

Figure 16.- Concluded.

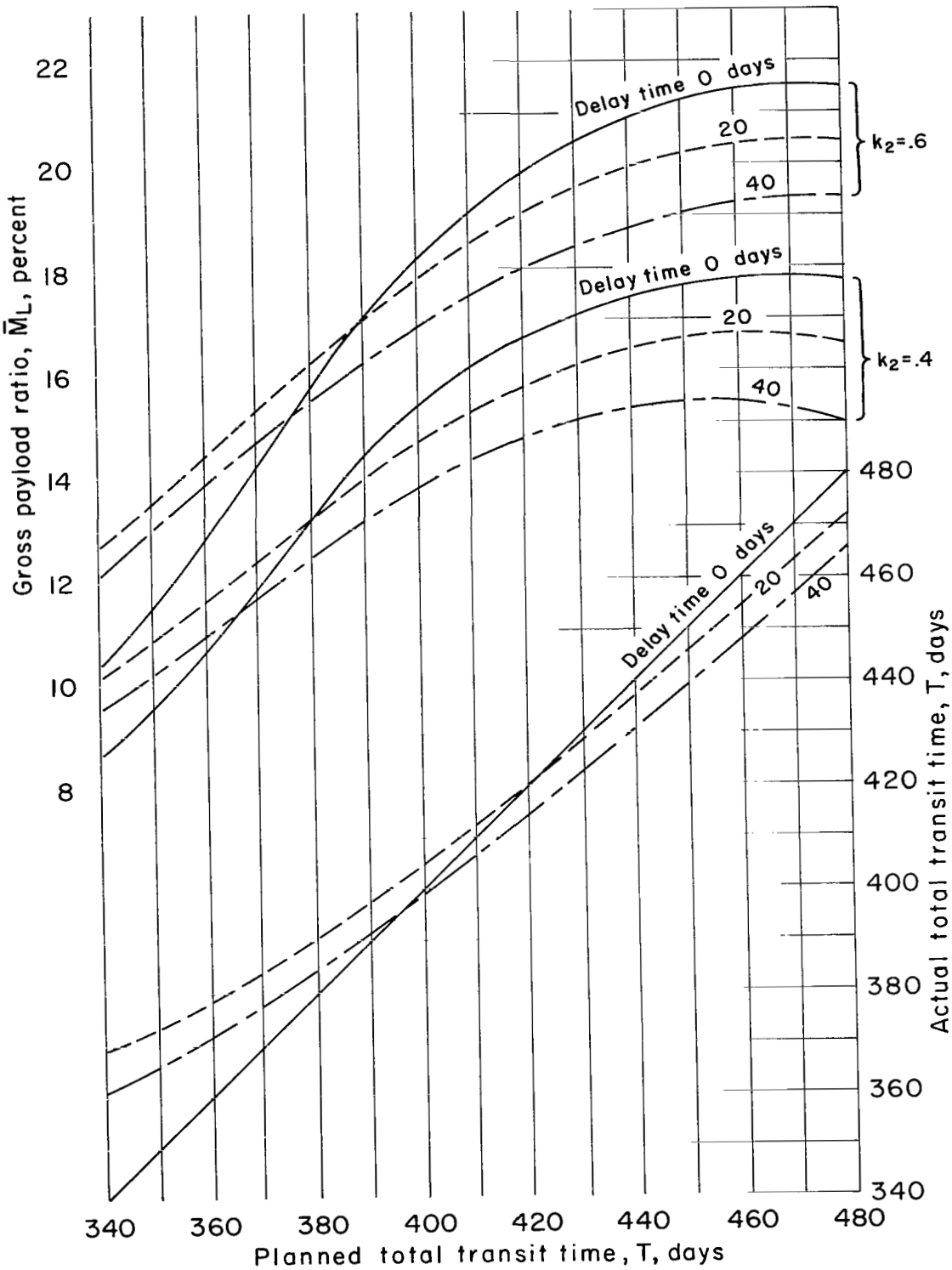

Figure 17.- Effects of delayed departures from Mars; rendezvous mode with propulsion braking at Mars; k_2 = 0.4; 1980.

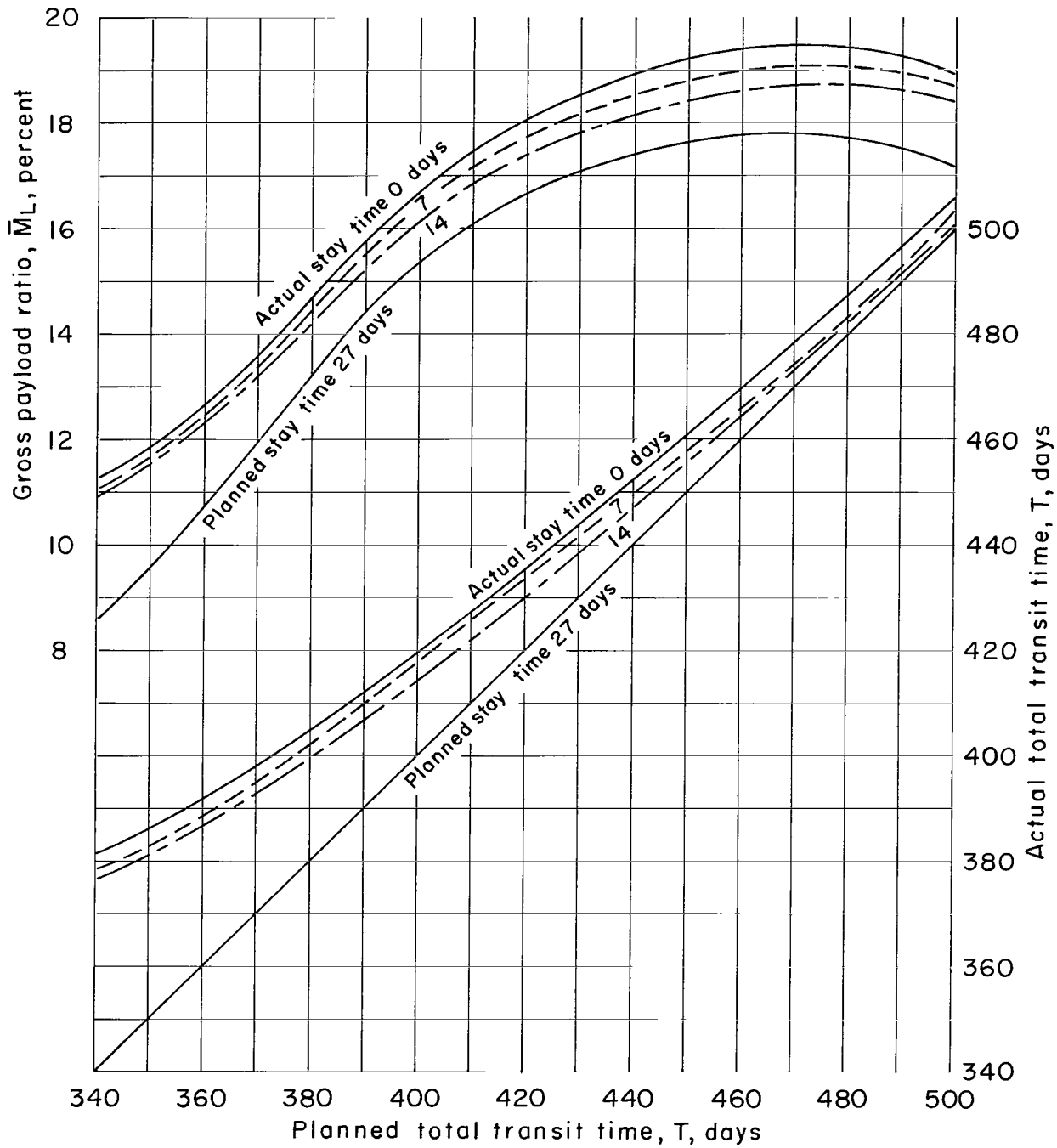

Figure 18.- Effects of early departures from Mars; rendezvous mode with propulsion braking at Mars; k_2 = 0.4; 1980.

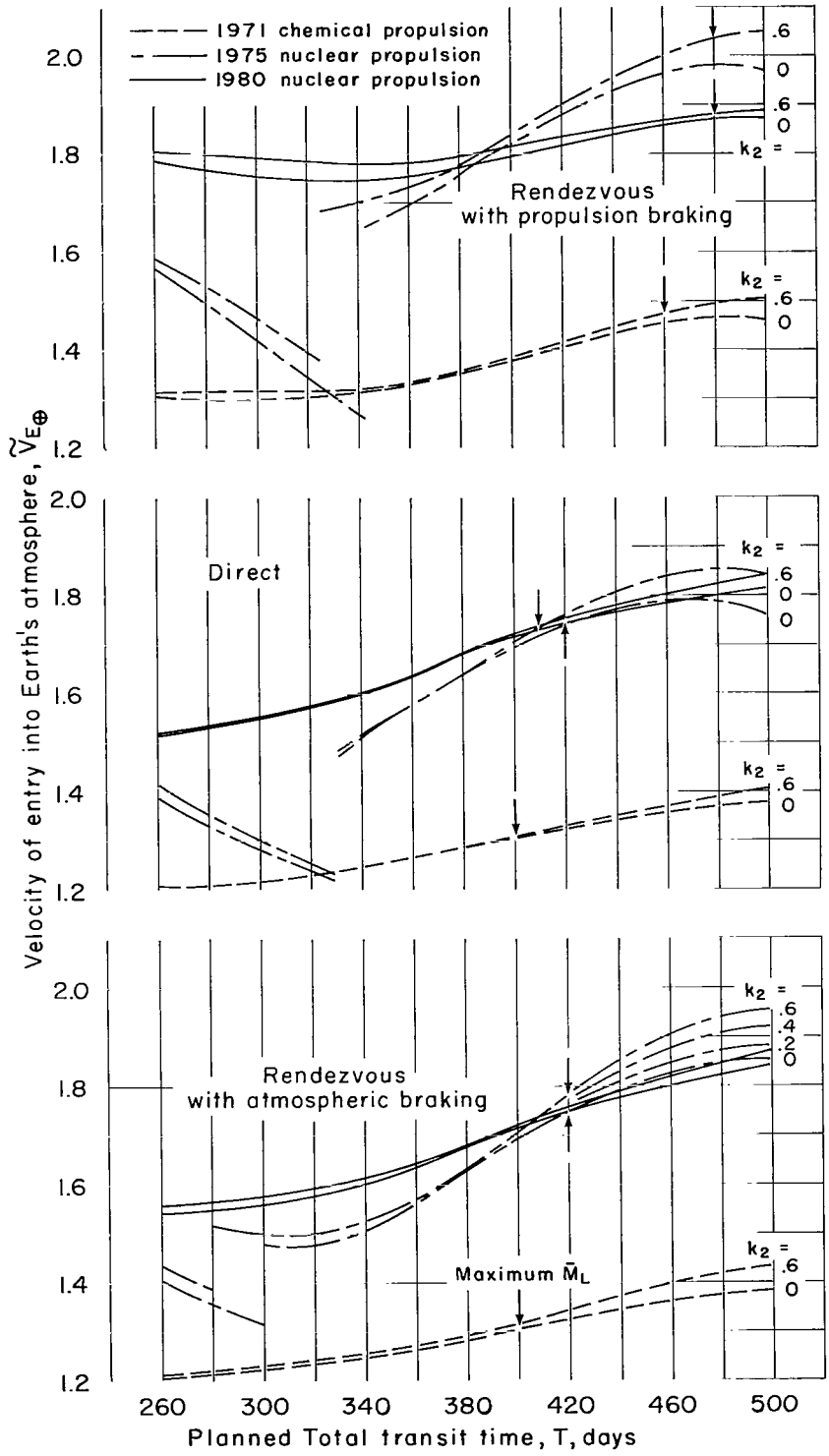

Figure 19.- Variation of velocity of entry into Earth's atmosphere with total transit time, mission mode, and period of mission; 7 day stay.

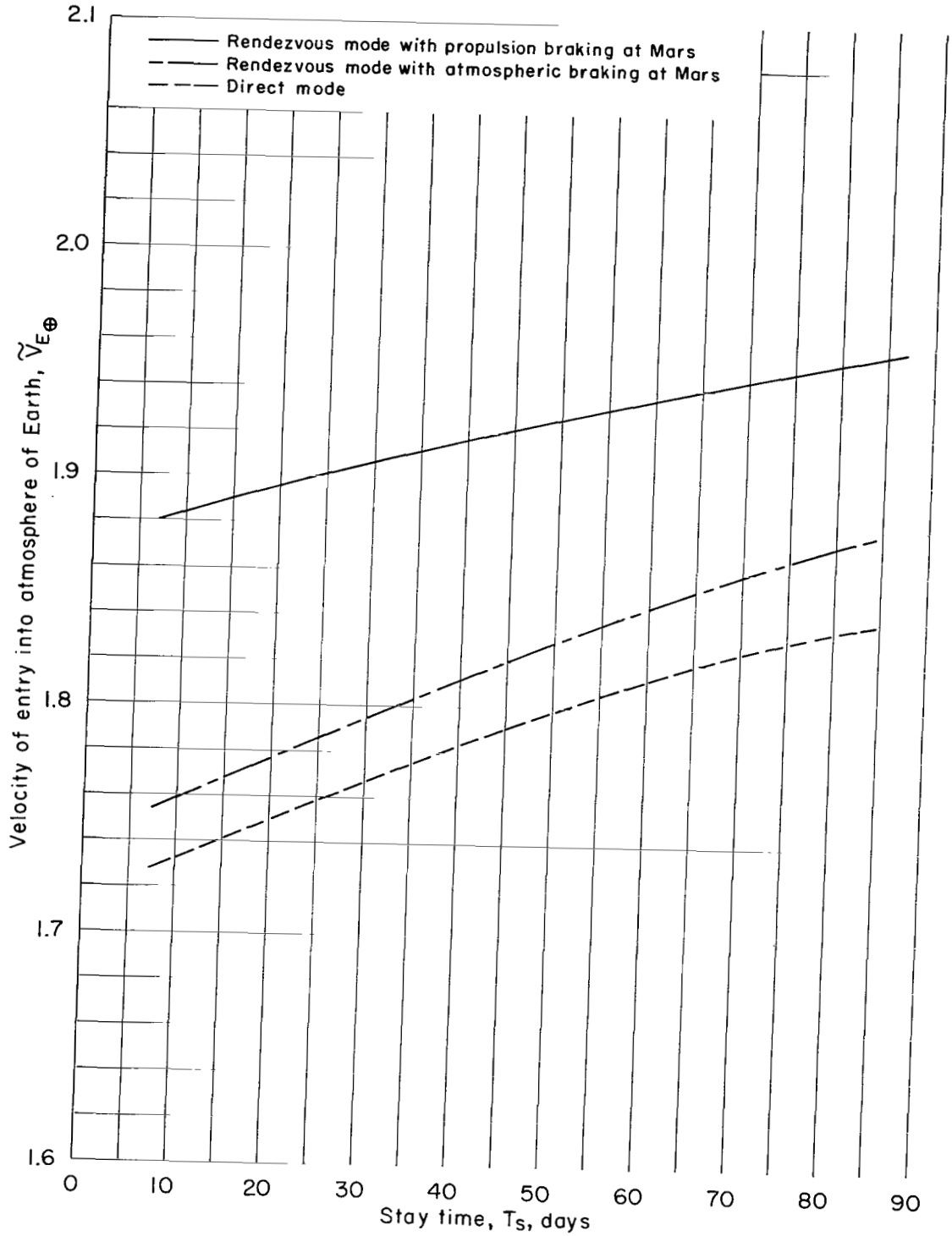

(a) Opposition of 1980.

Figure 20.- Effect of planned stay time at Mars on velocity of entry into atmosphere of Earth in the case of maximum gross-payload fractions; $k_2 = 0.4$.

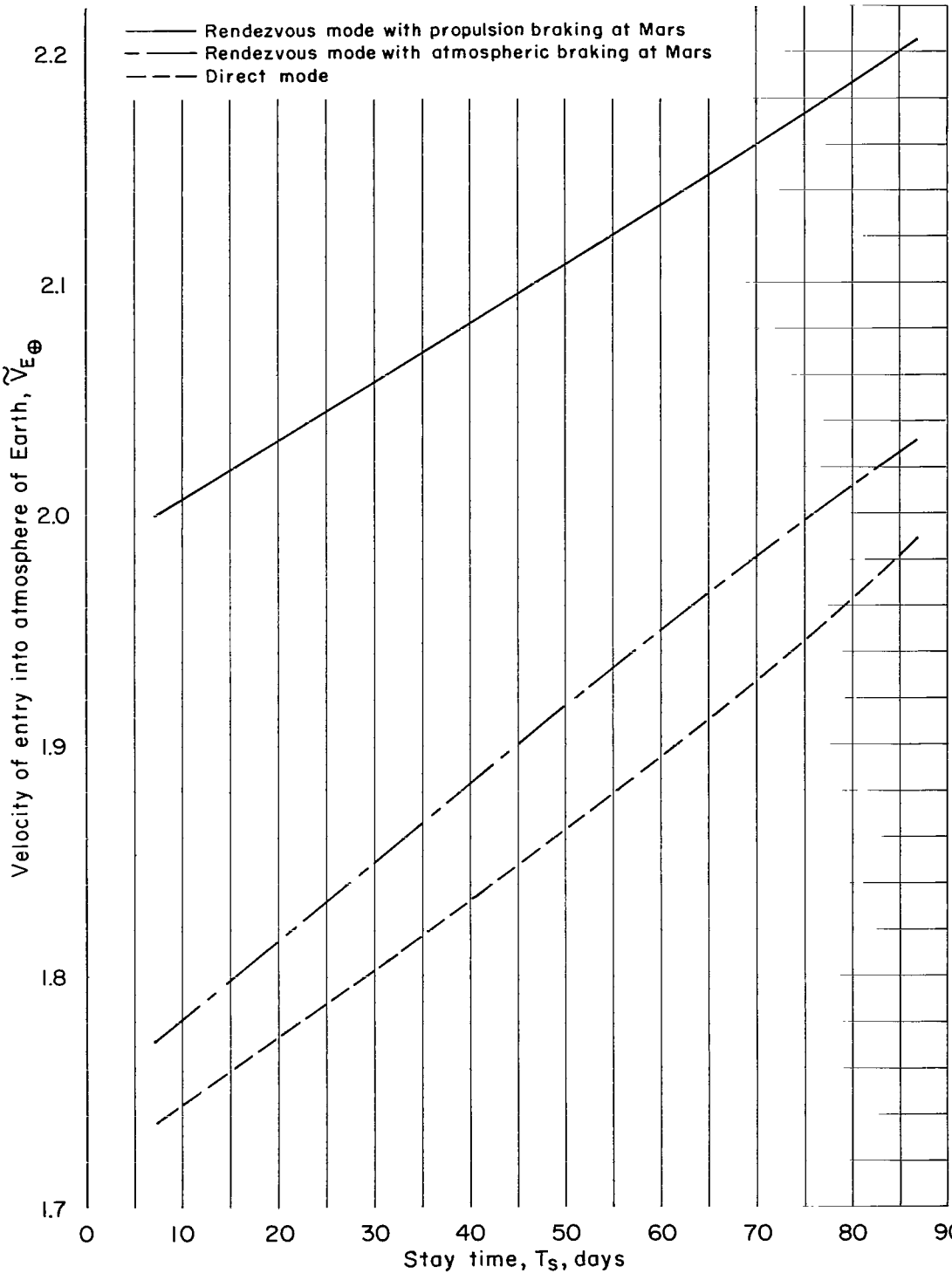

(b) Opposition of 1975.

Figure 20.- Concluded.

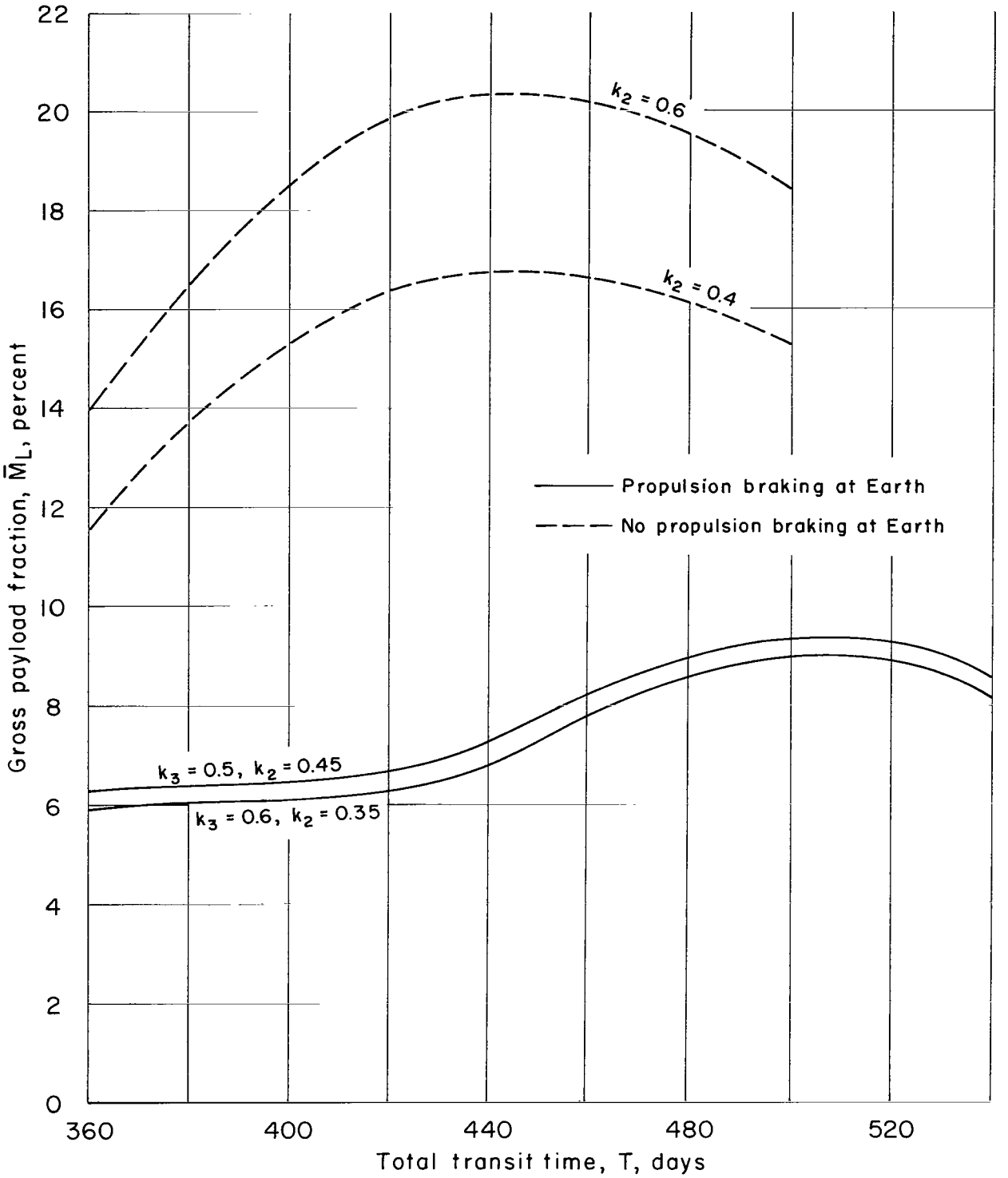

Figure 21.- Effect of using chemical propulsion to reduce Earth atmosphere-entry velocities to parabolic speed; rendezvous mode with propulsion braking at Mars; all other stages, nuclear propulsion; 47-day stay; 1975.

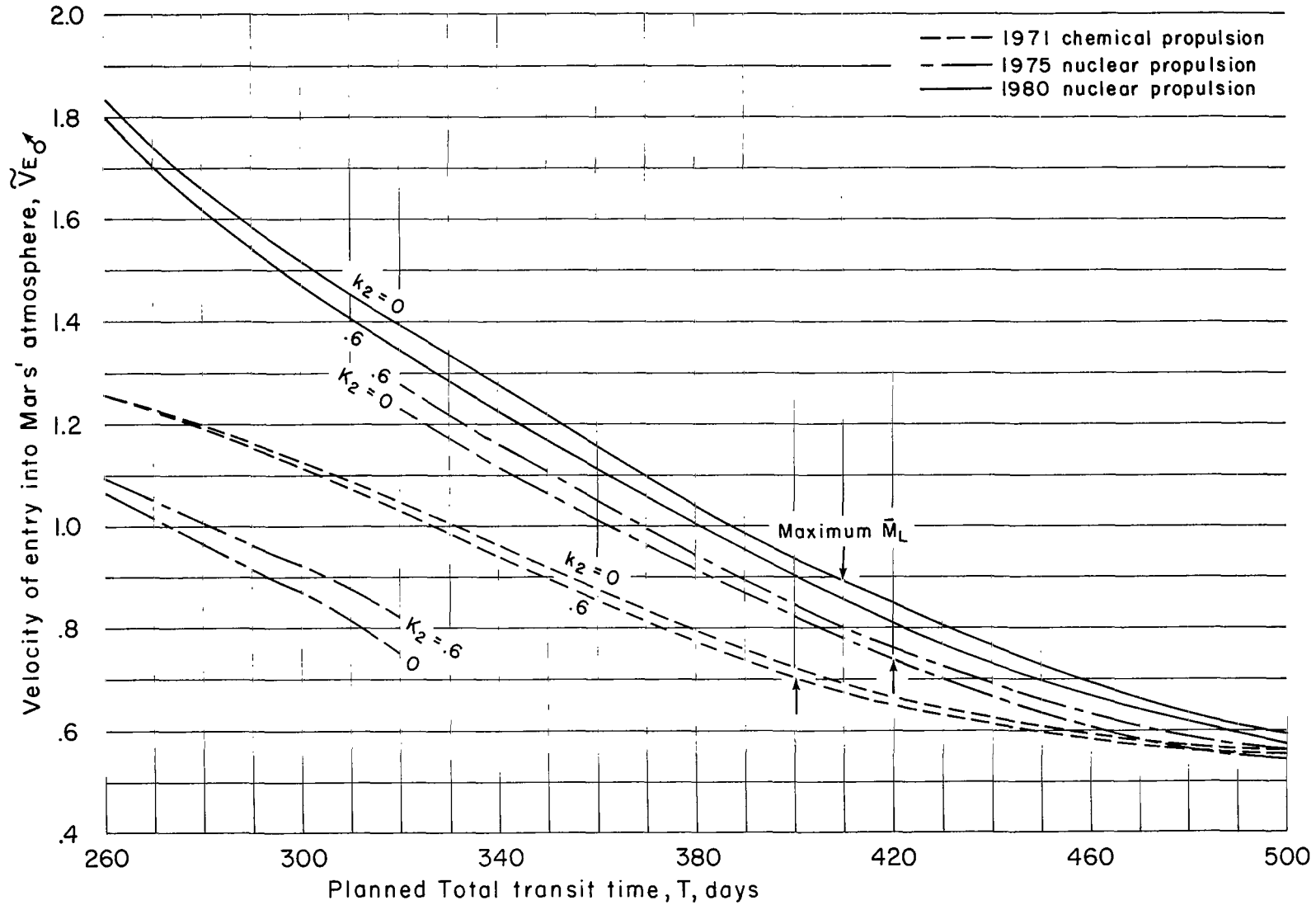

(a) Direct mission mode.

Figure 22.- Variation of velocity of entry into martian atmosphere with total transit time; 7-day stay.

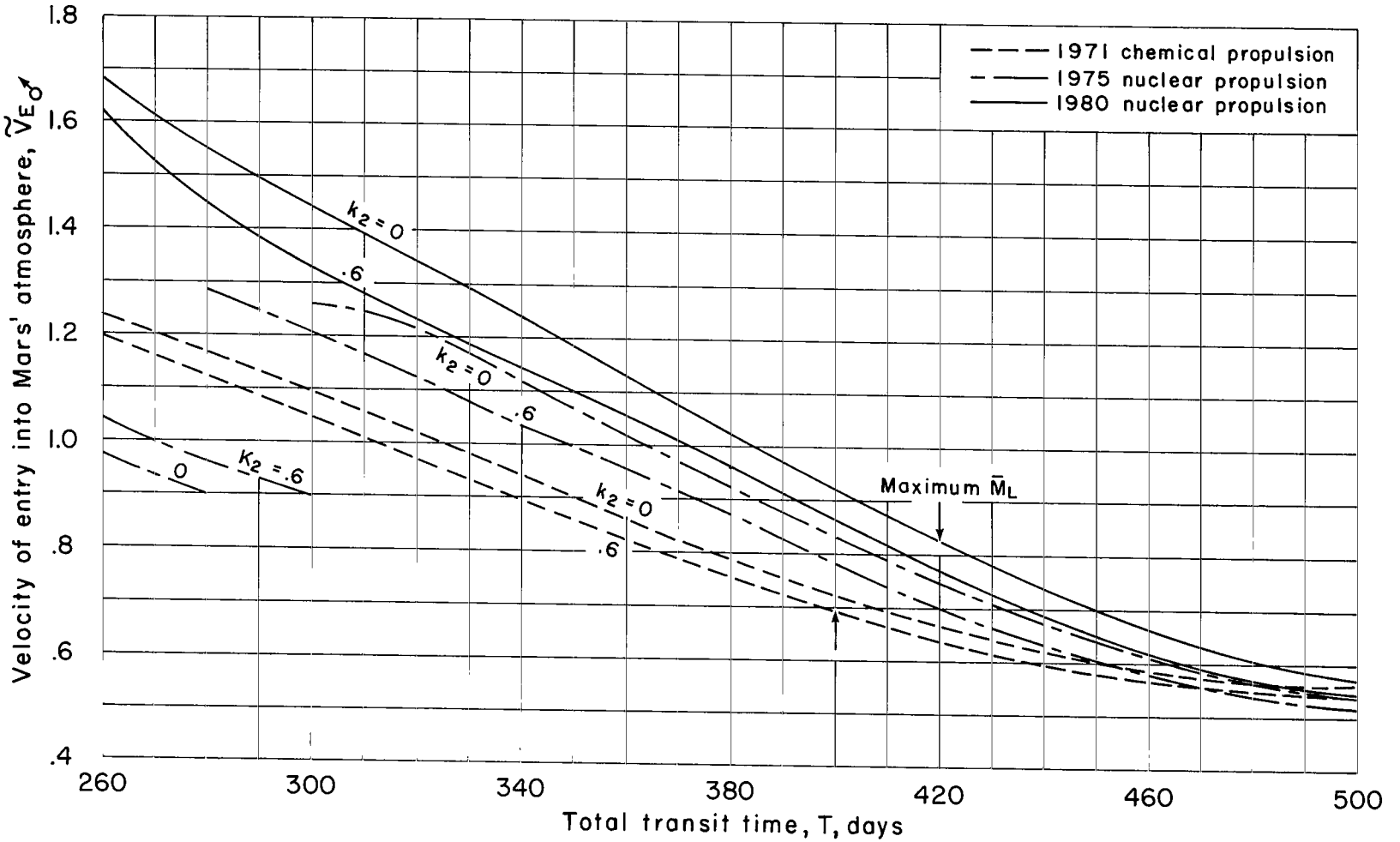

(b) Rendezvous mission mode with atmospheric braking at Mars.

Figure 22.- Concluded.

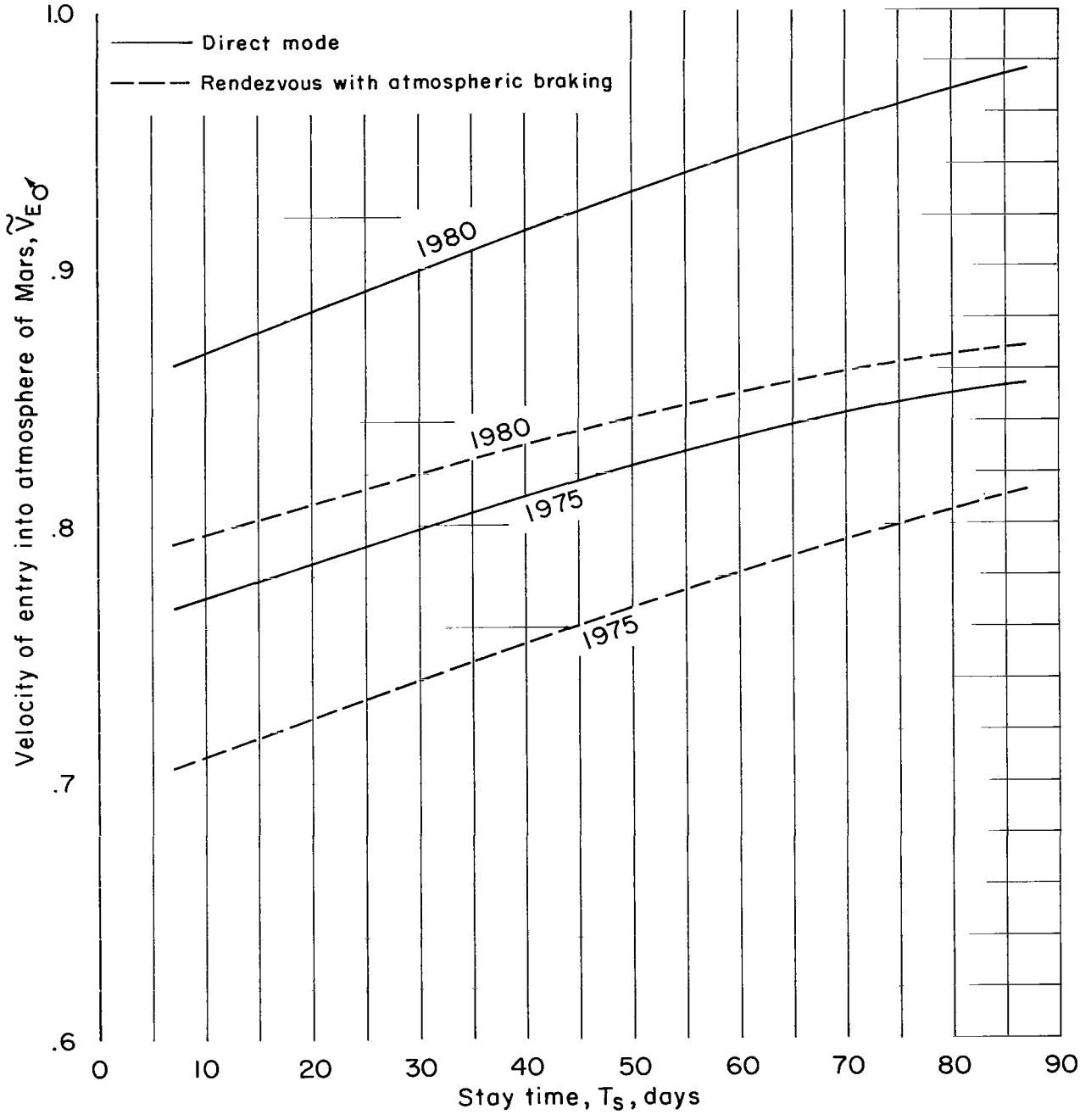

Figure 23.- Effect of planned stay time at Mars on velocity of entry into martian atmosphere in the case of maximum gross-payload fractions; $k_2 = 0.4$.

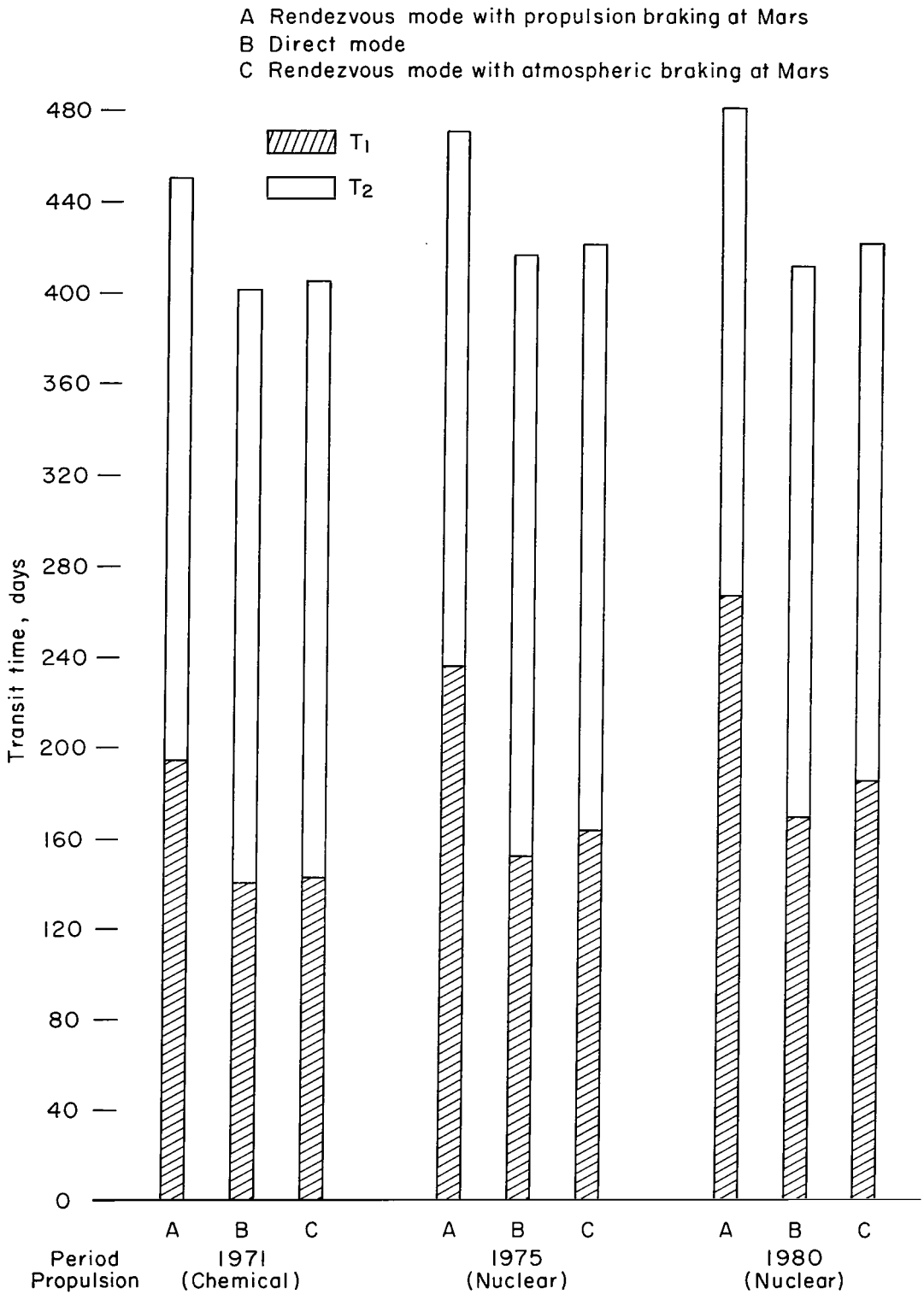

Figure 24.- Division of total transit time between outbound and return legs in the case of maximum gross-payload fractions; $k_2 = 0.4$; 7-day stay.

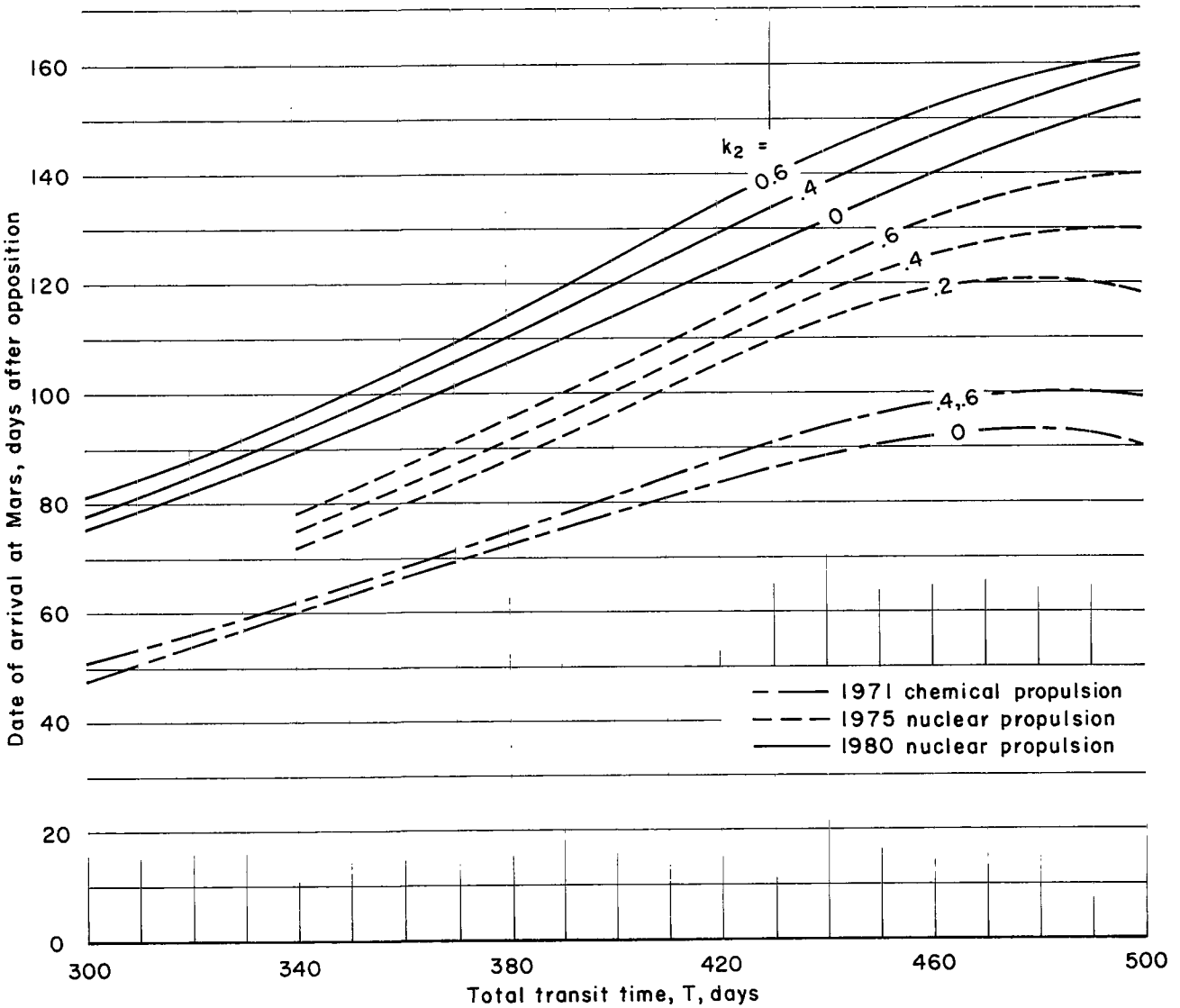

(a) Rendezvous mode with propulsion braking at Mars.

Figure 25.- Dates of arrival at Mars for best gross-payload fractions; 7-day stay.

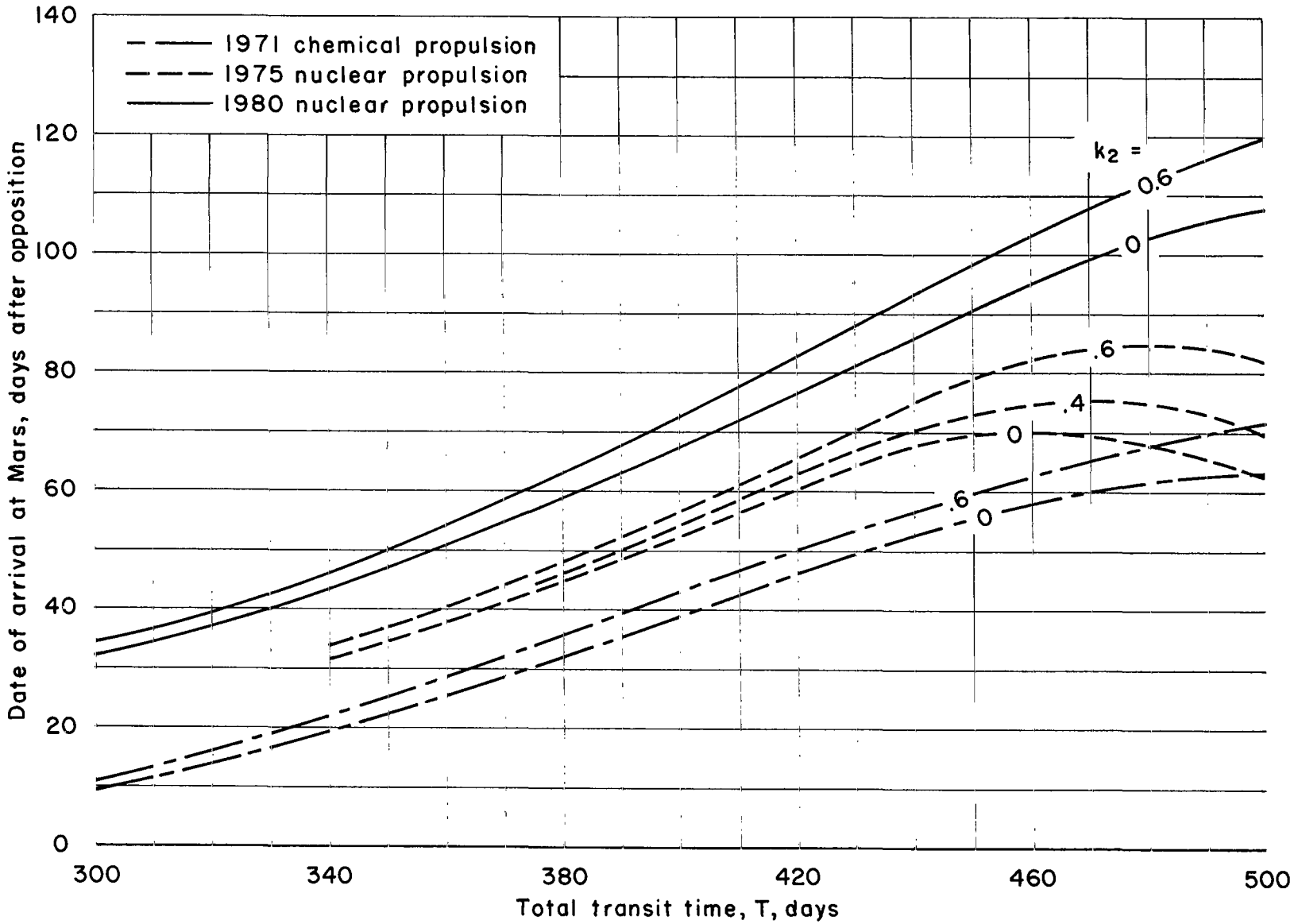

(b) Direct mode.

Figure 25.- Continued.

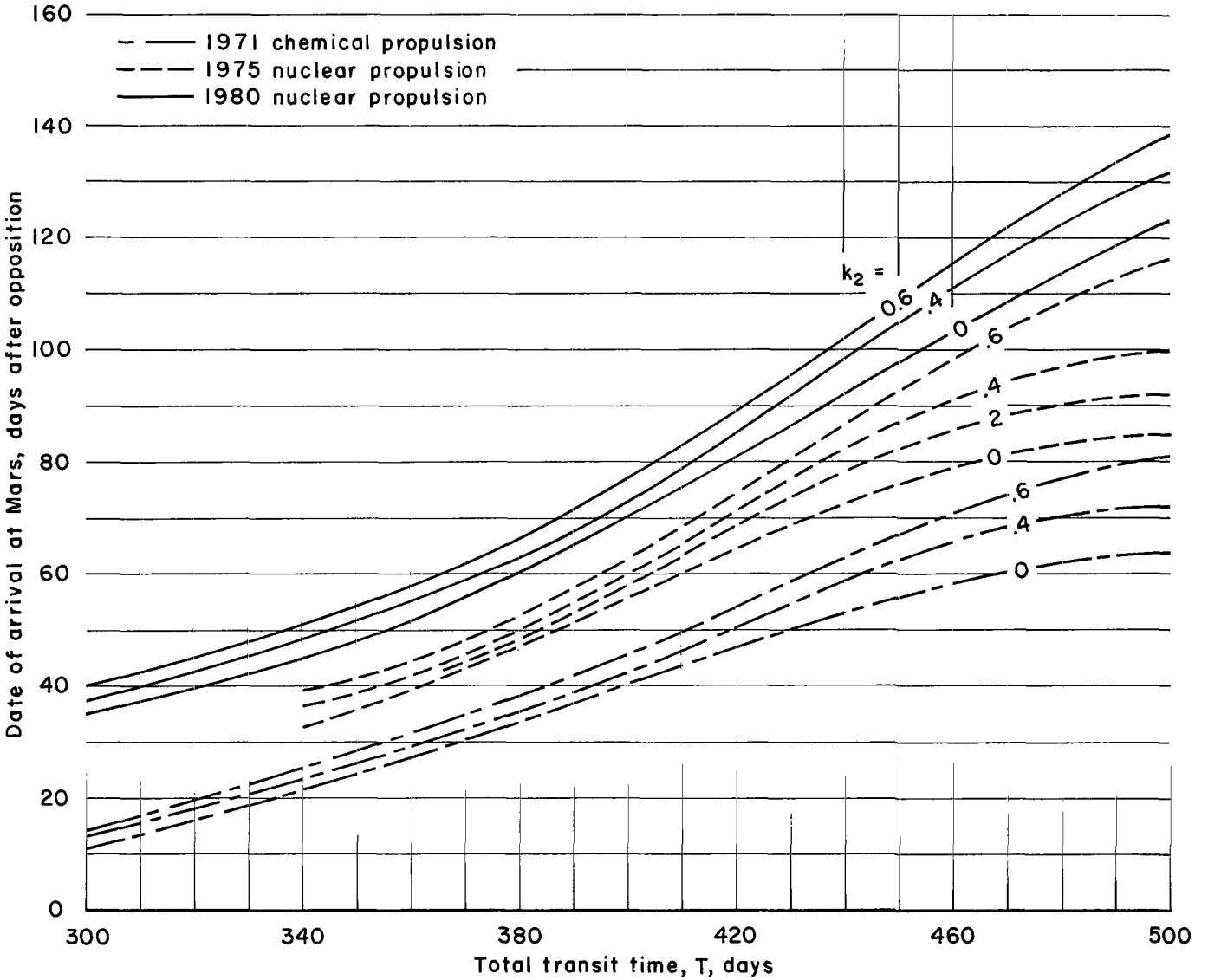

(c) Rendezvous mode with atmospheric braking at Mars.

Figure 25.- Concluded.

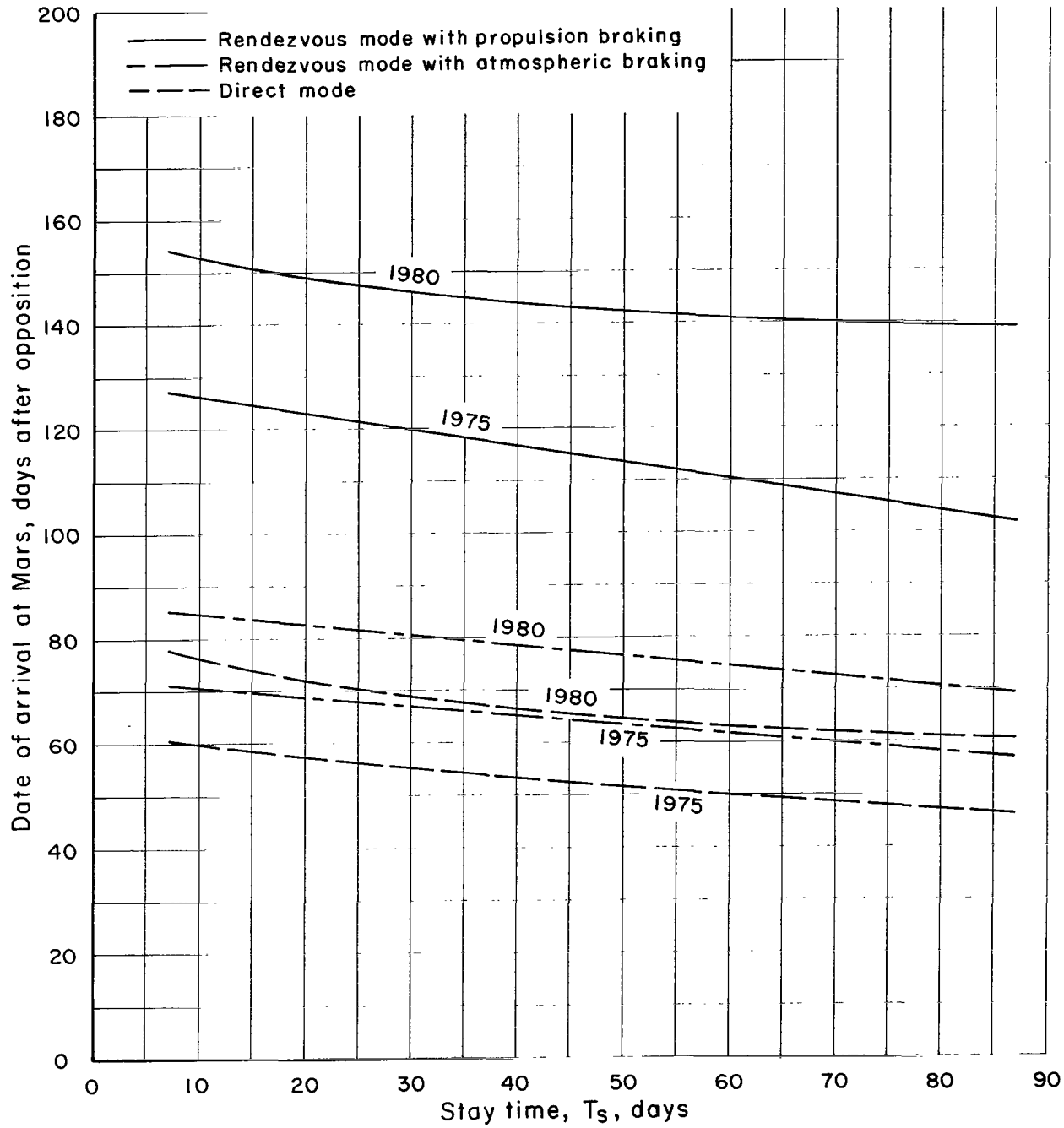

Figure 26.- Effect of planned stay time at Mars on date of arrival at Mars in the case of maximum gross-payload fractions; $k_2 = 0.4$.

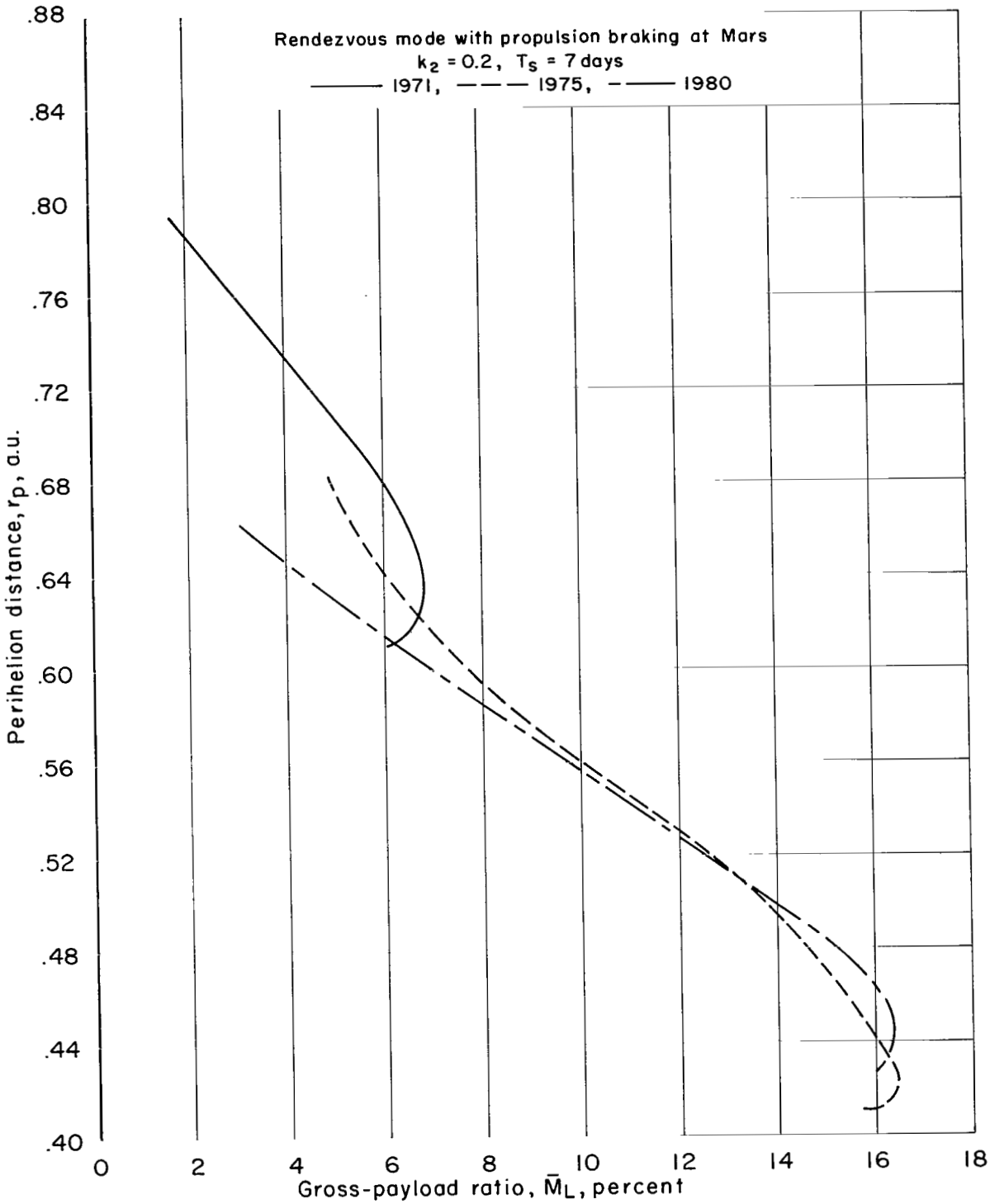

(a) Effect of date of opposition.

Figure 27.- Variation of perihelion distance with gross-payload fraction.

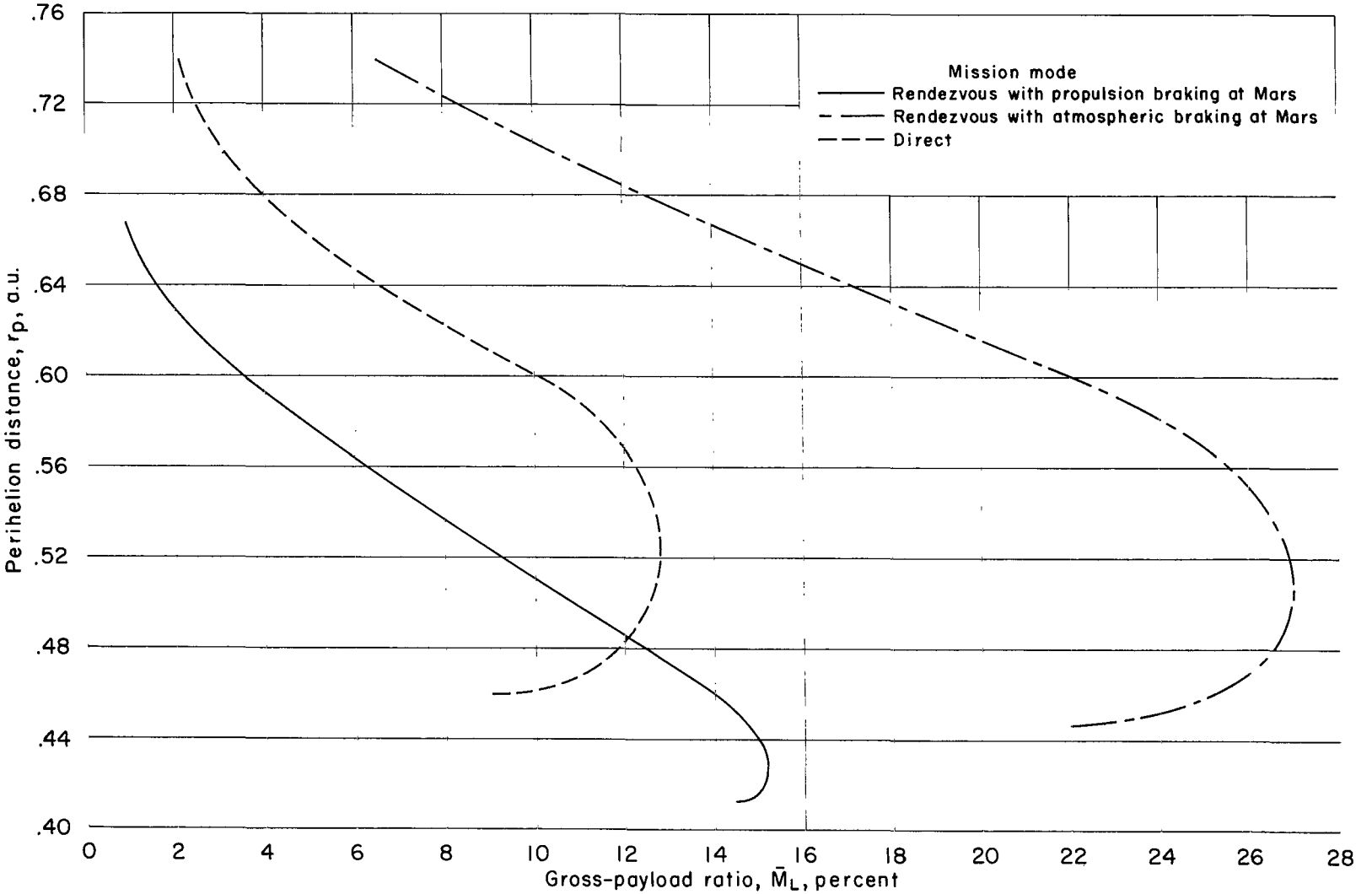

(b) Effect of mission mode; 27-day stay.

Figure 27.- Continued.

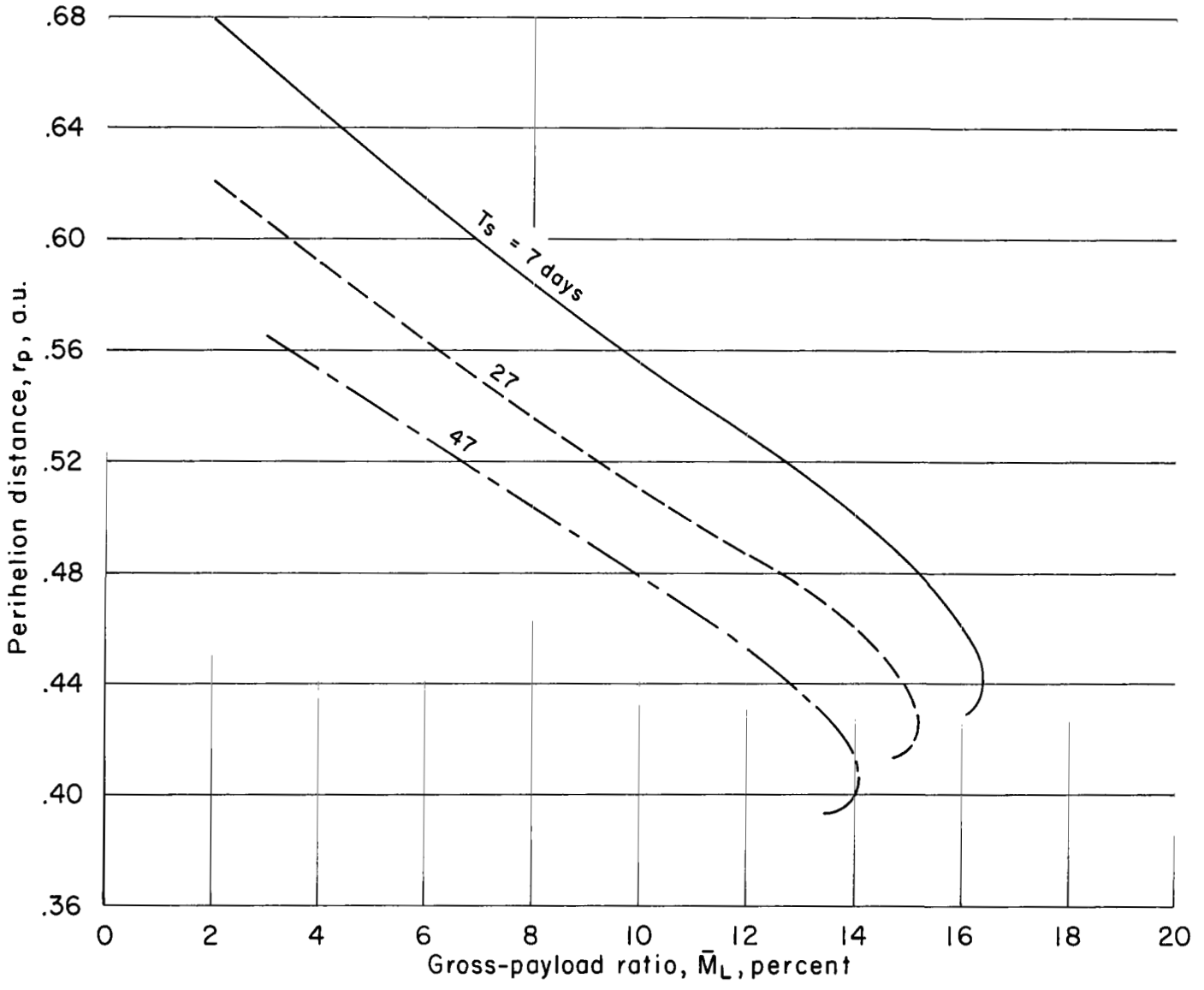

(c) Effect of stay time; rendezvous mode with propulsion braking.

Figure 27.- Concluded.

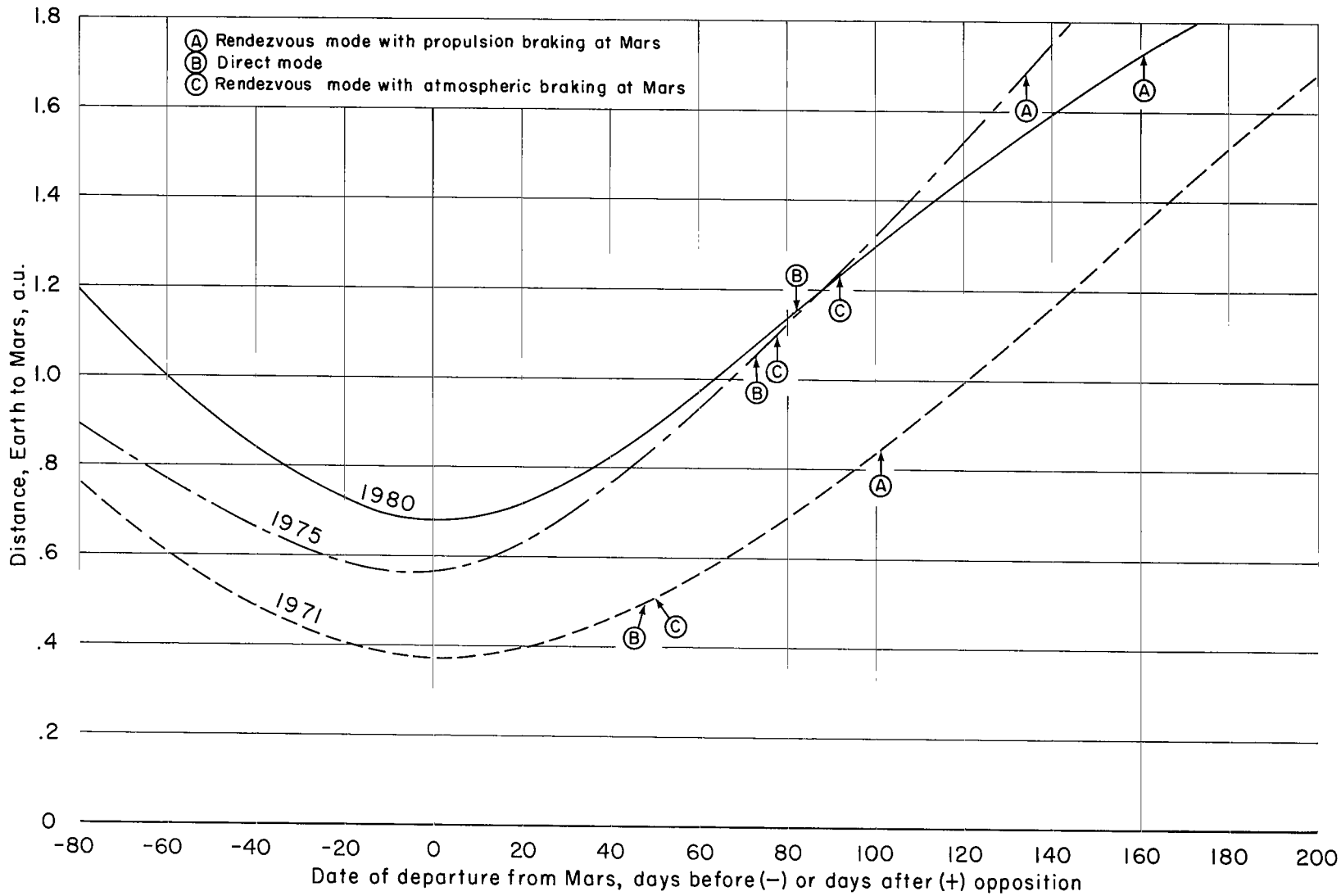

Figure 28.- Variation of distance between Earth and Mars during oppositions of 1971, 1975, and 1980 with time of departure from Mars.

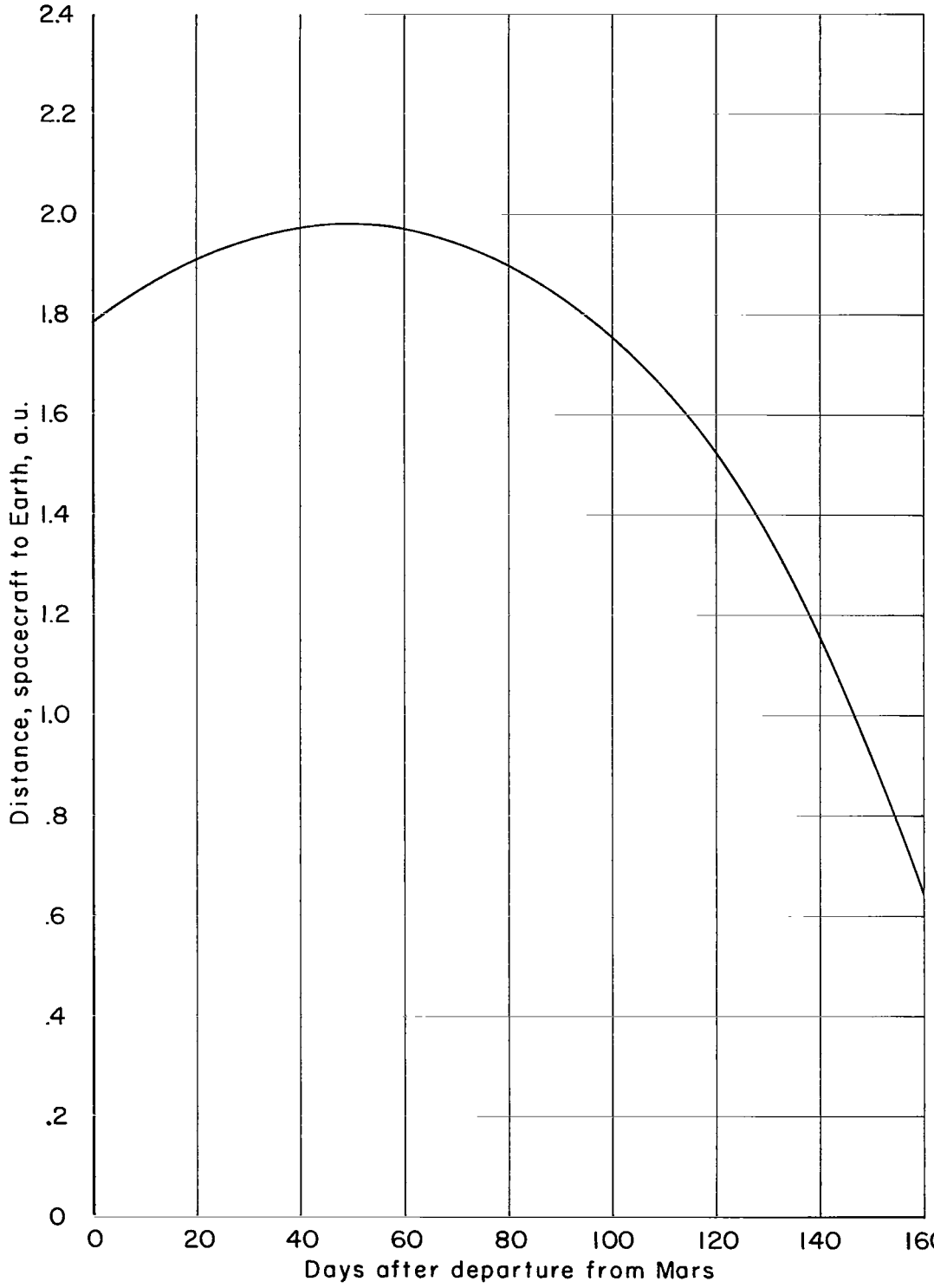

Figure 29.- Variation of communication distance with time after departure from Mars; rendezvous mode with propulsion braking at Mars; 1980; $k_2 = 0.4$, 27-day stay.

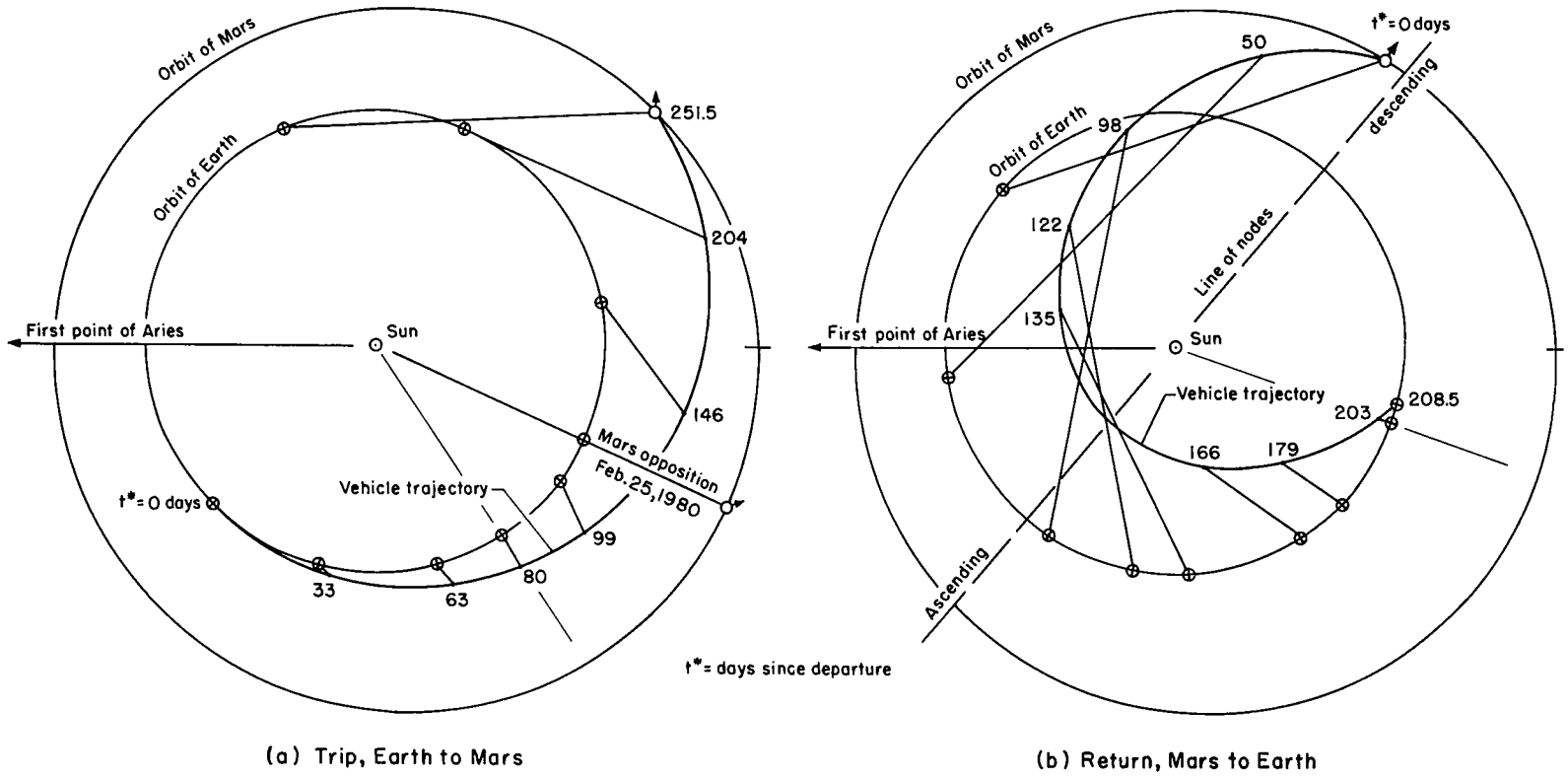

Figure 30.- Typical trajectories of mission; rendezvous mode with propulsion braking at Mars; $k_2 = 0.4$; 27-day stay; 1980 opposition.

2/7/85

"The aeronautical and space activities of the United States shall be conducted so as to contribute . . . to the expansion of human knowledge of phenomena in the atmosphere and space. The Administration shall provide for the widest practicable and appropriate dissemination of information concerning its activities and the results thereof."

—NATIONAL AERONAUTICS AND SPACE ACT OF 1958

NASA SCIENTIFIC AND TECHNICAL PUBLICATIONS

TECHNICAL REPORTS: Scientific and technical information considered important, complete, and a lasting contribution to existing knowledge.

TECHNICAL NOTES: Information less broad in scope but nevertheless of importance as a contribution to existing knowledge.

TECHNICAL MEMORANDUMS: Information receiving limited distribution because of preliminary data, security classification, or other reasons.

CONTRACTOR REPORTS: Technical information generated in connection with a NASA contract or grant and released under NASA auspices.

TECHNICAL TRANSLATIONS: Information published in a foreign language considered to merit NASA distribution in English.

TECHNICAL REPRINTS: Information derived from NASA activities and initially published in the form of journal articles.

SPECIAL PUBLICATIONS: Information derived from or of value to NASA activities but not necessarily reporting the results of individual NASA-programmed scientific efforts. Publications include conference proceedings, monographs, data compilations, handbooks, sourcebooks, and special bibliographies.

Details on the availability of these publications may be obtained from:

SCIENTIFIC AND TECHNICAL INFORMATION DIVISION

NATIONAL AERONAUTICS AND SPACE ADMINISTRATION

Washington, D.C. 20546